TÉCNICO LISBOA

Automatic cost estimation of aerospace composites components based on retrieved knowledge from historic process data

João Alexandre Martins Chícharo

Thesis to obtain the Master of Science Degree in

Mechanical Engineering

Supervisors: Prof. Elsa Maria Pires Henriques

Eng. António Pedro Dias Alves de Campos

Examination Committee

Chairperson: Prof. Rui Manuel Dos Santos Oliveira Baptista

Supervisor: Prof. Elsa Maria Pires Henriques

Members of the Committee: Eng. João Pedro Amaro Pratas

Prof. Bruno Alexandre Rodrigues Simões Soares

Prof. Inês Esteves Ribeiro

October 2020

Acknowledgments

First of all, I would like to thank my supervisors Prof.Elsa Henriques and Eng. António Campos, whose knowledge and contributions were fundamental for the development of this work. As well as Prof. Bruno Soares for his support. It was a privilege to work under their guidance, and a truly enriching experience.

Secondly, I thank the manufacturer, that granted me this unique opportunity to work so closely with them, and the openness and desire they have demonstrated for the success of this research. I would like to especially thank Eng. João Pratas, Eng. André Bogni and their team for welcoming me in my many visits, and for providing me with the tools and information that constituted the core of this work. Their good-humoured spirit was very refreshing.

To my friends and colleagues, that I was fortunate to have by my side through this journey, I deeply treasure every moment we shared.

Lastly, to my parents and family, that always supported and encouraged me throughout all my life. I owe them all my accomplishments, and for that, they deserve my sincerest appreciation.

Resumo

O crescente interesse em estruturas em compósitos desencadeou um desenvolvimento das tecnologias e métodos de fabrico até aos dias de hoje, cujo impulso é garantido de se manter. Em particular, na indústria aeronáutica, os compósitos tornaram-se o material predominantemente utilizado, dadas as suas vantagens sobre os materiais metálicos. No entanto, devido à competitividade económica do sector, os fabricantes têm de lidar de melhor forma com as exigências de custos.

Este trabalho descreve a captura e reutilização de dados históricos do processo, sobre múltiplos programas de aeronaves, com o intuito de desenvolver uma abordagem capaz de gerar boas estimativas de custos de novos componentes numa fase de concepção de projecto. As amostras recolhidas preenchem uma série de relações tecno-económicas, desenvolvidas para estimar os parâmetros e requisitos do processo de fabrico, a partir de um conjunto de propriedades geométricas dos componentes. Por sua vez, estes métodos são integrados num modelo de custos baseado no processo, que traduzem a informação gerada do mesmo, numa avaliação final dos custos de fabrico. Além disso, a abordagem tradicional determinística da estimação de custos é substituída por métodos estocásticos, que reproduzem as variabilidades dos processos. Desta forma, obtêm-se uma visão mais ampla dos custos esperados, consequência das variabilidades inerentes aos processos.

Os resultados obtidos indicam uma boa concordância com os custos do fabricante (MAPE=16,4%, NRMSE=5,1%), validando a aplicabilidade da ferramenta desenvolvida. Assim, é oferecida uma solução para a falta de avaliações do impacto económico de decisões de projecto e processo de um componente, antecedentes à sua industrialização.

Palavras-Chave: Compósitos; PBCM; Modelação de custos; Indústria Aeronáutica.

Abstract

The growing interest in composites structures triggered a development in composites manufacturing technologies and methods up to the present day, whose momentum is certain to be carried into the future. Particularly, in the aerospace industry, composites have become the predominantly used material given its many advantages over traditional metallic materials. However, because of the sector´s economic competitiveness, manufacturers have to better deal with cost requirements.

This research describes the capture and reuse of rich historic process data, over multiple aircraft programs, to develop an approach capable of generating good cost estimations of new components in a preliminary design stage. The collected samples populate a series of tecno-economic relations, developed to estimate manufacturing process parameters and requirements, based on a set of components' geometric properties. In turn, these methods are integrated into a process-based cost model, that translates the generated process information into the final manufacturing cost assessment. Additionally, the traditional deterministic approach to cost modelling is replaced in favour of developed stochastic methods that inherit process uncertainties. By doing so, a broader view of expected costs is provided, which reflects existing process variabilities.

Results obtained in this approach indicate close agreement with the manufacturer cost assessments (MAPE=16.4%, NRMSE=5.1%), validating the applicability of the developed cost tool in estimating projects' manufacturing costs. Ultimately, the tool provides a solution to the lack of readily available cost assessments prior to process industrialization and may help designers to overcome the challenge of evaluating design and process decision consequences on final product cost.

Keywords: Composites; PBCM; Cost Modelling; Aeronautics Industry.

Table of Contents

List of figures

List of Tables

List of Acronyms

C_{XY}	Contour complexity in XY view
C_{XZ}	Contour complexity in XZ view
C_{int}	Integration complexity
Δ$	Reduction in final component cost
Δt_b	Reduction in work center maximum cycle time
Δt_c	Reduction in work center most likely cycle time
μ	Micron
a	Triangular distribution minimum value
A	Surface area
ABC	Activity-Based Costing
Adstat	Adjusted statistic
AFP	Automated Fiber Placement
AFRP	Aramid Fiber Reinforced Polymers
ATL	Automated Tape Layup
b	Triangular distribution maximum value
c	Triangular distribution most likely value
CER	Cost Estimation Relation
CFRP	Carbon Fiber Reinforced Polymers
CLT	Central Limit Theorem
CNC	Computer numerical control
CSU	Cold Storage Unit
Cv	Critical value
DFC	Design for Cost
DTC	Design to Cost
EAC	Equivalent Annual Cost
GFRP	Glass Fiber Reinforced Polymer
H_0	Null hypothesis
HDF	Hot Drape Forming
INVCDF	Inverse Cumulative Distribution Function
k	Number of Non-quality occurrences
LCC	Life Cycle Cost
m	Median
MAPE	Mean Average Percentage Error
MLR	Multiple Linear Regression
NRMSE	Normalized Root Mean Square Error

P	Perimeter
p	Probability for success
PBCM	Process Based Cost Models
Pc	Pearson Coefficient
PDF	Probability Distribution Function
PMF	Probability mass function
R^2	R-squared
RQ	Research Question
SLR	Simple Linear Regression
V	Volume
WS	Workstation
X	Qualities

1. Introduction

Large competitiveness in commercial aircraft manufactures, stimulate a constant push towards producing more economically efficient airplanes to stay ahead of competitors and attract potential buyers. When doing so, manufactures are faced with the challenge of further developing established technologies and explore emerging ones on how to save manufacturing costs, through a more efficient use of its resources. Since the early 1990s composites have been making their way into the aerospace market and have been increasingly used [1]. This penetration has only become possible with the automation of layup processes such as Automated Tape Laying (ATL) and Automated Fibre Placement (AFP), which significantly increased the rate and consistency to which the material is placed when compared to the more traditional method of manual layup [2]. Even though composite materials are typically more expensive than the widely used aluminium alloys, they do come with the benefits of producing lighter components resulting in a lighter airplane that in turn consumes less fuel. Also, composites offer increased resistance to fatigue and corrosion allowing for some additional savings in aircraft maintenance costs. Both aspects drive overall operational costs down, allowing for a lower cost per passenger to be achieved which is of interest to commercial airliners when assessing aircraft acquisition. However, for the manufacturer to achieve profitable returns, a lot of effort should be put into the early stages of product development since a major part of the project cost is committed during this phase [3] and, once production takes place, excessive manufacturing costs are often irreversible [4]. Therefore, it is of the utmost importance to provide tools that allow designers and cost engineers to work more closely together and to support them during design iterations on how overall manufacturing costs are being influenced.

With the increased interest of manufacturers, in using Carbon Fiber Reinforced Polymers (CFRP), as well as other materials such as Glass Fibers (GFRP) or Aramid Fibers (AFRP), great improvements have been made in developing materials with better mechanical properties, as well as the technologies that process and shape these materials into working structures [5]. However, with newer and different technologies different technical challenges arise, to which engineers must adapt their designs (Design for Manufacturing), while making conscious decisions to achieve management imposed cost targets (Design to Cost), aware of each technology's strengths and weaknesses. Additionally, there is often an overlap between technologies, *i.e*. two or more different technologies that can achieve the same result in terms of mechanical performance but with significant differences in terms of manufacturing cost. Thus, the decision-making process becomes even more difficult and careful consideration of multiple process variables have to be taken into account. Understanding what drives the differences in the final manufacturing cost is extremely valuable for manufacturers who try to reduce production costs. But, more often than not, cost and design expertise are held by different people, requiring a combined effort and efficient sharing of information to successfully drive manufacturing cost down and achieve a more economically effective component. Additional challenges lie in the process and methods of determining the key factors that ultimately influence costs, often biased and subjective to one’s expertise on the matter, *e.g.* operational time, material quantities.

In order to achieve a better balance between cost and performance, there must be some enlightenment on what are the main aspects that ultimately affect costs. In turn, these aspects would provide relevant information that engineers could use in the early stages of design to steer and streamline development into a more affordable solution.

The nature of costs that impact final product costs, is distinct between different steps and areas of the manufacturing process. Another trait of manufacturing processes is their well-known variance, *i.e*. they do not always perform under the same conditions. For example, human work performance is variable by nature, leading to an inconsistency on final product costs – either by variations in cycle times or non-quality aspects such as scrap or reworks – meaning that producing the same component will not always have the same costs as initially planned, under normal operating conditions. Recognizing this fact, the present thesis focusses on making use of available industrial data, to translate labour, materials and machine costs, among other sources of cost, into a final assessment of the expected manufacturing costs in the environment of an aircraft manufacturer. Ultimately, the goal of this work is to provide an analytical tool that can help engineers to better understand, during the design process and early stages of process industrialization, possible future manufacturing costs in order to weight on the economic viability for possible changes to the manufacturing process, in a more streamlined way.

To achieve these objectives, this research was conducted at an aircraft manufacturer industrial setting that mainly focus on the manufacturing and assembly of composite aircraft components and structures that range from their executive, commercial and defense divisions. A typical composite part manufacturing process can be long and complex, sometimes taking multiple days to complete with many different steps in between. Understanding and capturing the process dynamics for each of the different parts manufactured was only made possible due to the visits to the factory on a weekly basis, for *in situ* observations of the processes, enabling key insights from both the operators and engineers to be documented. The main purpose of these visits was for the acquirement of manufacturing data, automatically recorded throughout the multiple process steps by company software. This data provided a wide spectrum of analysis, with a history that traces back to 2012/2013, for over 680 components, manufactured through various methods and supporting composite based technologies. Each component manufacturing process was broken down into its core steps - from raw material storage to non-destructive testing - and information from past production runs was analyzed with the intent of capturing the dominant features that impact and influence the different variables that ultimately drive costs – known as cost drivers. Regression analysis was employed throughout the study, to determine possible relations between identified cost drivers and component geometric attributes. These geometric attributes are therefore used as primary inputs, to develop probability distributions to model the cycle times of the various manufacturing steps as a stochastic variable. This information coupled with factory data for materials, machines, and other operational costs is added into Process-Based Cost Models (PBCM) [6] with the intent to simulate its manufacturing costs. Additionally, a Monte Carlo simulation is performed using the developed model, which enables a cost distribution to be obtained that reflects existing process variations. Ultimately, the developed model cost results enable the economic

assessment of currently available technologies at the factory, as well as explore manufacturing alternatives or future process improvements impacts on cost.

This document is organized in the following way: Chapter 2, provides a brief overview of composites' penetration into the aerospace industry, evolution, and prospects. Considering the industrial environment where this work is inserted, a description of some of the available composite technologies is also provided to familiarize the reader with its current capabilities and limitations. Lastly, a rundown over some of the most popular cost modelling methods is provided.

Chapter 3 describes the different manufacturing processes currently explored under the studied industrial framework, the different available data that was collected, and the methods used to develop the models that enable the cost estimations.

In Chapter 4, additional methods and tools are explored and developed, to enhance current PBCMs, by limiting the number of inputs required, to a reasonable amount of quantitative component's geometric characteristics, while at the same time introducing real manufacturing variability to the cost estimation.

The following chapter, Chapter 5, focusses on testing and verifying the developed model throughout the available set of components, and exploring its results. Additionally, the model is used to evaluate cost impacts stemming from technological or process improvements, which are essential to assess when making future process decisions.

Lastly, in Chapter 6, conclusions about the developed work are drawn out, and future work suggestions are provided.

2. State of the Art

The desire to enhance performance on aircrafts is constantly driving the development of high-performance structural materials. Composite materials play a significant role in current and future aerospace components, as they offer exceptional strength and stiffness to weight ratios, allowing for superior structures to be obtained. Composite materials come in many shapes and forms, but most commonly, they are composed of relatively strong and stiff fibers, embedded in a softer and more compliant constituent forming the matrix. Wood is an example of a natural composite material, composed of aligned cellulose fibers in a lignin matrix. Man-made composite materials used in aerospace and other industries are mostly comprised of carbon or glass fibers, both of which are very stiff for their density, but brittle, hence they are embedded in a soft polymer matrix. In a very simplistic way, this combination of materials with complementary properties, form a new material (Fiber Reinforced Polymer) with most of the benefits (high strength, stiffness, toughness and low density) and few or none of the weaknesses of the individual components. Aircraft manufacturers try to make extensive use of these materials, that although more expensive than most common metals, result in lighter airplanes, that in turn consume less fuel, becoming extremely attractive to commercial airliners that seek to acquire new planes, able to operate at lower costs and enable a reduced cost per passenger to be achieved.

2.1. History of Composites in Aerospace

Forty years ago, aluminum dominated the aerospace industry. It was considered to be lightweight and state-of-the-art, therefore as much as 70% of an aircraft was once made of aluminum, from the fuselage to main engine components. Other metals such as titanium and stainless steel also have applications in aerospace, and new alloys are constantly being developed to offer ever-increasing performance in structural pieces like fasteners, landing gears, and actuators that require raw strength rather than lightweight properties.

Despite the dominant run of metal materials in aerospace, with composite materials such as continuous carbon fibers becoming commercially available from 1966 [7] on-wards, the industry very rapidly began growing an interest for this new material even though the use of composite materials was not at all new, with reports of the use of a glass fiber sandwich on a fuselage skin dating back to 1945 [1].

Initially, composite materials were only used in secondary structures, but as experience and development of these materials increased, so did its use, becoming a common application in fuselages and wings. Percentage by structural weight was initially small and mainly used in military applications, at around 2% in the case of the F15, in 1972. But these numbers rose, and by the time of the F18 – around 6 years later – it had increased to 19% [8]. Commercial aircraft manufacturers quickly took notice of the advantages brought by these new materials:

Firstly, unlike conventional metallic materials that are isotropic *i.e*. their properties (strength, stiffness, etc.) are all the same in any direction, fibrous composites are anisotropic *i.e*. their properties vary

depending on the direction of the load with respect to the orientation of the fibres. Initially, this may seem as an undesired characteristic, but by stacking multiple layers of material with the fraction of a millimetre in thickness, and aligning the fibres according to the direction of the expected loads, engineers can tailor the properties of the laminate to better withstand the loads to which it will be subjected. By doing so, material and therefore weight can be saved, by removing unnecessary excess when compared to their metallic counterparts [9].

Secondly, more complex shapes can be achieved, with a bigger level of integration, meaning that two or more individual parts can be joined together and built as one single component. This in turn reduces the need for fasteners and joints to which the advantages are twofold: a fastener requires a hole, which therefore acts as a stress concentration point that may lead to crack initiation. Also, by removing fasteners, assembly times can be brought down, as well as overall component weight.

In the end, it falls to the manufacturer to balance his decision between cost and performance and whether to use composites materials or not, since traditionally, composites are more expensive than metallic materials.

Airbus took the first step in 1983 with their A300 and A310 models that featured a composite material rudder, and then in 1985 the vertical fin. The latter resulted in a reduction from 2000 individual parts to fewer than 100 in its composite counterpart, lowering its weight and production time. These early successes with composites prompted its use for the entire tail structure of the A320, as well as some other components, detailed in Figure 1, composing 28% of its airframe weight.

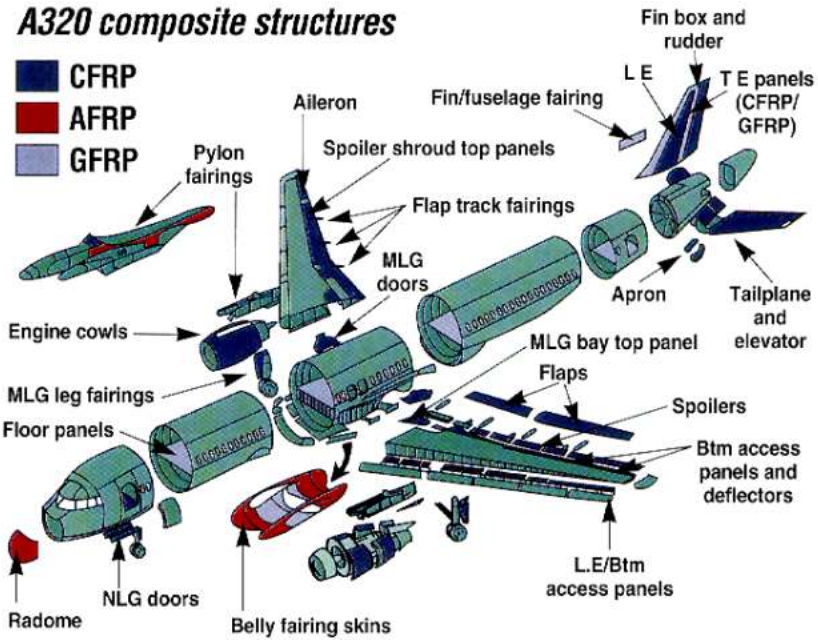

Figure 1 - Composite Materials Applications on Airbus A320 [8]

Similarly, the A340 and A380 models, also bear use to composite structures that contributed to weight savings around 20%, and between 15% to 30% respectively, along with some additional savings in production times when compared to their aluminium counterparts.

Boeing also made use of composites in its commercial aircrafts as early as Airbus, but in 2007 they took a striking step forward introducing the 787 Dreamliner with an unprecedented 80% and 50% of its airframe volume and weight respectively, comprised of advanced composites materials which included the first-ever carbon fibre fuselage and wings with an aerodynamic design that improved fuel efficiency, which could not be easily achieved in metallic wings [10]. This revolutionary design was mostly based on Boeing's attempt to respond to airliners' demands that, with the increase in fuel costs, underlined their interests in having more fuel-efficient aircrafts and to operate at lower per-passenger costs [11]. This extensive use of composites contributed to the aircraft's reduced weight, that coupled with a new generation, more-efficient jet engines, offered a 20% better fuel economy and an equal reduction in pollutant emissions. In addition to that, with the superior resistance of composites to corrosion and fatigue, Boeing developed a maintenance schedule that would allow airliners to extend maintenance checks and reduce total scheduled labour hours by 60%, which in turn, would also contribute to lower operational costs [12].

Airbus paid close attention to these developments, and 2 years later presented its competitor to Boeing's 787 Dreamliner, the Airbus A350XWB. This airplane explores the same benefits of composites as the Boeing 787 with 83% of its volume and 52% weight comprised of composite materials. Both models currently hold the most extensive use of composites on commercial aircrafts (Figure 2), and only confirms the upward trend of adopting composites as the favourable material to reduce weight and achieve higher fuel efficiency.

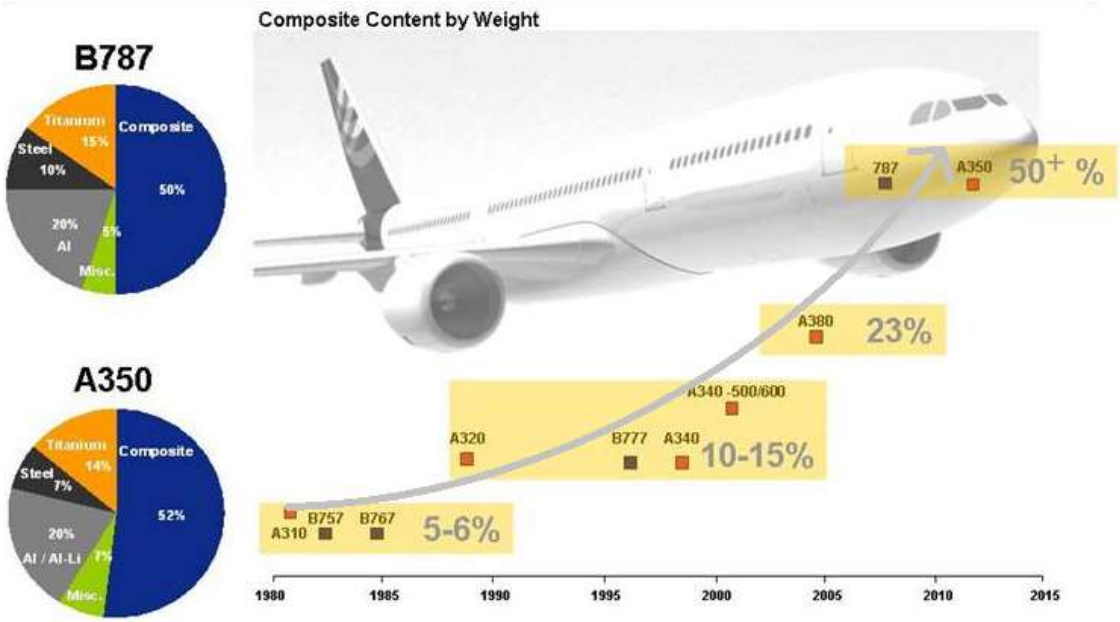

Figure 2 - Breakdown of weight content by material types in Boeing 787 and Airbus A350 XWB.

In the years to come, it is not certain whether these numbers in composite weight percentage will rise or not with yet to come aircraft programs, but composites demand and consumption are sure to increase as interest grows from other industrial segments [13][14][15].

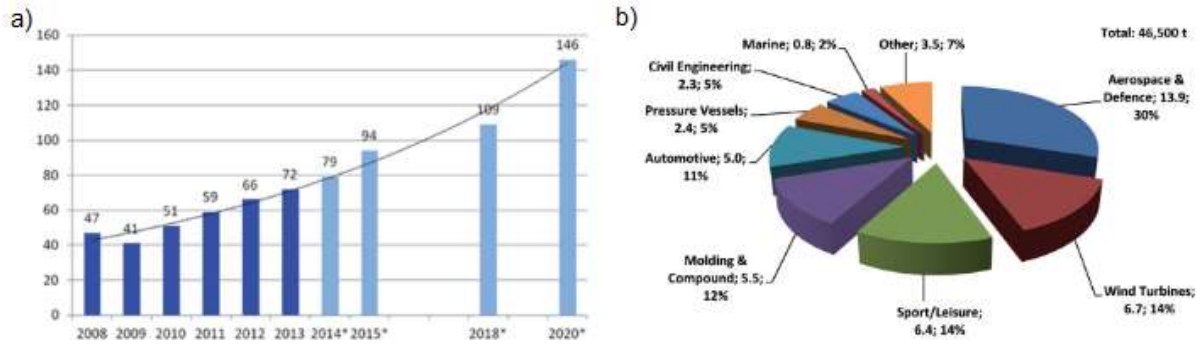

*Figure 3 - a) Global CFRP demand in thousand tonnes (*estimated). b) Global demand in CF by industrial sector in thousand tonnes (2013)* [14]

Boeing claims that its newest 777X model - with expected first deliveries by 2020 – will be the largest and most efficient twin-engine jet in the world with 10% lower fuel consumption and emissions as well as 10% lower operational costs than its competitors [16]. Early estimations indicate that each of these newer aircraft carbon fibre wings, will consume as much material as an entire 787 Dreamliner and that alone should increase and sustain carbon fibre demand in the aerospace sector for the next decade [17]. This increase in consumption naturally requires additional investments in technologies that give shape to these materials and allow for a steady production flow of parts. From this perspective, Boeing invested over 1 Billion dollars in new facilities that accommodate three of the world's largest autoclave units, together with automated layup manufacturing equipment from Eletroimpact Inc. which cements the interest in composites from one of the leading aerospace manufactures for years to come [18].

2.2. **Advanced Composite Manufacturing Technologies**

Carbon fiber composites manufacturing still requires a great amount of manual work due to parts intricacies that may be inaccessible to machines, or in situations where the machine acquisition investment might not compensate for the targeted production volume. Notwithstanding, for the past decades, the manual process of depositing sheets of composite material on top of each other – also referred as hand-layup – as the standard process for composites manufacturing is falling more and more out of use, as for larger components, the low rates of material deposition achieved (~1kg/h) are not on par with the current demands of production. Not only that, but manual processes are also highly variable, as the alignment of the fiber directions and correct positioning of the sheets are dependent on the worker level of skill and precision, which may not always achieve the same results, generating a lot of material waste and scrapped components in the process. Therefore, since the early days of composites,

manufacturers have been trying to develop equipment that would allow for an increase in material deposition rates, in order to unlock composites manufacturing to its full potential. These shortcomings in composites manufacturing are nowadays significantly reduced by automated processes that can perform at high levels of precision and consistency.

The two most common technologies currently in use in the aerospace industry are Automated Tape Laying (ATL) and Automated Fiber Placement (AFP). Besides these two, there is a wide range of other available technologies, each more suitable for a particular part characteristic of the component to be manufactured. However, there is not a single technology that is only suitable to a particular set of components, rather, there is a span of technologies that could achieve the same results but requiring different operational conditions. As it will be shown in the next sections, both ATL and AFP have some overlaps in terms of the types of components they produce, although each comes with its advantages and limitations. The question then lies in which technology achieves a better or equal result at a more affordable cost, resulting in a more cost-competitive component.

2.2.1. Automated Tape Layout (ATL)

Since carbon fibers became commercially available by 1966 [7] manufacturers started to wrap their efforts into developing technologies that could improve productivity and consistency when using these materials. The first ATL systems were conceived by the end of the 1960s and by the middle 1970s they were in applicable use, although, at that time, they were mostly built in-house as part of a component center production system (Figure 4).

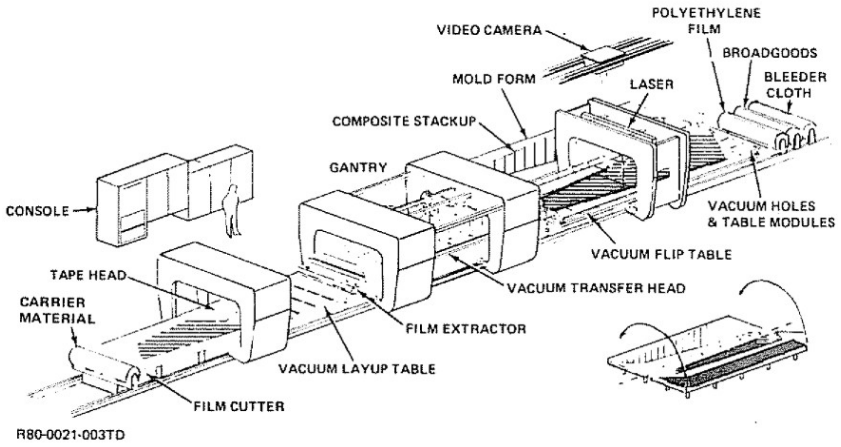

Figure 4 – Layout of an automated laminating system [19]

At that time, it was argued that the slow speeds of these systems did not yet achieve the desired productivity levels, and were reported to be on par with hand-layup processes in terms of deposition rates [19]. However, the big advantage already possessed by these systems, was the ability to greatly reduced layup errors, resulting in material savings between 70% and 90% comparatively to hand-up [20][21].

During the 80s and throughout the 90s, lots of developments and competing concepts emerged, yet, some limitations regarding the difficulty in depositing material over curved surfaces, accurate pressure and temperature control - that could ensure correct tack level of the laminate and enable tape attachment - still made it difficult to offset the high initial investment of ATL as productivity levels remained low (10-20m/min).

In today's time, most of these problems have been overcome, and ATL is a well-established technology in the manufacturing of composites parts, considered to be an additive process as the part is built by adding the material in opposition to material removal in machining [22]. These systems are usually built in horizontal gantries or vertical column configuration that hold the machine's head where the material is stored, and are responsible for delivering the material tapes onto the surface of the mold.

a) b)

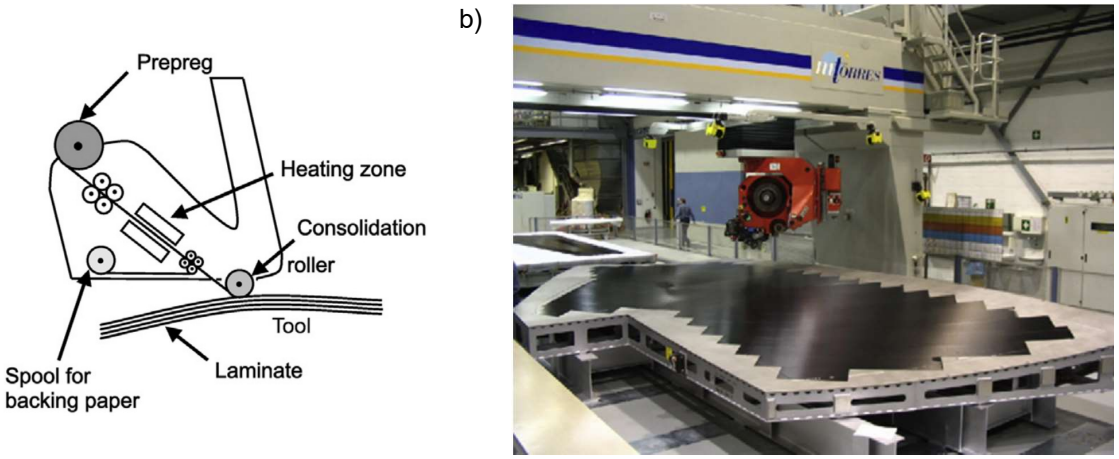

Figure 5 - a) Schematic of an ATL layup head [23] *b) Gantry type ATL machine, laying prepreg material onto an open mold* [24]

Depending on the level of curvature of the surface, these prepreg tapes could vary from 75 to 150 and 300 mm wide – with lower curvatures allowing for a wider tape - and are placed parallelly to each other with gaps no bigger than 1mm, so that it is not impactful to the mechanical performance of the component. The machine first attaches the tip of a pre-determined length of material on the mold, using a soft silicone roller, and then accelerates to deliver the remaining length of material using controlled force. At the end of the ply's course, the head decelerates and cuts the tape automatically, in order to start a new one. This is only possible due to the Computer Numerical Control (CNC) systems that execute these predefined paths with high accuracy and reproducibility, allowing the minimization of layup errors. Current systems are capable of reaching linear speeds up to 0.83 m/s and accelerations up to 0.5m/s^2 with layup rates varying from 10 to 150 kg/h depending on the level of complexity of the component [5][25]. In terms of material waste that result from the layup process itself (technical scrap), it is claimed that with increasing part size, these tend to decrease from 30% and can be as low as 2% to 4% [20], meanwhile, efficiency follows an opposite trend, and increases with part size [26][6]. This has to do with the fact that with bigger parts the machine spends most of its time at maximum laying speed, not having to decelerate and cut the material to readjust its position and start a new ply as often.

2.2.2. Automated Fiber Placement (AFP)

The first AFP system introduced in 1974, was based on an ATL machine with the ability of slicing down the wide tape into smaller 3.2mm slices that could be delivered at individual speeds, allowing for a better deposition of material onto curved shapes (Figure 6).

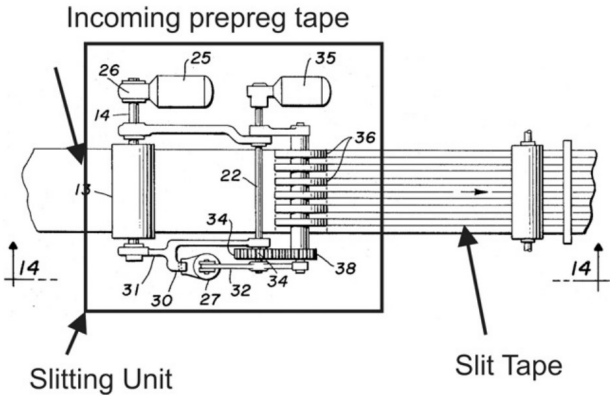

Figure 6 - Schematics of tape slicing mechanism of the first AFP system [27]

Controlled pressure and temperature are just as important as in ATL for the same reasons, however, due to the increase in the number of narrower independent tapes placed at the same time, an even greater accuracy control is needed, otherwise, it will result in gaps between the material that may affect the mechanical performance of the component [28]. Another challenge that emerges in AFP, has to do with the possible welding of the tape ends, known as splicing, that required the development of better cutting systems to mitigate its effect.

Current AFP structures are very similar to ATL (Figure 7), with most equipment employing the horizontal gantry or vertical column configuration, while some might use robotic arms that offer better tailoring for specific applications [5].

Figure 7 - AFP gantry structure with tow holder on top of the horizontal column, laminating over an open mold [29].

These systems deposit multiple tows of material - stored inside the machine head or on-top of its gantry structure - with widths typically of 3.2, 6.4, or 12.7 mm, termed bands. A band forms a course, and a

sequence of courses forms a ply that covers the desired surface area of the mold in a specific direction. Presently, up to 32 tows can be delivered at a time, with the ability to independently control each tow speed as well as the number of tows delivered at the time, enabling a better layup over complex geometries and curves, as well as deposition along curvilinear paths [5]. This ability - known as tow steering - is very useful as it allows for better optimization of the laminate directions producing highly efficient load-bearing parts. Another advantage of this independent tow control is the possibility to individually cut and adjust the number of tows, which in turn leads to lower scrap rates when compared to ATL (Figure 8).

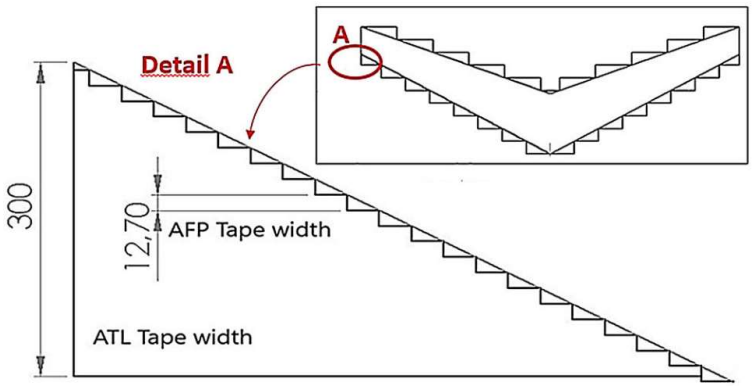

Figure 8 - Difference in technical scrap generated in ATL and AFP, resulting from the larger surface of material deposited than the part surface [6].

Performing at speeds up to 1 m/s and accelerations 2 m/s^2, it is possible to achieve deposition rates up to 150 kg/h. This productivity falls significantly when depositing material over more complex surfaces, despite its better ability to perform under these conditions compared to ATL.

2.2.3. Hot-Drape Forming (HDF)

Hot Drape Forming (HDF) is a thermoforming process that was originally developed for forming thermoplastic composites in the 1980s as an alternative and more efficient way to achieve geometrically complex composite parts, but nowadays it is also applicable to thermosets [30][31]. Unlike ATL or AFP, HDF is not considered as a lay-up technology, as no material is deposited during its process, instead, it can be seen as an auxiliary technology to be used in combination with any of the previous two, or even hand-layup.

The idea behind this technology is to firstly produce a flat prepreg stack either by any automated process or hand-layup and then conform the material to the curved geometry of a tool. Deformation of the material is achieved inside the equipment (Figure 9) by the application of heat and vacuum between the tool and a membrane above the material, pressing it against the tool during a certain period, dependent on part geometry and dimensions (Figure 10). Finally, the preformed curved part is cured inside an autoclave or oven, under applied pressure to consolidate and produce the final composite component.

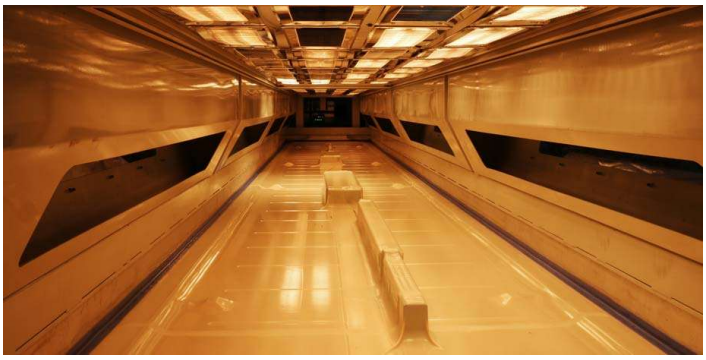

Figure 9 - HDF machine cycle source: https://pinetteemidecau.eu/en/preforming-solutions/hdf-hot-drape-forming-preform-production

Figure 10 - Illustration of the composite forming process [32]

By using this method, it is possible to significantly reduce the layup time of the component onto three-dimensional tools, into a single step forming process, therefore reducing part costs. However, some technical challenges may hinder the process. Heat is applied to soften the material and reduce the highly viscous resin on prepreg surfaces that generate high interply friction between multiple sheets of material [33]. This friction reduces the slippage between the material sheets, causing interply shear stress that ultimately results in ply wrinkling or fiber buckling, both highly undesired as they compromise the structural integrity of the component. For this reason, some studies suggest that HDF may not be suitable for manufacturing large and thick components [34].

As previously mentioned, heat can be applied to reduce the effects of fiber wrinkling and buckling, but even this more conventional method has its limits, as prolonged exposition to high temperature could initiate the curing process, which is undesirable during the forming cycle. Recent studies propose the application of dry lubrification layers in between the prepreg layers to reduce interply friction [32]. These lubricant layers can be formed either by thin veils or powders, that not only promote interply slippage but have also been reported to increase the component interlaminar fracture toughness [35][36].

Overall, HDF is a viable solution when evaluating potential manufacturing alternatives and has been successfully implemented in thermoset composite structures [37][38]. Ultimately, whether a manufacturer chooses to employ this technique or not, will come down between the balance in potential time savings in its other equipment such as ATL or AFP, freeing up space for other components to be produced, and the initial investment that has to be made in order to acquire the machine.

2.3. **Cost Modelling in Aerospace**

With the development of automated technologies, newer processes and methodologies to manufacture composites components emerged, becoming ever so difficult to make a conscious and informed decision on the most cost-effective manufacturing route. This is true not only in the aerospace industry but in any other industry. Being cost an important decision metric in assessing product viability, a lot of effort is put in trying to control possible manufacturing costs with design decisions at the very early stages of engineering design, and it is usually done under two different approaches: design for cost (DFC) and design to cost (DTC). DFC makes conscious use of engineering process information during design to reduce life cycle cost (LCC), whereas DTC is driven by management-imposed cost targets resulting in iterative redesigns of a project until the content of the project meets a given budget [39].

However, it is believed that imposing strict cost targets leads to inferior designs that ultimately still overshoot estimated costs [40]. Rather, emphasis should be put in providing designers supportive costing tools that could determine cost impacts based upon design decisions.

Despite this rather obvious statement, cost modelling is knowledge intensive and usually requires expertise in several different disciplines for an accurate understanding of a company's processes and ensure that the model is provided with accurate data, to generate a meaningful cost estimate in a timely manner.

Cost modelling is defined as:" the process of predicting or forecasting the cost of a work activity or output by interpreting historical data" [64]. Currently, there are three well-recognized methods used in the evaluation of potential costs: analogous, parametric, and bottom-up.

(1) Analogous

The analogous method is also synonymous with case-based reasoning tools. This method is characterized by adjusting the cost of similar past projects relative to differences between it and the target product. Past project data are organized and stored to later retrieve its information and help identify a cost value for a new project, but in order to do so, it is required to first capture the knowledge of experts that can formalize the process into similarity functions and analogy rules [41]. Those could later be used to attain the desired estimates, but formalizing this knowledge can be a very complex process that still requires some assumptions to be made, and its utilization is subject to the expertise and understanding of the user [42][43].

One of the strengths of this method is the possibility to utilize a single historical data point as support for the estimate of a new project that does not incorporate many different design features or utilize new processes for the company. However, there is always an associated risk in affecting the accuracy of those estimates when dealing with a limited set of information, and its effectiveness relies heavily on the ability to correctly identify the differences between the two cases. Standardization helps to ensure that the process is as rigorous as possible, seeking to achieve better results. Examples can be found in the literature [44], as well as cost estimates using this methodology [43].

(2) Parametric

Parametric cost models were developed in the 1950s by the Rand Corporation [45] and have thus become very popular within the aerospace industry. This cost estimating techniques usually employ cost estimating relations (CER's) in the form of mathematical algorithms to establish cost estimates. It usually relies on linear regression for the development of CER's, where the focus is in establishing possible relationships between different parameters – referred as cost drivers - that are observed to change as cost changes [46]. These are typically project parameters know to be highly influential in the change of costs.

With the use of historical data, it is then possible to establish relations between cost as the dependent variable, and the selected cost drivers as independent variables and infer the statistical accuracy of these relationships to check for their validity. The process of establishing CER's is performed across all the relevant cost sources - from the cost of materials, fabrication, inspection, etc. - and combined, they account for the product's total cost.

This way, it is then possible to generate a cost estimate for a similar product, or products, inside the range of the historical data set used, mindful that the accuracy of this estimate is only as good as the combined correlation accuracies of all the individual CER's.

(3) Bottom-up

Bottom-up cost modelling relies on detailed engineering analysis and calculation for the various system components, and the aggregated sum of each estimate equals the estimate of the entire project. This approach is the most accurate in estimating project costs, but it also requires the most time. The process typically starts by entailing each team responsible for a basic task in the work structure of the project with the opportunity to produce the estimate relative to their work. Because each team is performing the work relative to its estimate, it is believed that they are in a better position to achieve accurate results. However, as mentioned earlier, this process requires detailed information about the project designs, which may not be readily available at an early stage, hence, if an early estimate was to be produced, it would require the use of parametric or analogous methods.

Advanced estimating techniques

More recently, different methods are starting to emerge that follow more complex methodologies, attributed to advances made in other disciplines, such as computer science that ultimately set off the development of such methods. A few examples are (1) Feature-based modelling, (2) fuzzy logic, and (3) neural networks.

(1) Feature-based modelling

Feature-based modelling - as suggested by its name - uses the design features of the manufactured object as relational drivers of costs. By doing so, objects can be categorized into classes of similar features, giving the possibility for the cost functions to be attributed to the classes itself, and not the individual object. Another result from this process is that by linking costs to certain object features, that

information itself can be fed back to the designer who ultimately becomes more conscious of design decisions and how themselves can directly influence costs.

One example is to associate certain product features with the production time and resultant costs to achieve that same feature. However, this process can become cumbersome, when multiple operations are carried out for groups of inter-related features which makes it difficult to allocate the exact cost for each feature. With the growth of CAD technology and 3D modelling, most manufacturers have a good supply of readily available geometric data where it is possible to draw which features should be selected and linked to the company's historical manufacturing data to evaluate costs.

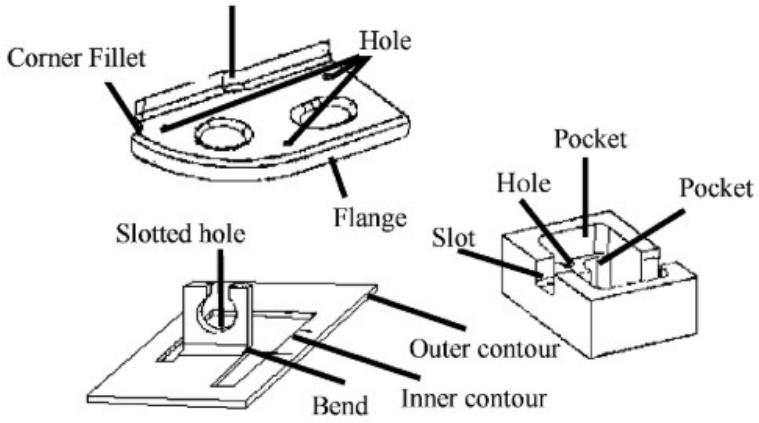

Figure 11 - Examples of design feature definitions

Typically, the more features a product has the more designing, manufacturing, and planning it will require [47], leading to an increase in costs. Although not yet fully established, companies appreciate the concept as this methodology is usually a more apparent way for engineers to decompose and define costs based on design.

(2) Fuzzy logic

Most traditional cost modelling tools are deterministic and do not account for the uncertainty of many of the parameters in the industrial environment. Fuzzy logic was originally created to bridge the gap between the binary world of digital computing and that of continuous intervals, as displayed in nature, but it also proved to be capable to quantify vagueness in human knowledge in a formal manner. By applying fuzzy logic approach, it is possible to address the uncertainty in cost estimation and it is appropriate in situations where the understanding of very complex models is limited or judgmental and heavily based on human perception and decision making [48][49]. It can be viewed as a form of Artificial Intelligence that formulates the human thought process and has been applied to the realm of aerospace cost estimating.

(3) Neural networks

Neural networks have been implemented in cost modelling applications with the view of linking historic costing information with design stimuli [50]. In its essence, it is a computational model, that is fed with a range of product-related attributes and historic cost data and simulates the various procedural permutations and combinations between the product related attributes and costs to repeatedly arrive at a logical cost conclusion. This is referred to as training of the network, and during this process, the network learns to develop the links between cost as the effect and attributes as the cause. It is stated, that these methods, under the correct conditions, can produce better cost estimates [51][52], however, this technique does not simplify the overall analysis, as it must still define the problem domain and supply the model with relevant cost data perceived to be important, where the accuracy of the estimate is only as good as the quality and quantity of the input learning data.

Another important observation is the “black box” nature of the process, as the relationships developed within the model are not as explanatory as regression approaches where the cause and effect are clearer. Consequently, this approach may not be appropriate for users that need a transparent analysis of the reasons behind the cost estimate, which is a fundamental requirement for the designer who wants to be able to learn from the estimating procedure on how his designs influence costs.

3. Data and Methods

This chapter provides an overview of all the gathered data, detailing the type and source of data that was made available by the company, as well as the methods that were used for its cleaning and exploration. The resulting samples were used to populate the developed methods that form the core of this thesis. In turn, the developed methods provide vital pieces of information that must be known within the cost modelling problem, allowing for a manufacturing cost assessment to be obtained.

Understanding the dynamics in the manufacturing processes is of key relevance in cost modeling, as it underlines each cost origin, and provides the necessary insight to develop appropriate cost models. Therefore, in this chapter, the reader is initially presented with a description of the factory framework and the different manufacturing methods that currently take place in the manufacturer's composite facilities.

Lastly, a thorough description of the process-based cost model (PBCM) and its cost relations are given, which translate the various manufacturing process data into its manufacturing costs.

3.1. Manufacturing Process Description

In this section, a generic manufacturing process is presented, to give a perspective over the multiple steps necessary to obtain a carbon fiber composite component and point out the fundamental characteristics of each process step, in order to capture their potential impacts in final component cost.

The first step (S_1) in the manufacturing process begins with the necessary prepreg materials being removed from cold storage units (CSU 1 and CSU 2 in Figure 12), twenty-four hours prior to their use. These cold storage units are needed because most of the materials are pre-impregnated with bonding resins – hence the name prepreg – and must be stored at sub-zero temperatures otherwise, the curing process starts to take place. During this twenty-four hour period at room temperature, the materials become more malleable, and at the same time, any moister that could negatively impact the mechanical properties of the final part evaporates [53]. Once at room temperature the materials are rendered useless if not processed during a certain time window.

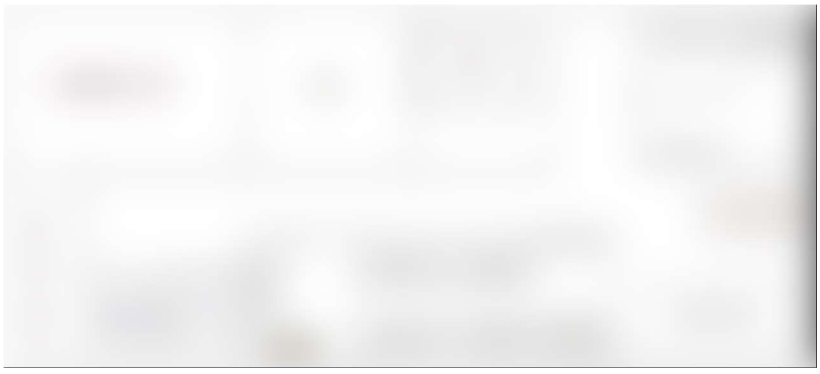

Figure 12 - Simplified factory plant and workstations. (To respect confidentiality, this information has been concealed)

In the second step (S_2), the materials are laid onto a CNC cutting table where multiple sections of material are cut to the specified dimensions. Afterwards, these material sections are stored and packed into labelled plastic bags (Figure 13), to avoid contamination from air particles and facilitates its transportation to the succeeding manufacturing steps.

Figure 13 - Labelled prepreg material KIT [54]

Step three (S_3), starts with the preparation of the mold in either workstation 1 (WS_1) or workstation 2 (WS_2). Here, the mold is cleaned, a release agent is applied onto its surface and only then the materials prepared in S_2 are manually deposited in the appropriate positions with the aid of LASER projection systems, that provide reference points for the operators performing the task. Depending on the component being produced, the combination of materials used may change, but there are normally three standard options: Glass Fibre, Copper Mesh, and Carbon Fibre. Whether all three or any other combination of these materials is applied, depends on the type and application of the component. As an example, if the component is part of any external structure, a copper mesh is usually applied onto its outer surface to promote a low resistance path to discharge points, warding against any damage to the plane structure or electrical equipment from potential lightning strikes [55]. After the careful placement of these different material layers, the mold surface is sealed by covering its area with a special plastic film and by placing an adhesive tape along its contour, that eliminates any gaps between the mold surface and the plastic material so that vacuum can be created. Once the pressure is lowered inside this sealed area, the plastic material presses onto the prepreg layers previously laid, compacting them into each other to reduce its volume and decrease any intralaminar voids from air trapped between the layers, in a process often referred as debulking. At this point, the manufacturing process is ready to be moved to a further step – step 4 (S_4).

S_4 is characterized as the major material deposition step in the process, often performed by one of the available automatic laying processes - either ATL or AFP - depending on the component's type. The mold is placed under the layup machine gantry structure, and the layers are individually added. Each deposited layer is visually inspected by the machine operator to ensure that there are no overlapping or wide gaps between the prepreg strips, or any wrinkles that may have formed during the process, which could cause the operator to redo the deposition of that layer or individual strip. This action of pausing the machine, visually inspecting and resuming the operation is time consuming and greatly contributes to the increase in the cycle time of this step.

Once all the layers have been deposited by the machine, step 5 (S_5) can take place either in Workstation 3 (WS_3) or Workstation 4 (WS_4), respectively depending on the previous step being ATL

or AFP. Here, similarly to S_3, manual work is performed. Additionally, the component receives an identification tag, and thermocouple probes are inserted along its surface in non-structural areas of the laminate for temperature control during the autoclave curing cycle. Once all the preparations are over, the mold containing the laminate is moved inside the autoclave, where the curing cycle takes place (S_6).

Inside the autoclave, the prepreg material is cured by undergoing a high temperature and pressure cycle that takes several hours. The increase in temperature promotes the polymerization of the resins present in the material, accelerating the curing process whereas pressure further compacts the material layers onto the mold surface to acquire its shape and to reduce intralaminar voids that may have formed from air entrapment during the layup cycles. If present, these voids will negatively impact the mechanical strength and integrity of the component [56]. The demolding step – step 7 (S_7) – begins after the curing cycle, where the multiple layers of laminated material have been stiffly bonded onto each other, granting the component its mechanical strength and shape once it is removed from the mold.

In the next step (S_8), the part is held in place with auxiliary tools in a CNC machine where a cutting tool follows the edges of the part to achieve the components' final geometry by trimming any excess materials. The trimming process requires a lot of precision and must comply with two important technical aspects. First, the cut must be precise enough to guarantee the tight tolerances that are often practiced in the aerospace industry, which can be as low as a micron ($\mu = 1 \times 10^{-6}$ m). Second, the cut must be clean enough to ensure that no delamination between the composite layers occurs or that the surface is left with any burs or chips, that could lead to future damage propagation and result in the component's failure [57]. Both these conditions should be met, otherwise the component may fail to pass non-destructive testing, resulting in either a repair to be issued or, if the damage is too severe, for the complete scrapping of the part. Material trimming is followed by light manual finish (S_9) and carries the component into its final step - step 10 (S_10) – where non-destructive testing of the component is performed. There, ultrasound equipment is used to detect the presence of potential flaws hidden inside the material that could affect its integrity. This process is typically performed by automated equipment on larger surfaces, as well as manual scanning on areas inaccessible to the machine.

From this point onward the component is forwarded to the assembly line for its installation in an aircraft structure, which is later moved into the shipping area where it is packed and stored, waiting to be transported to another factory and assembled into the aircraft. The described manufacturing process is illustrated in Figure 14, where each block represents a different manufacturing step.

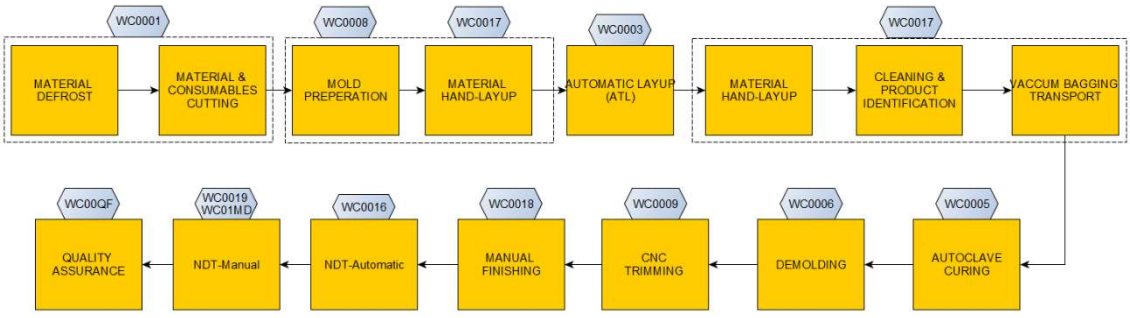

Figure 14 - Generic ATL / AFP manufacturing process steps

In Figure 14 WCXXXX labels, refer to work centers. These work centers, labelled accordingly by the company, designate the type of activities and the equipment used, as well as its physical space, or spaces. For example, workstations 1 through 4 (WS 1 to WS 4 in Figure 12), performed activities are simultaneously designated by the labels WC0008 and WC0017, as those areas are responsible for the mold preparation, and manual lay-up of materials, respectively.

One should note that after going through the manufacturing processes described above, the produce parts follow to the assembly line, which by itself must deal with the assembly of thousands of individual elements that compose the final structure. However, focused on the development of tools that, based on historical data, can estimate the manufacturing cost of parts made of composite materials, the assembly costs were excluded from this work.

3.2. **Components and Manufacturing Processes**

Composites manufacturing technologies allow the production of components with different shapes and sizes. Currently, the manufacturer makes use of its automatic layup technologies to mostly manufacture multiple skins and spars. In this current sample, there are some noticeable differences in the components' overall dimensions and technical requirements, resulting in a diversified range of manufacturing processes and technologies used (Table 1).

Aircraft	Part Description	Main Technologies
A	Skin 1	ATL
A	Skin 2	ATL
A	Skin 3	ATL
A	Skin 4	ATL
B	Skin 1	ATL
B	Skin 2	ATL
B	Spars 1	AFP
B	Spars 2	AFP
C	Spars 1	ATL+AFP+HD
C	Spars 2	ATL+AFP+HD
C	Skin 1	ATL+HD
C	Skin 2	ATL+HD
C	Skin 3	ATL+AFP+HD
C	Skin 4	ATL+AFP+HD
Total		

Table 1 – List of manufactured components and respective technologies used in its processes

There are two different manufacturing processes currently explored in the manufacturing of the spars, with both sharing some similarities in the initial and closing manufacturing stages. The main differences lie in the way they are laminated. While one follows the more generic approach of directly adding the multiple layers of material on top of a mold with the desired shape (Figure 14), the other instead deposits the carbon fiber plys onto a flat surface, where the material is then manually relocated to an appropriate mold and together they are transferred to the hot drape forming machine for attaining its final shape (Figure 15). In a parallel task, some sacrifice layers are deposited following a similar approach which are then manually added to the outer surfaces of the already conformed spar. These layers provide no

structural benefits to the spar but, they offer some surplus of material, ensuring that the desired dimensional precision is achieved during the CNC machining step.

Figure 15 - Manufacturing process flowchart for aircraft C spars. Orange steps are performed synchronously to the main manufacturing process in yellow. (Information has been omitted to respect confidentiality.)

Co-cured reinforced skins involve manufacturing processes with significantly higher complexity. Typically, wing type structural elements of an aircraft are composed of an outside skin, reinforced with spars, ribs, and stringers. In some cases, these elements are manufactured separately and then put together in the assembly line. With composites elements, however, it is possible to layup the materials for these components individually - in this case, the skin and stringers - and then, these uncured parts are pre-assembled together before the autoclave cycle, where the curing and bonding occur at the same time resulting in a single reinforced component (Figure 16 and Figure 17).

Figure 16 - Manufacturing process flowchart for aircraft C skins 1 & 2. Orange steps are performed synchronously to the main manufacturing process in yellow. (Information has been omitted to respect confidentiality.)

Figure 17 - Manufacturing process flowchart for aircraft C skins 3 & 4. Orange steps are performed synchronously to the main manufacturing process in yellow. (Information has been omitted to respect confidentiality.)

These manufacturing processes require additional investments, as both skin and stringers manufacturing tasks must be performed at the same time, parallel to each other, in order to reduce the overall process cycle time while at the same time ensuring the proper alignment between components, just like an assembly line would, with the use of assembly jigs and appropriate support tooling.

There are multiple advantages when performing this manufacturing technique. The bonding between the two surfaces usually overwrites the need for mechanical fasteners mounting, which would otherwise need a hole to be made and act as a potential stress concentration point. Not having to perform any of these tasks, greatly reduces assembly times and part count, thus reducing costs [58]. However, careful considerations must be made to assess the economic viability in the additional tooling investments needed for the manufacturing stage, in detriment of investments for the assembly stage, as well as the technical challenges that arise when performing this complex process.

3.3. **Data Collection**

In today's manufacturing environments data plays an important role to make thoughtful business decisions and to provide insights on how plants are running by observing trends in production and labour times. With the information retrieved from adequate data, manufactures are able to reduce waste and processes' variabilities allowing for improvements in product quality and yield [59].

For aircraft manufacturers, data not only works as a source of useful information from a management point of view, opening many of the previously stated opportunities, but it is also used as a source of validation of the quality and integrity of any part that is produced.

Since the start of factory activities, until when the data was retrieved, more than six-hundred and eighty composite parts have been successfully manufactured, split among 14 different components. Table 2 shows the corresponding manufactured quantities of each different component and the associated technologies used in its manufacturing.

Aircraft	Part Description	Main Technologies	Percentage of Total Produced Parts
A	Skin 1	ATL	21.6%
A	Skin 2	ATL	21.1%
A	Skin 3	ATL	23.3%
A	Skin 4	ATL	22.2%
B	Skin 1	ATL	0.7%
B	Skin 2	ATL	1.2%
B	Spars 1	AFP	3.6%
B	Spars 2	AFP	2.9%
C	Spars 1	ATL+AFP+HD	1.0%
C	Spars 2	ATL+AFP+HD	0.7%
C	Skin 1	ATL+HD	0.4%
C	Skin 2	ATL+HD	0.4%
C	Skin 3	ATL+AFP+HD	0.4%
C	Skin 4	ATL+AFP+HD	0.3%
Total			**> 680**

Table 2 – Parts data set and respective manufacturing technologies used.

The following sections go into detail on how the available industrial data was collected, filtered, and stored so that it could be later employed in the developed cost estimation models as a reliable and meaningful source of information.

3.3.1. Cycle Times

Prior to the beginning of any operation, the operators confirm in the workstation's computer, that they are about to start their tasks. This action stores a timestamp, as well as the current operation that is about to take place for that specific component. When an operation is concluded, the operators close it. Both these interactions with the computer – starting and ending of the operation – feeds the information to a database, and the internal software automatically calculates the difference between end and start time, resulting in the operation duration (Figure 18).

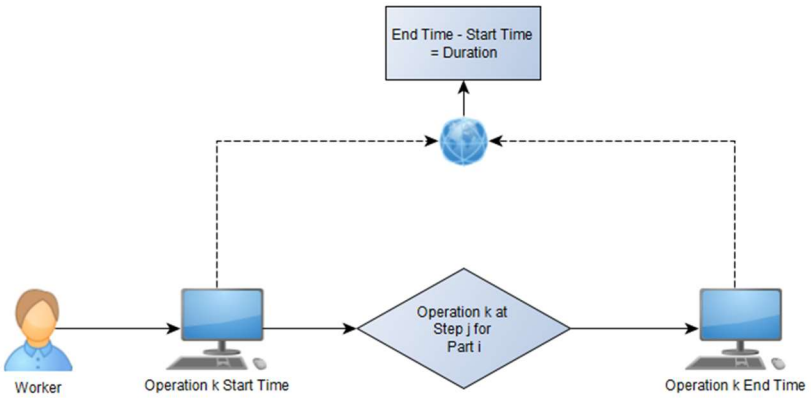

Figure 18 - Cycle time data gathering representation

This process is repeated throughout the different manufacturing steps, which can have one of more individual operations, as shown in Figure 19.

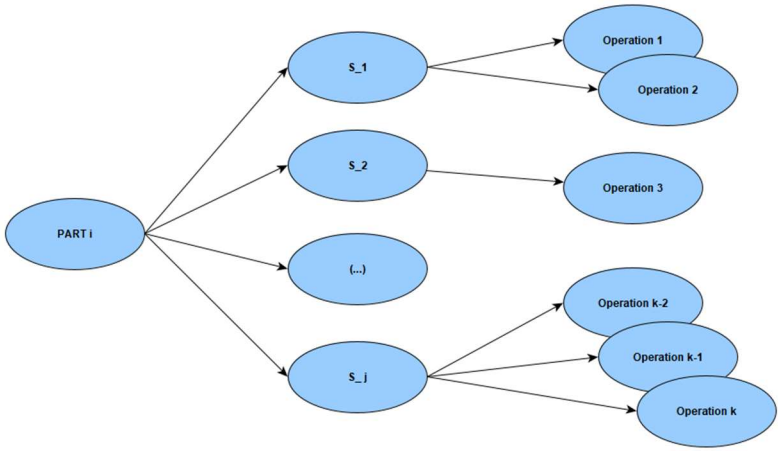

Figure 19- Part operations plan example

The set of 14 different components, manufactured across multiple steps, along several years and in different quantities (Table 2), resulted in the collection of over 48,000 individual operations time entries. These were filtered and rearranged to allow for preliminary data exploration. The collected data presented some inconsistencies: in a very small number of operations the durations - automatically calculated by the internal software - were incorrect, while a more considerable amount had either extremely small or exceedingly long durations. Independent of the magnitude, these situations indicate that the operators did not follow the normal procedure (Figure 18), and closed the operation before performing the task, or forgot to register its conclusion. It is important that both these cases of software and operator misstep are avoided in the future, as it defeats the purpose of monitoring tasks for data analysis. For the purpose of this work they were filtered out to allow for any significant analysis to be performed.

In addition, the software calculated entries accounted for the duration of labour performed by a single worker in a single operation, meaning that the sum of durations of all the operations in that step would be equal to the total labour performed by all the workers, and not the process step cycle time itself. It is important to separate these two quantities, as labour and cycle times account for different cost drivers. Figure 20 shows an example of a set of operations performed in a random manufacturing step. Each bar accounts for the duration of an operation performed by a certain worker which is the difference between end time (y_i) and start time (x_i). Total labour time is defined by the sum of each operator's task duration (Equation 1) while cycle time is the difference between the last operation end time, and the first operation start time, minus any idle time in between (Equation 2).

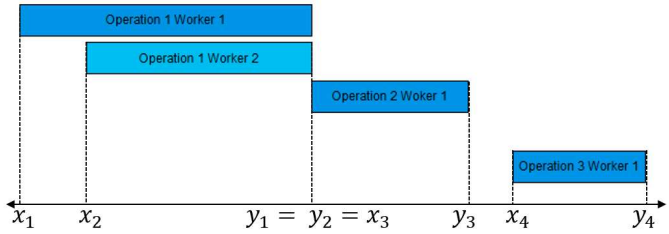

Figure 20 - Representation of duration times for a manufacturing component step

With this in mind, a MATLAB script was created that imported every timestamp entry to calculate the multiple cycle times of each step according to Equation 2 and as illustrated in Figure 21, before being stored to an EXCEL sheet for future use.

$$Labour\ Time = (y_1 - x_1) + (y_2 - x_2) + (y_3 - x_3) + (y_4 - x_4) \quad (1)$$

$$Cycle\ Time = (y_4 - x_1) - (x_4 - y_3) \quad (2)$$

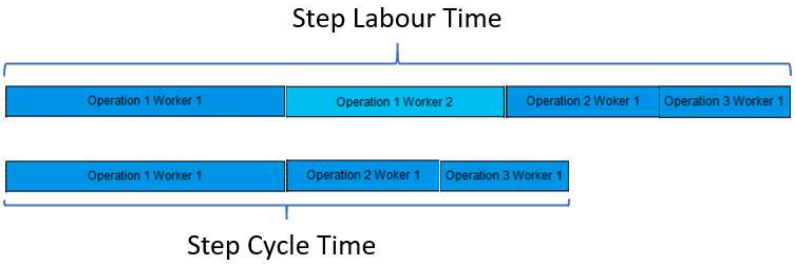

Figure 21 – Representation of Labour and Cycle Time difference

From the data set, a total of 7,589 individual cycle times were outputted. This number is much lower than the initial input sample of 48,000 registers because, rather than summing and counting the durations of every elementary operation performed by the operators involved in a particular process step (Figure 19), the multiple entries are aggregated into the duration of the process step considering labour overlapping. Also, the elimination of the cycle times that are either too short or too long - from operator or software inconsistencies - reduced the amount of outputted cycle times.

Aircraft	Part Description	Main Technologies	Output Cycle Times
A	Skin 1	ATL	1688
A	Skin 2	ATL	1648
A	Skin 3	ATL	1664
A	Skin 4	ATL	1653
B	Skin 1	ATL	43
B	Skin 2	ATL	52
B	Spars 1	AFP	201
B	Spars 2	AFP	130
C	Spars 1	ATL+AFP+HD	116
C	Spars 2	ATL+AFP+HD	100
C	Skin 1	ATL+HD	108
C	Skin 2	ATL+HD	78
C	Skin 3	ATL+AFP+HD	55
C	Skin 4	ATL+AFP+HD	53
Total			**7589**

Table 3 – Number of cycle time outputs by manufactured component from MATLAB script filtering, representing the final working data set for cycle times.

From Table 3, it stands out the significant difference between the number of outputs for aircraft's A components, compared to other components. This is mostly attributed to aircraft's A manufacturing program being much older than any of the other two, hence a larger number of its units had been produced until the moment when the data was collected (May 2019). Also, it should be noted no distinction between left or right components is made in the description, as in fact, they are mirror images of each other, with equal manufacturing processes. Therefore, the data sets of either left or right components were combined.

3.3.2. Non-Qualities

Depending on the manufacturing step, there is always a probability of any sort of defects to occur. While some might not be significant, others might impact not only the component integrity but also the process performance and component cost, as extra resources may be needed, and extra work must be performed to address the issue. Another important element is the point in time the defects are uncovered and identified. The further the component has progressed in its manufacturing process, the more expensive a defect becomes. If for example, a miss-aligned ply is placed during a hand-layup cycle in the initial steps of the manufacturing process and is only detected in the last step of NDT, it could potentially mean that all the labour and resources allocated until that final evaluation step could go to waste if the component has to be scrapped. However, if this issue were uncovered much earlier in the process, a significant portion of these costs are avoided (Figure 22).

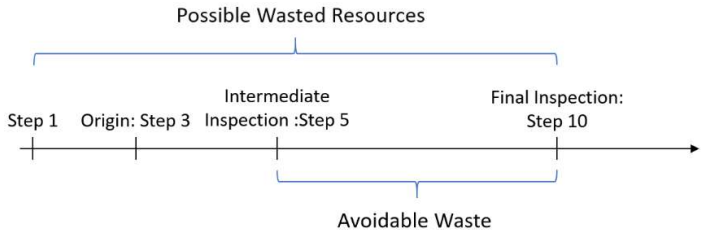

Figure 22 – Avoidable wasted resources by implementing intermediate inspection

Manufactures understand this dynamic and mitigate its effects by implementing intermediate inspections throughout the manufacturing process, which opens a chance for defects to be detected and addressed, before moving forward to more critical steps where the impact in production costs would be greater.

In this study, we make use of data collected across intermediate inspection operations as well as final NDT inspections. From the initial set of nearly seven hundred parts, there were † counts of non-qualities, that were possible to trace back to their origin and detection steps in each of the manufactured parts (Figure 23).

These † non-qualities are divided into 4 different categories: Scrap, Repair, Rework and Use as Is (Figure 24)

- Scrap: It is the most severe of non-qualities as this means that the defect encountered is beyond repair and the complete component is lost.
- Rework: A rework is ordered when the defect (normally a common one) can be corrected and the solution is already set in place to solve it. The affected area is reworked following the established procedure.
- Repair: Similar to a rework, it is possible to salvage the component, but additional analysis has to be made to evaluate the extent of the damage and repair, thus incurring additional indirect costs before being able to develop the proper rework procedure.

† Total number of non-qualities has been omitted to respect confidentiality.

- Use as Is: It is the most common of non-qualities and the least impactful, as no further action has to be made and the component can move forward in the manufacturing steps.

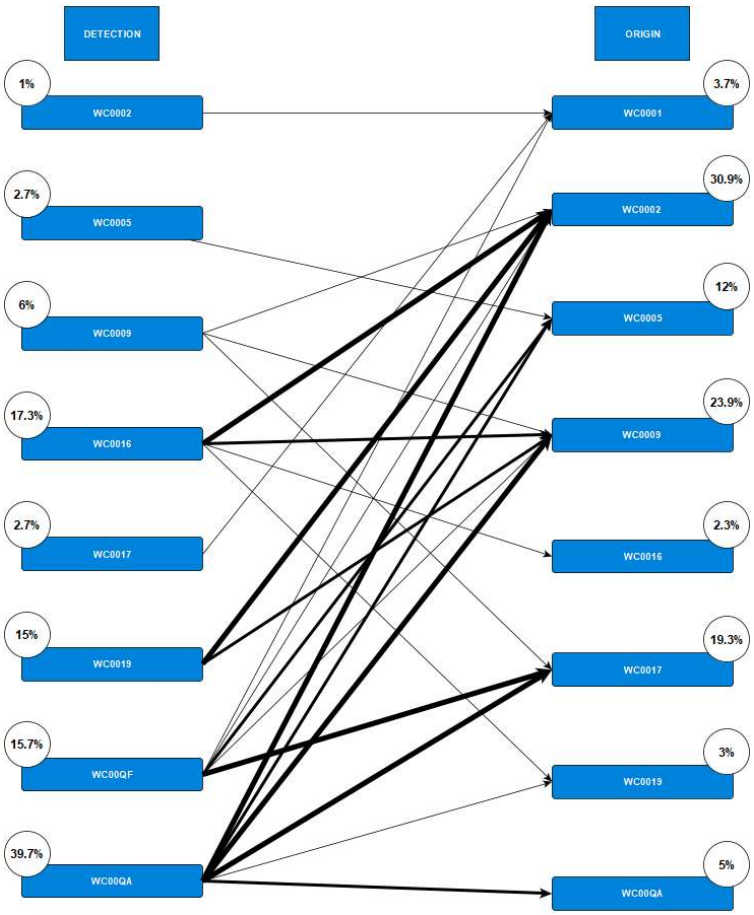

Figure 23 – Aircraft A components non-qualities origin and detection distribution. Wider arrows represent a bigger weight of non-qualities assigned from the detection to the origin center. Percentages represent the proportions of overall non-qualities occurrences at each "step" for that specific component.

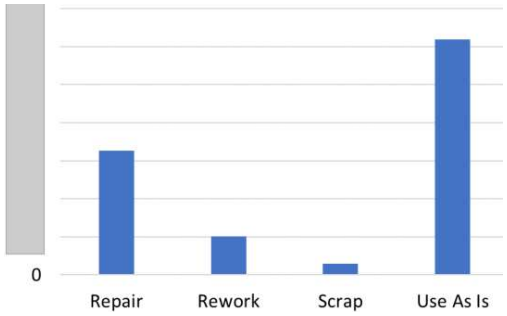

Figure 24 – Non-qualities total occurrences by category. (To respect confidentiality, the total number of occurrences has been omitted)

It is worth noting that, to finish nearly seven hundred good parts (Table 2), it was necessary to launch more into production, since some of them are scrapped during the process. This is an important observation, as yield determination should take into consideration the set of initiated parts that ended up as scrap.

At first, when a non-quality is detected, a preliminary evaluation is performed to assess its condition. This evaluation results in the component being tagged into any of the four different categories. However,

this does not imply that this first assessment is exempt from changes as shown by the sanky diagram in Figure 25. A component with an initial flaw identified as Use as Is, could evolve into a more severe and unanticipated problem further down the production line, hindering the process and issuing the need for a repair or rework, or, at the worst possible case a scrap.

Figure 25 – Sanky diagram representation of non-qualities category changes and final classification of "non-quality" parts. (Information is omitted to respect confidentiality.)

Conversely, in the case of an initially issued repair or rework, there is the possibility for the procedure to be either successful or unsuccessful. If it is successful, the component status is updated and cycles through its remaining manufacturing stages, as for the later, it opens again the possibility for a second attempt of repair/rework, unless there is substantial damage that could lead to the inevitable scrapping of the part.

In short, no initial decisions regarding the status of a non-quality are final, with the exception for scrap. This exchange between decisions, results in additional non-quality occurrences, with each interaction having a different cost impact that must be accounted for.

3.3.3. Materials and Equipment

Another major cost driver in manufacturing is the raw materials used, as well as the equipment and manufacturing tools that must be acquired in order to produce the composite's components. For the available set of 20 parts (Table 1), it was possible to collect the various material quantities and respective average unit prices for each part, as illustrated in Table 4 for aircraft's A skin 4.

Material Description	Quantity [m^2]	Price [$/$m^2$]
Copper Mesh	7.82	
Glass Fiber Epoxy Prepreg	12.28	
Carbon Fiber Epoxy ATL tape	92.76	
White polyvinyl film	1.493	

Table 4 – Example of material data for aircraft A skin 4. (The remaining parts' material data, as well as the unit costs have been omitted in order to respect confidentiality)

Detailed geometric data about the tooling used in each parts' manufacturing process was also collected, *e.g.* dimensions and surface area. For a company, acquiring manufacturing toolings such as molds and

jigs represents an additional expense that is diluted on the number of parts produced. Knowing this, a summary of each parts' tooling acquisition cost was also provided by the company so that they could be considered in the cost analysis (Annex 1). Minor and secondary tools such as portable automated cutters, x-cutters, scissors, or spatulas used throughout the manual steps of the processes were unaccounted, as their costs are orders of magnitude lower than other previously mentioned tools.

Lastly, acquisition costs for the equipment and machinery used throughout the process were also collected. These include the cold storage units, automated material cutting table, ATL, AFP, Autoclave, Hot-Drape Forming, CNC trimming machine as well as NDT equipment (Annex 1).

3.3.4. Geometric and Complexity Part Data

Part specific data, CAD files and drawings (Figure 26) of the parts were equally made available by the company, so that information about the geometric properties could be collected, namely the surface area of the part in contact with the mold, its volume, and perimeter that encompass both the outside contour and inner cut-out openings that serve as access points during assembly tasks (Table 5).

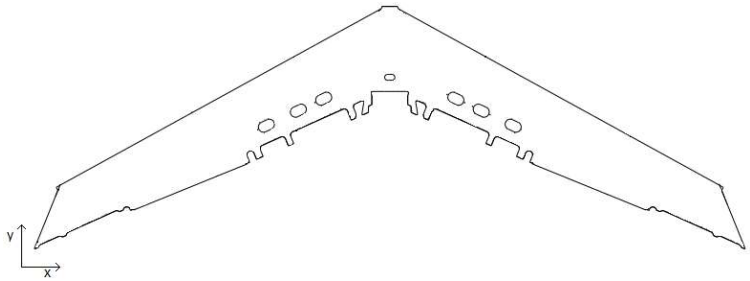

Figure 26 - 2D drawing of aircraft A skin 4

Area [m^2]	4.51
Volume [m^3]	0.014
Perimeter[m]	18.18
Dimension X [m]	6.81
Dimension Y [m]	2.29

Table 5 - Geometric properties of aircraft A skin 4

Part complexity data is considered throughout the literature to have an impact on process step times [25]. ATL and AFP are the most affected, as the part geometry influences the operation layup rates, having a high impact on cycle times. Hence, geometry complexity indicators are usually taken into consideration to calculate these rates, as part area, or any other simple geometric property alone is not able to accurately explain and define layup rates and thus estimate the cycle time.

Therefore, three complexity metrics were defined and computed, with the purpose of capturing the relation between manufacturing times and geometric properties, increasing the information that characterizes each part and allowing a better estimation of operations cycle times. One of these complexity metrics is defined in respect to the integration of stringers or secondary parts to the primary part, which is regarded as an increase to the complexity of the manufacturing process. This metric is calculated as in Equation (3), where $N^{\underline{o}}{}_{stringer}$ is the number of stringers integrated into the primary part, $A_{constrg}$ is the contact area between the stringer and the primary part, and A_{pp} is the surface area of the primary part in contact with the mold surface.

$$C_{int} = 1 + N^{\underline{o}}{}_{stringers} \times \frac{A_{constrg}}{A_{pp}} \tag{3}$$

The other two metrics are retrieved from 2D technical drawings, available for each part at two different views. A top view, in the XY plane (Figure 26), and a side view, in the XZ plane. From these two views it is possible to extract the complexity metric of the part contour (C_{xy}) and its overall curvature (C_{xz}), respectively. In order to do so, an algorithm was implemented in MATLAB in which the component's 2D shapes are analyzed and a complexity metric is defined based on Lempel-Ziv complexity [60]. The algorithm's objective is to measure the part contour complexity since it can be directly tied to specific operations cycle times (*e.g.* shape contour directly impacts trimming cycle times). The algorithm starts by reading the part's image and transforming it into a series of points (Figure 27a). Then, this initial set of points is reduced to the essential number of points that represent the geometry of the part (Figure 27b), eliminating those that do not add relevant information, thus reducing the computing power needed to perform the complexity measurements. Visual confirmation of the final result is performed, to ensure that no information from the original shape has been lost that could otherwise compromise the final result.

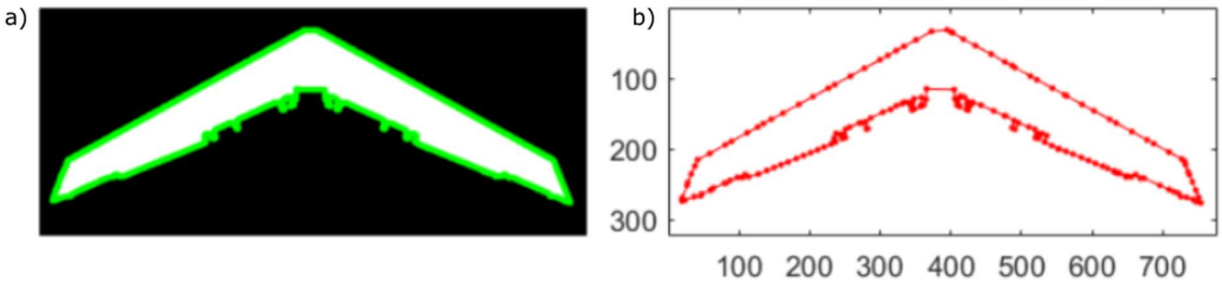

Figure 27 - a) Original 2D shape contour with 1750 points. b) Simplified 2D shape with 175 points

Then, angle measurements between the normal vector to the part's contour and the horizontal are made along the contour points. Lastly, the complexity metric is obtained by employing the Lempel-Ziv complexity to the array of angle measurements, and the result grows as the sequence grows in length and irregularity, in this case, the angle variations between neighboring points.

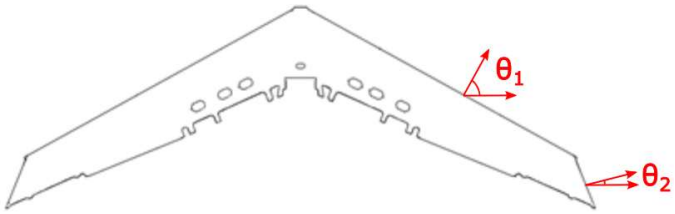

Figure 28 – Example of local points angle measurements between countor normal vector and horizontal reference.

This method was applied to every component, and a summary of each part geometric properties, as well as its complexity metrics, are presented in Annex 1 .

3.4. **Process-Based Cost Model**

After understanding the different manufacturing processes and having gathered data on relevant cost drivers, the challenge, then, is how to model and represent the interrelationships between part and process information and part final cost, in order to achieve a tool that allows cost estimation during a process planning stage. Process-Based Cost Models (PBCM) are one adequate approach that has been fairly studied in the literature, not only for their ability to calculate costs based on technical relations, empirical estimates, best guesses and literature input data, but also as a tool for strategic analysis of the impact of design, material, and process choices on the product final cost.

The following sections detail the cost model structure employed, and the analytical models developed to combine these different variables across the different manufacturing steps into a cost metric.

3.4.1. PBCM Concept and Structure

One of the interests of using cost as a basis for decision making is the simplicity and tangibility of the metric. The notion of cost is a part of everyone's day-to-day experience, therefore serving as a well-established metric for evaluating process and product alternatives. It is often necessary to make decisions in terms of process and product, long before the consequences of these choices are known, hence a strong effort has been driven to devise methods to predict its economic consequences.

Process-Based Cost Models follow a structure decomposed into three interconnected models: a technical process model, a production operation model, and a financial accounting model (Figure 29).

1) At the core of any manufacturing process, there is a set of technologies, employed to accomplish productions that have requirements in terms of equipment, labor, materials, and energy. The process model overviews the set of operations that have to take place within the processes, structuring the problem and underlying the technical needs to achieve the desired goal, providing an answer to the question of "What is needed?".
2) While the process model deals with the identification of what is needed, the operations model aims at determining the amount of resources used and consumed - including the operational inefficiencies - in order to achieve the desired production output.
3) After the enumeration of needs and respective quantities have been carried out, the financial model converts these amounts of resources into their economic costs, by simply accounting the factors required by their purchase price.

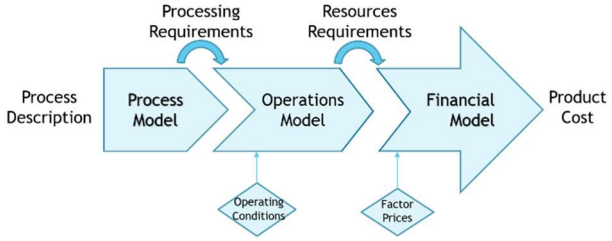

Figure 29 - Process based cost model decomposition

In the developed models, production costs are calculated on a per year basis and are divided into two categories: variable and fixed costs (Table 6). Fixed costs are usually calculated based on annual equivalent rents associated with the capital investments in equipment, tooling, and building, and are therefore independent of the production volume. This means that as more parts are produced, the lower the per unit cost, as there are more parts to dilute the costs. However, depending on the accounting method employed by the company, this last statement does not always hold and will be discussed further into this work.

Conversely, annual variable costs are dependent on the production volume, as they are mostly associated with the materials, energy, and labour. They increase with annual production volume but are kept constant on a per unit basis, as they are the same between equal components.

Variable Cost	Fixed Cost
Material Cost	Equipment Cost
Energy Cost	Tooling Cost
Labor Cost	Building Cost
Scrap Cost	Fixed Overhead Cost

Table 6 - Variable and fixed cost in PBCM

3.4.2. PBCM Requirements and Cost Estimating Relations

The preliminary overview of the processes – discussed in section 3.1 - is the first step in process cost modelling, as it allows for the identification of the major cost drivers and technological needs (*e.g.* equipment, tooling, materials, time) in each of the process steps, while at the same time filtering out minor steps that otherwise, would only add complexity to the analyses for marginal gains in results credibility.

Operational Model

The materials and time requirements drive almost every quantification of resource consumption or usage included in the operational model.

To quantify the required raw materials it is necessary to include the materials that are integrated into the final parts together with the materials losses along the process. There are two types of material losses: scrap and technical scrap. Technical scrap are material losses inherent to the technologies involved. One example would be the excess material that is deposited extending over the edges of the part surface, or any material cutting operations that are required to adjust the material to the correct dimensions, resulting in losses of material. On the other hand, scrap accounts for material losses due to the parts in the process that, facing some sort of problem during its production, have to be discarded.

In order to account for the effects of these issues, a mass balance is performed across every step, to determine the amount of materials required and the work-in-process parts passing through each step to achieve the expected production volume (Equation 4). In its simplest form, the input of process step $i + 1$ is the output of process step i (Figure 30), and it is constructed backwards, with the required production

volume as the output in the last step leading to the material input in the first process step, accounting for the material losses in between.

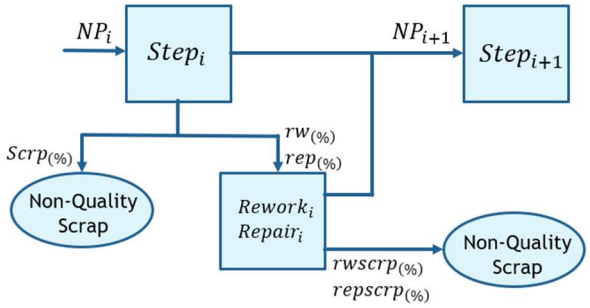

Figure 30 - Framework of non-quality losses in process step i.

$$NP_i = \frac{NP_{i+1}}{1 - (Scrp_i + rw_i \times rwscrp_i + rep_i \times repscrp_i)} \tag{4}$$

In Equation 4, $Scrp_i$, rw_i and rep_i are the percentages of scrapped, reworked, and repaired parts from the overall volume of production in process step i, respectively. Meanwhile, $rwscrp_i$ and $repscrp_i$ are the percentage of parts that do not pass rework or repair *i.e.* the number of parts from the total volume of production, with some sort of defect which the operations of rework or repair were not able to fix.

As a result, material quantities for each of the j different materials, and material losses ($Scrap_i$) can be directly calculated from Equation (5 & 6), respectively, at every *i*th process step.

$$Mat_{quant\ i,j} = Mat_{quant\ j\ per\ part} \times NP_i \tag{5}$$

$$Scrap_i = \sum_{j=1}^{n} (Mat_{quant\ i,j} \times \rho_j) \times NP_i \times (TechScrap + scrp_i + rw_i \times rwscrp_i + rep_i \times repscrp_i) \tag{6}$$

Where ρ_j is the material area density in (kg/m^2), so that material losses are accounted in kg.

In the steps of manual labour, there is usually the application of materials such as peel-ply, breather, and vacuum bag. These will fall into a category called consumable materials and their expenditure is assumed to be equal to the part surface area upon which they are applied.

$$Consumable_{quant\ i} = Part\ Surface\ Area \times NP_i \tag{7}$$

Also, knowing that some parts may need reworks or repairs, the required materials to perform these activities are included in the analysis to account for their costs. Each j material is calculated separately, as a small percentage of its initial required quantity.

$$Rework\ material_{i,j} = Mat_{quant\ i,j} \times rw_{i\ \%} \times Mat\ req\ in\ rework_{\%} \times NP_i \tag{8}$$

$$Repair\ materials_{i,j} = Mat_{quant\ i,j} \times rep_{i\ \%} \times Mat\ req\ in\ repair_{\%} \times NP_i \tag{8}$$

The equipment time usage necessary to accomplish the required yearly production volume is another important cost driver. It should be noted that in a factory environment, equipment time can be split into available and unavailable time.

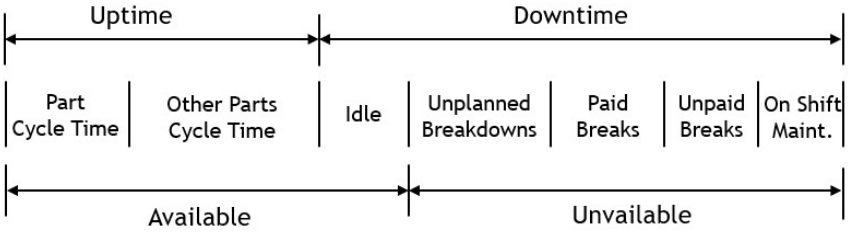

Figure 31 - Factory environment equipment utilization times

Unavailable time accounts for the time parcels in which it is not possible to produce parts, due to unplanned breakdowns, workers paid and unpaid breaks, or on-shift maintenance (Figure 31). This time, associated with the idle time (equipment not working but available to work), corresponds to the total downtime.

In opposition, the uptime represents the portion of time when the equipment is operational, and the production is taking place. In an environment where the same equipment can be used to produce different components (non-dedicated equipment), this uptime can be further divided to account for the time consumed for each of the different components. Whether the company assigns the according time consumptions to each individual part or, the total uptime divided by the total number of parts produced, is the difference between activity-based costing (ABC) and absorption costing, respectively, which are two of the most common accounting methods. In this study, we employ the former, by determining the allocation of equipment for each part as in Equation 9.

$$Alloc_i = \frac{Treq_{\,i}}{Uptime_i} \tag{9}$$

$$Treq_i = CT_i \times NP_i \tag{10}$$

$$Uptime_i = Days\ per\ year \times 24\,h - (Idle + Unpl.Breakdowns + Paid\ Breaks + Unpaid\ Breaks + On\ Shift\ Maint) \tag{11}$$

Where $Treq_{\,i}$ (Equation 10) is the total cycle time required in step i (CT_i) to achieve the targeted production volume (NP_i), and $Uptime_i$ (Equation 11) is the total operational time minus the aforementioned downtime at that same step.

This allocation, $Alloc_i$, represents the percentage of uptime at step i that is dedicated to the manufacturing of a specific part and influences the equivalent annual cost of the equipment and building associated to that part only. Under this approach, equipment costs and building costs are no longer viewed as a fixed cost, as they are in fact, no longer independent from production volume, meaning that an increase or decrease in the latter, will no longer influence the cost per unit. Nevertheless, we will keep referring to equipment and building costs as fixed costs to stay coherent with the aforementioned notation (Table 6).

Financial Model

At the core of the financial model of the PBCM, is a set of relations responsible for translating the requirements and necessary quantities defined for consumptions (materials and energy) and resources time usage (labour, equipment, space, tooling) into costs. The sum of all cost items results in the component final cost.

Material Cost

Knowing the necessary quantities of each material across the multiple manufacturing steps for the annual production volume, it is then possible to multiply these quantities by their specific acquisition costs and obtain the costs of materials for the intending production volumes.

The cost of the part raw materials can then be calculated by Equation (12), in which $Cost_{sqm\ i,j}$ is the specific cost of each material *j* (cost per unit of area):

$$Mat_{cost\ i} = \sum_{j=1}^{n} Cost_{sqm\ i,j} \times Mat_{quant\ i,j} \tag{12}$$

Consumables and additional materials needed for rework and repair operations are accounted separately, but then later added as part of material expenses.

$$Consumable_{cost\ i} = Cost_{sqm} \times Part\ Surface\ Area\ \times NP_i \tag{13}$$

$$Rework\ material\ _{cost\ i} = \sum_{j=1}^{n} Cost_{sqm\ j} \times Rework\ material_{i,j} \tag{14}$$

$$Repair\ material\ _{cost\ i} = \sum_{j=1}^{n} Cost_{sqm\ j} \times Repair\ material_{i,j} \tag{15}$$

Unlike metal materials that could be recycled and provide an additional source of revenue, in composites, material losses need to be disposed of, incurring additional costs during that process. These costs are determined by multiplying the material losses (in weight) by the cost of disposal per kilogram of materials ($Cost_{kg\ i}$).

$$Scrap_{cost\ i} = Cost_{kg\ i} \times\ Scrap_i \tag{16}$$

Labour Cost

Labour cost can be defined as

$$Labour_{cost\ i} =\ CT_i \times n^{o}w_i\ \times ded_i \times w_{\$\ i} \times NP_i \tag{17}$$

where $n^{o}w_i$ and ded_i are the number of workers and the percentage of their dedication to the process step i, $w_{\$\ i}$ is the average wage per hour, and CT_i is the cycle time of that process. In processes involving

machine operations, cycle time includes part loading, unloading, and inspection together with the machine operation time itself.

Energy Cost

Energy cost is the power consumption of the equipment used in each manufacturing step i (PC_i), multiplied by the energy unit cost (EC) and the total time required to achieve the desired production volume.

$$Energy_{cost\,i} = PC_i \times EC \times NP_i \times CT_i \quad (18)$$

Machine, Tooling and Building Fixed Costs

For the equipment, facilities, and tools, initials investments must be made. To account the impact of these investments in the manufacturing costs across the multiple years of operations, these initial investments are discounted into a set of annual payments, called equivalent annual cost (EAC), that translate the annual cost of owning, operating and maintaining an asset over its life span. It is a useful measure often used by companies to compare the cost-effectiveness of different assets.

The initial investments can be determined by the following equations:

$$Machine\ investment_i = Machine\ aquisition\ cost_i \times nºunits_i \quad (19)$$

$$Tooling\ investment_i = Tools\ aquisition\ cost_i \times nºunits_i \quad (20)$$

$$Building\ investment = (1 + Idle\ space_{\%}) \times spreq \times build_{cost} \quad (21)$$

$build_{cost}$ represents the infrastructure cost per unit of area, and $spreq$, the area required for the manual and/or automated activities to take place. These investments (I_j) are then translated to their respective equivalent annual costs as

$$EAC_j = I_j \frac{(1+r)^{n_j} \times r}{(1+r)^{n_j} - 1} \quad (22)$$

where n_j, is the useful life in years of asset *j*, and r its discount rate.

Knowing each of the respective EAC, it is possible to calculate the machine, tooling, and building costs.

$$Machine\ Cost_i = EAC_j \times (1 + Maintenance\%) \times Alloc_i \quad (23)$$

$$Tooling\ Cost_i = EAC_j \quad (24)$$

$$Building\ Cost_i = EAC_j \times Alloc_i \quad (25)$$

Machine costs also account for maintenance, determined as a small percentage of the EAC of the machine. Both building and machine costs are multiplied by the allocation in order to account for the portion of individual cost incurred from each part's volume of production, for using the equipment and space associated with the related step where the operations took place, as previously discussed. In opposition, one should note that tooling is part-specific, therefore its cost is fully allocated to the respective part.

Fixed Overhead Costs

Overhead costs are associated with the engineering support or any other form of indirect expense to the manufacturing process, and are determined as an additional percentage of direct labour costs.

$$Fixed\ Overhead\ Costs_i = Labour\ Costs_i \times (1 + Overheads_{\%}) \quad (26)$$

Final Costs and intermediate model verification

Under the described approach, five different PBCMs were created in EXCEL spreadsheets, each tailored to a specific manufacturing process and set of technologies. In each model, every block in the process flowcharts corresponds to a process step, where both variable and fixed costs are calculated employing the aforementioned cost relations, using the gathered data (section 3.2) as inputs (Figure 32).

Model inputs are divided into two main groups. Global inputs that are transversally used across all PBCM (Table 7), and process step specific inputs that correspond to the necessary quantities in each step, such as the number of workers and machines to perform that particular step (Table 8).

Annual Production Volume	parts/year
Days per Year	days/year
Unit Energy Cost	$/kWh
Wage	$/h
Discount Rate	%
Equipment Life	years
Building Unit Cost	$/m2
Building Life	years
Production Life	years
Idle Space	%

Table 7 - Process global inputs

Workers	units
Dedication	%
Floor Space	m2
Machine Units	units
Aquisition Cost	$/unit
Energy Consumption	kWh
Cycle Time	h
Maintenance	%
Overheads	%

Table 8 - Process step specific inputs

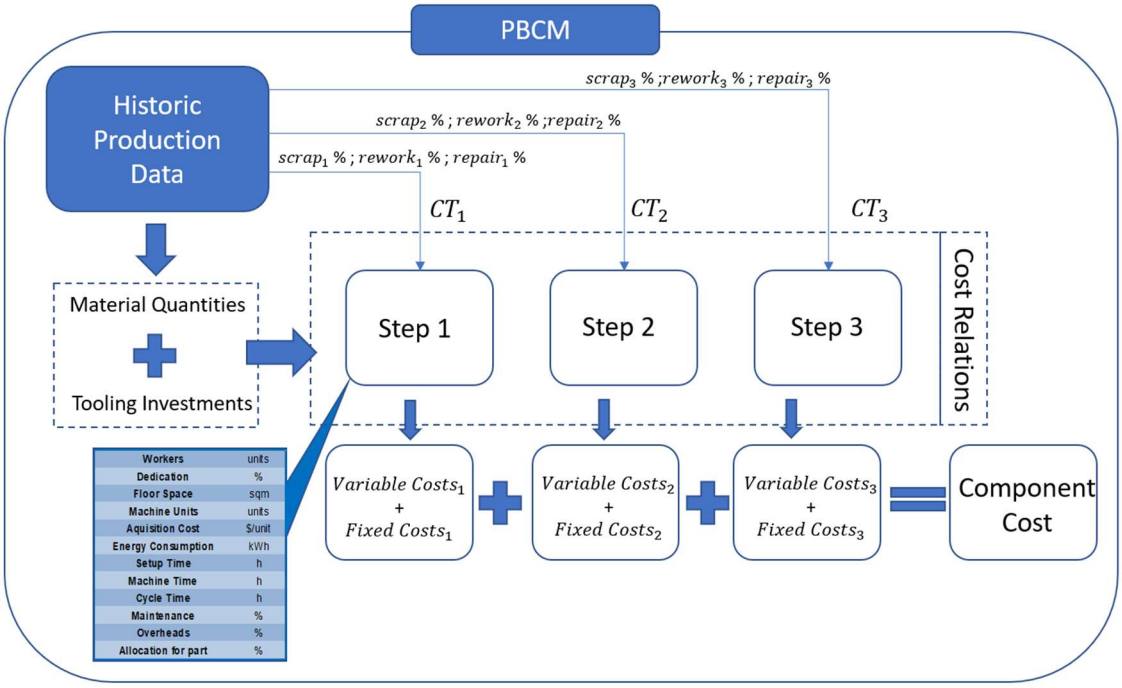

Figure 32 – PBCM cost estimation flowchart

The component final cost is obtained by adding each cost item across the multiple process steps. The results are plotted in Figure 33. An initial cost model evaluation was performed by comparing the models' estimations with the manufacturer's cost accounting results, which are assumed as the true/real manufacturing costs of each component. As a first model iteration – hereinafter referred to as α-PBCM – the obtained results display a good approximation to real costs, with a mean average percentage error (MAPE) of 15.1% and normalized root mean square error (NRMSE) of 4.3%.

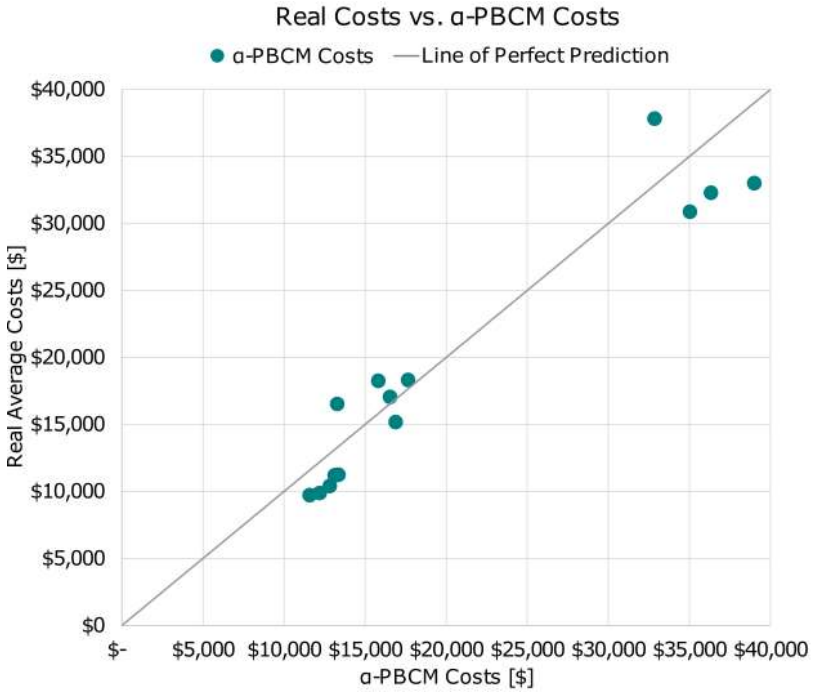

Figure 33 - Scatter plot of each component cost result from the developed model (α-PBCM), compared to the real component cost average provided by the manufacturer.

This comparison serves as an intermediate gauging on the agreement between the two different models results – the company cost accounting and the PBCM based cost – and, in a way, ensures that a proper translation of manufacturing inputs into costs is being made by the developed cost relations.

Nevertheless, additional work must be performed to overcome one of the biggest challenges of these estimates when assessing the production costs of a new component at the very front end of its process design. Usually, some of the required inputs for these estimates are analogously determined using historical process data from a similar component. By doing so, the accuracy of the resulting data is highly dependent on the experience and knowledge of the estimation expert [43]. One should want to move away from this methodology, as biased inputs could significantly affect cost results of the final estimate. Thus, more appropriate methods should be employed, in order to attenuate many of the human fallibilities that could have a negative impact on the accuracy of the cost result. With the abundance of available data in this study - both in process historic data and in component specific data – the following research question arises (RQ): **Can techno-economic relations/regressions be constructed based on historical parts data with enough merit to be used in the cost estimation model of the new component?**

This question is addressed in the following chapters, along with one very important trait, often ignored in most cost estimation methods – process variability. Manufacturing processes do not always perform under the same conditions, leading to variations in cycle times that ultimately impact production costs. Still, these are often left unaccounted by most cost estimation practices. With the current model as it stands, there is also little chance to replicate these processes' variabilities in a timely manner.

However, it is possible to further develop the current model, and build additional modules that would allow for an automated replication of real process variations to be introduced. Consequently, cost results could, therefore, be an economic reflection of the physical process variability.

Moreover, cycle time, tooling costs, and material quantities are known to be dependent on the components' geometric properties. Based on historical data, relations between the components' geometric characteristics and cycle times, material quantities, and other cost items will be explored. The set of developed relations shall estimate the aforementioned quantities and feed the information to the cost model that ultimately estimates cost. Additionally, by basing the relations on geometry inputs - obtained at a conceptual level of process design – it is expected to enable an early cost estimation response, where it is most valuable.

4. Modelling Process Variability

Depending on the component - as previously stated - there are intrinsic characteristics that could lead to differences in the manufacturing processes that they undergo, resulting in changes in the equipment, tooling, and materials used. Also, no two equal components take exactly the same time or face the same problems, leading to significant cost differences that may be overlooked when estimating costs deterministically or based on a few production runs.

One of the main objectives of this work is, based on historical data, estimate cost considering (1) the introduction of the effect of process variability, retrieved from past data, in the different activities across the manufacturing processes, (2) and turning knowledge explicit through empirical relations, between part geometry and process requirements. In this way, future component estimates could be made regarding its processes' requirements, solely based on the new component specifications.

The following sections describe in further detail how, with the gathered data, it was possible to create the relations between part characteristics and process variables, such as cycle times, non-quality occurrence, tooling, and material costs.

4.1. Cycle Times as stochastic variables

The analyzed composite manufacturing processes are highly automated in critical tasks such as material lay-up and trimming through the use of computer numeric control equipment, but there is still a significant contribution from manual sources of labor, as even these machines need some level of human interaction. While the automated processes themselves perform at reproducible speeds, operators do not, and could arguably influence operations cycle times and consequently the final component cost.

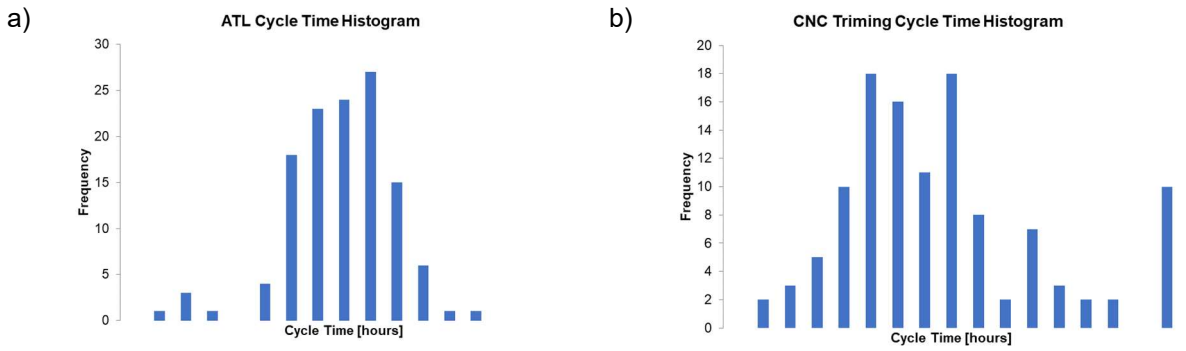

Figure 34 - a) ATL cycle times histogram; b) CNC trimming cycle times histogram. Samples obtained from past production runs of the same component. (Cycle time values have been omitted to respect confidentiality.)

Figure 34 a) and b) show two examples of gathered cycle times from past production runs in two different manufacturing steps for the same component. It is possible to observe a considerable variability in cycle times, with some significantly deviated observations representing the incorrect measurements described in section 3.3.1. These outliers are removed from the data samples, to minimize the introduction of bias

and error in subsequent analysis. The elimination was mostly supported on information gathered from the interactions with factory workers and engineers and their empirical knowledge on each individual step and component. Thus, the cleaned data set is assumed as representative of the cycle time behaviour and variations in every manufacturing process.

Probability functions are a common method to represent and describe stochastic variables in real-world data and industrial settings. Most commonly, data is interpreted and assumed as normally distributed, allowing for the obtainment of valuable information on processes performances and its variabilities [61]. To assume the normality of data, graphical exploration, and formal statistical tests are frequently used and necessary.

There are a significant number of these tests available, among the most common are the Shapiro-Wilk, Kolmogorov-Smirnov, and Anderson-Darling tests [62]. Performing the Anderson-Darling test at a 5% significance level returns that both samples are not normally distributed, with adjusted statistic (adstat) values above their respective critical values (cv) as shown in Table 9.

	ATL	CNC Triming
n (sample size)	124	117
adstat	0.998	5.685
cv	0.747	0.747

Table 9 - Anderson-Darling Normality Test Results on ATL and CNC Trimming cycle time data sets, for one of the manufacturer's components.

This test yields similar results across all other work centers data, where each component manufacturing operations take place. Thus, a different probability distribution method needs to be followed.

Beta and Triangular distributions are two methods that could be built based on the existing data samples and used to model historic cycle time data [63]. Triangular distributions pose as a more appealing method, given the simplicity in the estimation of its parameters [63]. A typical application consists in establishing a minimum (a) and maximum (b) parameters, and a most likely value (c), from the cycle time data samples.

The most likely value (c), is usually determined based on the median, which introduces less skewness to the data when compared to other methods based on the average. Equation 27 gives the value for *c* when the sample median (m) falls in the interval of $[b - \frac{b-a}{\sqrt{2}}, a + \frac{b-a}{\sqrt{2}}]$ [64].

$$c = \begin{cases} b - \dfrac{2(b-m)^2}{(b-a)} & m < \dfrac{a+b}{2} \\ a + \dfrac{2(a-m)^2}{(b-a)} & otherwise. \end{cases} \tag{27}$$

Given all three parameters, it is then possible, through Equations 28 and 29, to represent the probability density function (PDF) and inverse cumulative distribution function (INVCDF), respectively [65].

$$f(t) = \begin{cases} \dfrac{2(t-a)}{(b-a)(c-a)} & a < t < c \\ \dfrac{2(b-t)}{(b-a)(b-c)} & c \leq t < b. \end{cases} \tag{28}$$

$$F^{-1}(u) = \begin{cases} a + \sqrt{(b-a)(c-a)} & 0 < u < \dfrac{c-a}{b-a} \\ b - \sqrt{(b-a)(b-c)(1-u)} & \dfrac{c-a}{b-a} \leq u < 1. \end{cases} \tag{29}$$

Continuing with the two previous examples in Figure 34, and selecting the parameters a and b as the minimum and maximum values of the data set, respectively, enables the use of Equation 27 to calculate c (Table 10).

	ATL	CNC Triming
median (m)	7.58	6.15
a	4	2
c	8.27	5.77
b	10	11

Table 10 - Triangular distribution function parameters

These parameters (Table 10), are then applied to Equations 28 & 29, in order to generate the PDF and INVCDF, respectively (Figure 35).

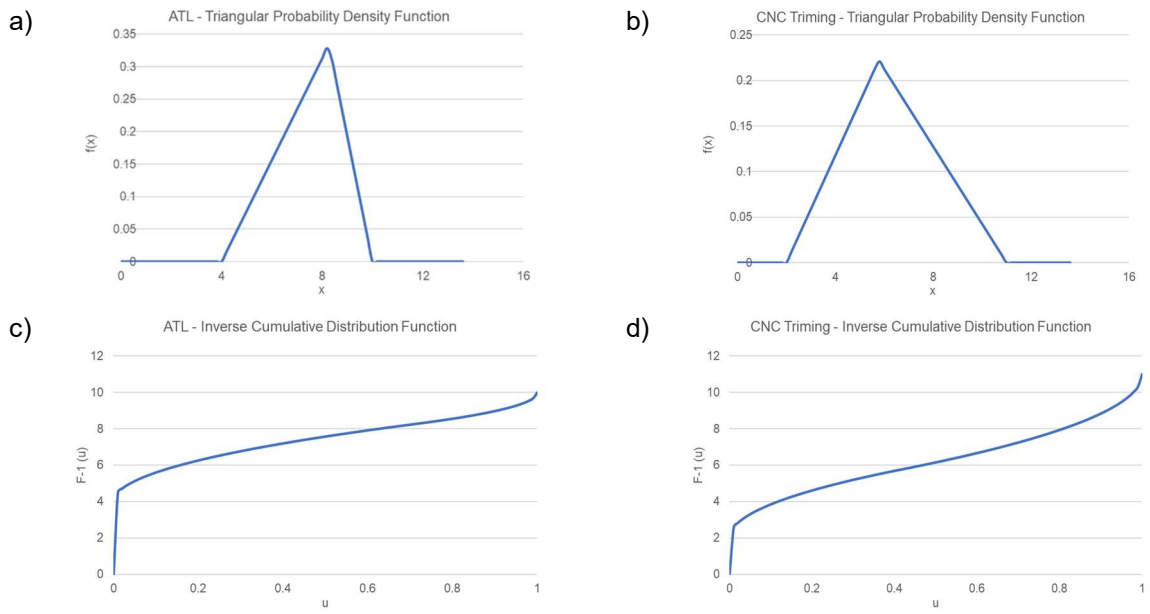

Figure 35 - a) ATL step triangular PDF b) CNC trimming step triangular PDF c) ATL step triangular INVCDF d) CNC trimming step triangular INVCDF

While the PDF represents the likelihood of a cycle time of a specific component to fall between given ranges, it is the INVCDF that holds the best practical use. By assigning random values u, between [0,1], it is possible to generate multiple cycle times, within the defined bounds [a,b], that follow the same behaviour as the original data and could replicate the variability of each manufacturing work center (Figure 36).

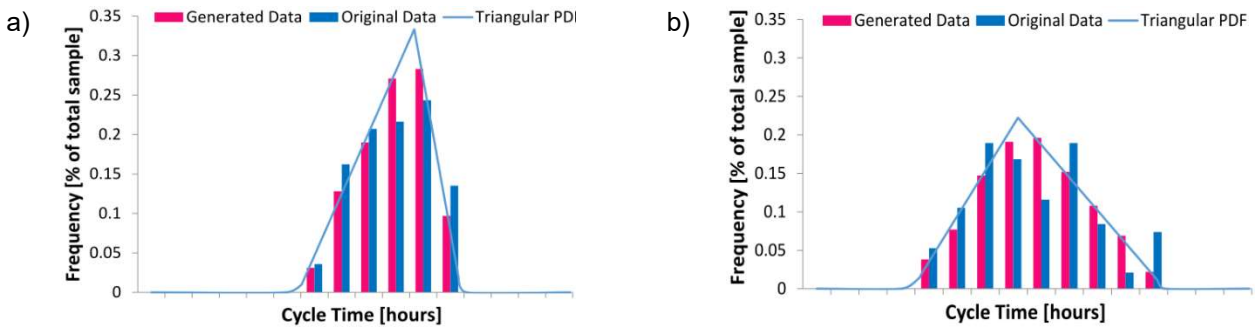

Figure 36 - Comparison between Original and Generated Cycle Times for: a) ATL; b) CNC Trimming (Cycle time values have been omitted to respect confidentiality.)

This method (Figure 37) can be applied across the multiple manufacturing steps of each component in order to generate synthetic cycle times that follow the historical patterns observed for the sample of 14 different parts. The next section presents the research done intending to understand how these cycle times are correlated with the parts geometric and technological characteristics.

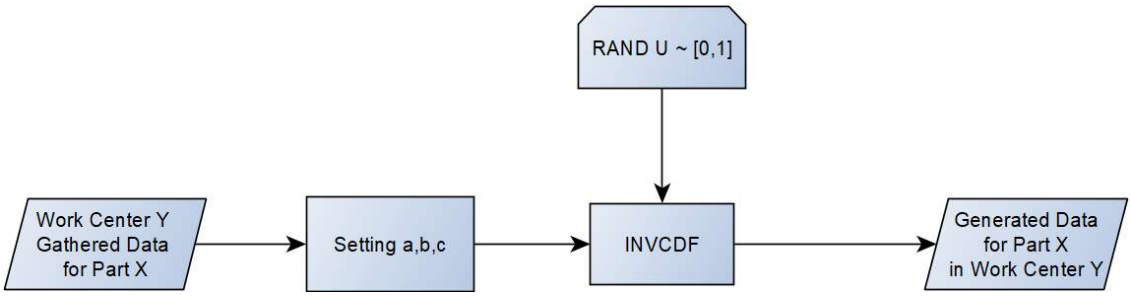

Figure 37 – General procedure to generate synthetic Cycle Times

4.2. Modelling Cycle Times as a function of part characteristics

Each component process step requires 3 parameters (a, b, c) to model its cycle time distribution. The current sample of components and their respective manufacturing steps resulted in 486 manually set parameters. This procedure is time consuming and is dependent on having past recorded data for a particular part. If a new component has to be produced it would most likely have different and unknown cycle times distributions. Thus, new parameters would need to be set, even if the part goes through the same process steps. In order to overcome these issues, and more easily take advantage of the historical data to determine cycle times of new components, new methods should be implemented.

It can be argued that a new component with a larger surface area should result in increased cycle times during the ATL layup process. Similarly, in the case of CNC trimming, a component with a larger contour/perimeter is also expected to take a longer time to finish its cycle – assuming constant feed rates - but by how much? The hypothesis that, depending on the type of operation, there is one or multiple component properties that clearly influence cycle times deserves to be investigated.

The challenge lies in identifying which of the component properties hold a stronger relationship with each process step cycle time. Ultimately, if the hypothesis is validated it will enable the estimation of the triangular distribution parameters to model the new distributions. This will allow the modelling of cycle times at each work center as a function of the chosen component geometric properties.

Simple Linear Regression (SLR) and Multiple Linear Regression (MLR) were used as a medium to assess the relationship strength- or if any correlation does exist - between the dependent and independent variables, *i.e*. cycle times and component properties, respectively. Additionally, in the future, it can be used to predict the dependent variable for new values (within the domain) of the independent variables. This is possible by writing the linear combinations of the determined β-coefficients that scale the independent variables x into the dependent variable y, resulting from the regression studies. Equation 30, represents a multiple regression model with k predictor variables $x_1, x_2, \dots, x_k$ (part characteristics) and an estimated dependent variable $\hat{y}$ (cycle time), where β_0 is the linear intercept when the independent variables are set to zero.

$$\hat{y} = \widehat{\beta_0} + \widehat{\beta_1} x_1 + \widehat{\beta_2} x_2 + \cdots \widehat{\beta_k} x_k \tag{30}$$

The process of finding the set of component geometric properties that better describes each work center cycle time is done by generating 100 synthetic cycle times - from the initially determined distributions - for each component whose manufacturing tasks are performed in that respective work center. These generated cycle times form the dependent variables working set, while the independent variables are their respective properties namely: component's surface area in contact with the mold surface (A), perimeter (P), volume (V), and complexity metrics (C_{XY}, C_{XZ}, and C_{INT}) (Figure 38).

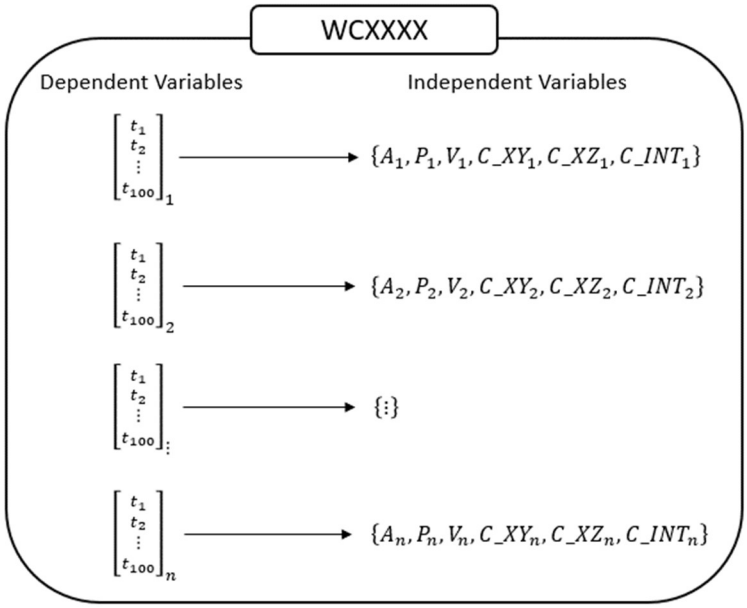

Figure 38 – MLR data assembly for each manufacturing work center. n stands for the number of different parts that go through the particular work center.

Surface area, perimeter, and volume are studied both separately and in combinations of two, while C_{XY}, C_{XZ}, and C_{INT}, are paired in combinations with the previous 3, contributing for 9 additional multiple

regression models. In total, the search is performed across 15 different models, for each work center within the studied industrial environment. For this set of potential models, the best subset of properties is identified based on three different criteria: R-squared (R^2), Pearson Coefficient (Pc), and p-value.

- R^2 is a measure that represents the proportion of a dependent variable variance, which is explained by the independent variables. This coefficient ranges from 0 to 1. In general, the higher it is, the better the current model replicates the outcomes of the dependent variable.
- Pc measures the correlation strength between the dependent and independent variables. It has a value between 1 and -1, where 1 indicates a perfect positive linear correlation, and -1 a perfect negative linear correlation.
- p-value tests whether the current model is statistically significant, by testing the null hypothesis (H_0). The null hypothesis (H_0) states that there are no useful linear relationships between the independent and dependent variables and that any correlation is most likely due to scattering and randomness of data. For a confidence level of 95%, if the p-value is less than 0.05, the null hypothesis is rejected.

Figure 39a) and Figure 39b) illustrate the scatterplots of SLR and MLR models, respectively, for the example of the cycle times of ATL stage using the component surface area (A) and C_{INT} as independent variables.

a)

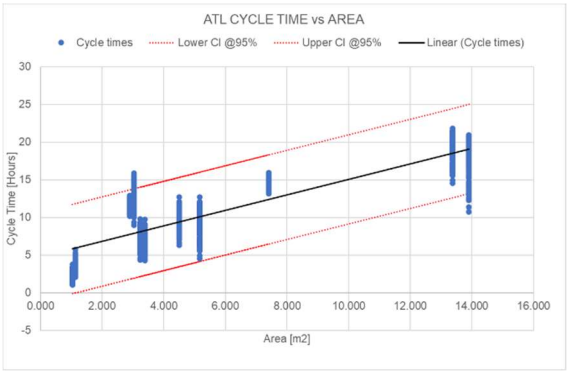

b)

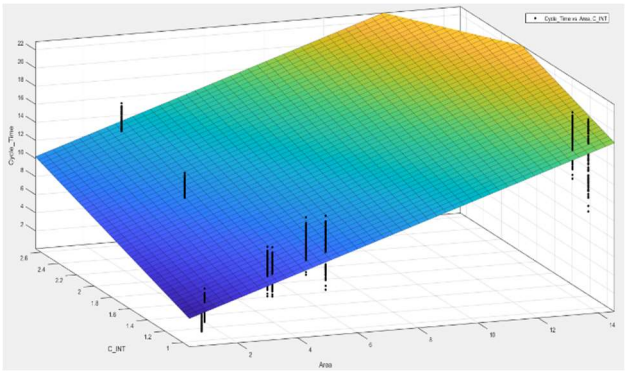

Figure 39 - a) ATL cycle times as a simple linear regression of parts area; b) ATL cycle times as a multiple linear regression of parts area and C_XY.

Despite both of these models holding statistical significance, considering the low p-values (Table 11), the one that considers as independent variables the area and the complexity metric is superior. This additional metrics ($x_2 = C_{Int}$) resulted in an increase of 11.4% and 21,6% in Pc and R^2, respectively, pointing to a better fitting of cycle times.

	x_1=Area	**x_1=Area, $x_2=C_{Int}$**
Pc	0.82	0.93
R^2	0.68	0.87
p-value	2E-273	0

Table 11 - Comparison between SLR and MLR fitting criteria

This same analysis was performed across each work center for the set of 15 models (Table 13) in order to identify the independent variables that demonstrated the stronger correlations. The best fits of each work center are recorded in Table 12.

Work Center	Sample Size	Independent Variables		Goodness of fit	
		x_1	x_2	Pc	R^2
WC0001	1400	V	C_{XZ}	0.43	0.18
WC0002	1100	A	C_{INT}	0.93	0.87
WC0003	600	A	C_{XZ}	0.74	0.55
WC0004	400	V	C_{XZ}	0.32	0.1
WC0008	900	A	V	0.72	0.53
WC0017	1400	A	C_{INT}	0.91	0.84
WC0006	900	V	C_{INT}	0.52	0.27
WC0009	1400	P	C_{INT}	0.83	0.69
WC0016	1400	A	C_{XY}	0.88	0.77
WC0018	1400	P	C_{INT}	0.9	0.82
WC0019	1400	P	C_{INT}	0.83	0.69
WC00QF	1400	P	C_{INT}	0.66	0.43
WC01MD	1000	V	C_{XY}	0.68	0.46
WC00QA	600	A	C_{XY}	0.97	0.94

Table 12 – Independent variables best fit of cycle times multiple linear regression for each work center.

Interestingly, it can be observed that almost every work center's best fit is a linear combination of a geometric property and a complexity metric (Table 12). Also, in most of the analysed cases, the pairing between the two geometric properties did not significantly contribute to an increase in the overall precision of the model. In statistical analysis, there is often the risk of collinearity between predictor variables *i.e*. when two variables express a linear relationship between themselves. Because most geometric shapes properties are correlated – even if not linearly – the combination between two of them contributes very little to a better fitting of the models, as observed, in Table 13.

On the other hand, complexity metrics do not face the same problems of correlation, and thus, when paired with one of the geometric properties, they positively add relevant information to the models, resulting, in some cases, in increases up to 87% in R^2 and 98% in Pc values when compared with the simple regression of that geometric property alone.

WORK CENTER		x_1=A	x_1=P	x_1=V	x_1=A; x_2=V	x_1=A; x_2=P	x_1=V; x_2=P	x_1=A; x_2=C_{XY}	x_1=A; x_2=C_{XZ}	x_1=A; x_2=C_{INT}	x_1=P; x_2=C_{XY}	x_1=P; x_2=C_{XZ}	x_1=P; x_2=C_{INT}	x_1=V; x_2=C_{XY}	x_1=V; x_2=C_{XZ}	x_1=V; x_2=C_{INT}
WC0001	Pc	0.10	0.13	0.05	0.17	0.15	0.23	0.35	0.41	0.24	0.35	0.39	0.22	0.33	**0.43**	0.24
	R^2	0.01	0.02	0.00	0.03	0.02	0.05	0.12	0.17	0.06	0.12	0.15	0.05	0.11	**0.18**	0.06
WC0002	Pc	0.82	0.76	0.79	0.86	0.82	0.79	0.82	0.83	**0.93**	0.79	0.79	0.90	0.76	0.78	0.92
	R^2	0.68	0.57	0.62	0.74	0.68	0.62	0.68	0.69	**0.87**	0.63	0.63	0.81	0.58	0.60	0.84
WC0003	Pc	0.51	0.51	0.49	0.51	0.51	0.51	0.62	**0.74**	0.67	0.53	0.74	0.49	0.68	0.73	0.55
	R^2	0.26	0.26	0.24	0.26	0.26	0.26	0.38	**0.55**	0.44	0.28	0.55	0.24	0.46	0.54	0.30
WC0004	Pc	0.14	0.22	0.16	0.30	0.16	0.22	0.33	0.33	0.15	0.29	0.18	0.16	0.33	**0.32**	0.22
	R^2	0.02	0.05	0.03	0.09	0.03	0.05	0.11	0.11	0.02	0.09	0.03	0.03	0.11	**0.10**	0.05
WC0008	Pc	0.67	0.56	0.65	**0.72**	0.67	0.65	0.67	0.67	0.67	0.66	0.65	0.65	0.57	0.58	0.57
	R^2	0.44	0.32	0.43	**0.53**	0.45	0.43	0.45	0.45	0.44	0.44	0.43	0.43	0.32	0.34	0.33
WC0017	Pc	0.64	0.50	0.58	0.76	0.64	0.58	0.66	0.65	**0.91**	0.58	0.59	0.89	0.50	0.54	0.54
	R^2	0.41	0.25	0.33	0.58	0.42	0.34	0.43	0.43	**0.84**	0.33	0.35	0.80	0.25	0.29	0.29
WC0006	Pc	0.33	0.36	0.21	0.46	0.36	0.41	0.48	0.48	0.33	0.48	0.24	0.29	0.48	0.37	**0.52**
	R^2	0.11	0.13	0.04	0.21	0.13	0.17	0.23	0.23	0.11	0.23	0.06	0.08	0.23	0.13	**0.27**
WC0009	Pc	0.37	0.18	0.37	0.76	0.37	0.57	0.40	0.38	0.82	0.37	0.37	**0.83**	0.19	0.19	0.80
	R^2	0.14	0.03	0.13	0.58	0.14	0.33	0.16	0.14	0.67	0.14	0.14	**0.69**	0.03	0.04	0.64
WC0016	Pc	0.71	0.71	0.73	0.71	0.73	0.73	**0.88**	0.75	0.71	0.83	0.78	0.74	0.83	0.73	0.74
	R^2	0.50	0.50	0.53	0.51	0.54	0.54	**0.77**	0.57	0.51	0.69	0.60	0.55	0.69	0.53	0.55
WC0018	Pc	0.85	0.82	0.90	0.85	0.90	0.90	0.86	0.85	0.85	0.90	0.90	**0.90**	0.82	0.82	0.86
	R^2	0.72	0.68	0.80	0.72	0.80	0.80	0.74	0.73	0.73	0.80	0.81	**0.82**	0.68	0.68	0.73
WC0019	Pc	0.27	0.08	0.28	0.74	0.28	0.57	0.35	0.42	0.82	0.32	0.42	**0.83**	0.10	0.32	0.81
	R^2	0.07	0.01	0.08	0.55	0.08	0.32	0.12	0.17	0.68	0.10	0.17	**0.69**	0.01	0.11	0.66
WC00QF	Pc	0.24	0.09	0.26	0.58	0.27	0.51	0.30	0.24	0.64	0.31	0.27	**0.66**	0.11	0.09	0.63
	R^2	0.06	0.01	0.07	0.34	0.07	0.26	0.09	0.06	0.41	0.10	0.07	**0.43**	0.01	0.01	0.39
WC01MD	Pc	0.58	0.47	0.59	0.67	0.59	0.65	0.66	0.67	0.59	0.65	0.68	0.61	**0.68**	0.60	0.53
	R^2	0.33	0.22	0.34	0.44	0.35	0.42	0.43	0.44	0.35	0.43	0.47	0.38	**0.46**	0.36	0.28
WC00QA	Pc	0.96	0.96	0.87	0.96	0.97	0.97	**0.97**	0.97	0.96	0.91	0.90	0.87	0.97	0.96	0.96
	R^2	0.92	0.93	0.75	0.93	0.93	0.94	**0.94**	0.94	0.92	0.82	0.82	0.75	0.94	0.93	0.93

Table 13 – Statistical criteria summary of regression study for all work centers

Some work centers have poor fits (WC0001, WC0004, WC0006), but others offer a strong correlation and predictive power that may balance the overall manufacturing process cycle time estimation.

This exploratory search was a stepping block to determine which component geometric properties could offer the best cycle time estimates for each work center. Knowing which properties are more useful for determining the cycle times for the different work centers, new multiple linear regression models were built involving the triangular distribution parameters (a,b,c) as independent variables. This enables the determination of cycle times distributions that inherit the process variabilities, given the component geometric properties. A benefit of the approach of fitting the distribution parameters is to estimate the cycle times variability for new parts avoiding any manual input, based on human expertise. The approach allows to obtain an expected distribution of cycle times based only on the parts' characteristics, namely part's geometric properties and complexity metrics, and on past variability of similar parts. From the estimated parameters, the INVCDF can be determined, and cycle times within a particular work center can be estimated for any desired component, as represented in Figure 40.

Table 14, summarizes the β-coefficients for each work center that formulate the MLR models to estimate the minimum (a), maximum (b), and most likely (c) distribution values, according to Equation 30.

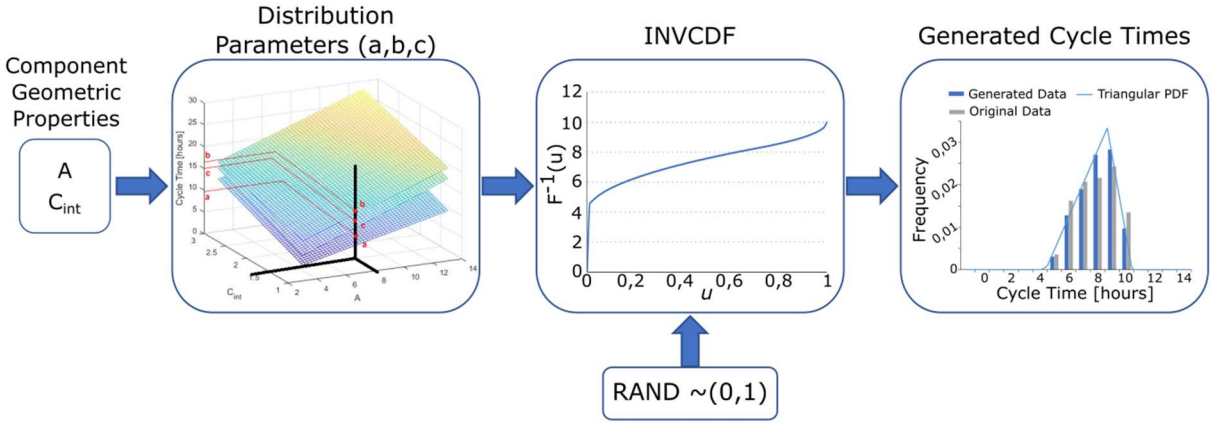

Figure 40 - New component cycle times distribution estimation and cycle times generation flowchart

.

WORK CENTER			a	c	b
WC0001	Ind.Variables	β_0	0.52	1.55	2.36
	x_1= V	β_1	3.73	2.67	23.68
	x_2= C_{XZ}	β_2	0.00	0.27	0.60
WC0002	Ind.Variables	β_0	-2.93	-2.18	2.45
	x_1= A	β_1	0.79	1.29	1.20
	x_2= C_{int}	β_2	4.21	4.28	3.32
WC0003	Ind.Variables	β_0	-5.12	-5.44	-0.78
	x_1= A	β_1	3.12	4.00	3.74
	x_2= C_{XZ}	β_2	5.75	6.95	7.60
WC0004	Ind.Variables	β_0	0.17	0.71	1.20
	x_1= V	β_1	35.67	35.00	109.61
	x_2= C_{XZ}	β_2	-0.04	0.03	-0.10
WC0008	Ind.Variables	β_0	0.02	1.00	1.30
	x_1= A	β_1	0.15	0.15	0.15
	x_2= V	β_2	3.85	3.85	3.85
WC0017	Ind.Variables	β_0	-3.06	-0.58	-1.06
	x_1= A	β_1	0.52	0.66	0.56
	x_2= C_{int}	β_2	3.73	3.13	6.13
WC0006	Ind.Variables	β_0	0.32	0.54	2.48
	x_1= V	β_1	-0.56	49.72	113.32
	x_2= C_{int}	β_2	0.06	-0.04	-0.70
WC0009	Ind.Variables	β_0	-7.59	-12.38	-4.32
	x_1= P	β_1	0.30	0.46	0.37
	x_2= C_{int}	β_2	6.39	10.92	9.58
WC0016	Ind.Variables	β_0	15.22	30.84	34.65
	x_1= A	β_1	2.52	3.45	3.25
	x_2= C_{XY}	β_2	-3.28	-5.60	-5.63
WC0018	Ind.Variables	β_0	-2.99	-3.61	-1.26
	x_1= P	β_1	0.19	0.34	0.36
	x_2= C_{int}	β_2	0.40	0.36	-0.25
WC0019	Ind.Variables	β_0	-15.38	-12.80	-16.34
	x_1= P	β_1	0.50	0.36	0.54
	x_2= C_{int}	β_2	10.85	15.94	19.36
WC00QF	Ind.Variables	β_0	-5.14	-6.75	-5.55
	x_1= P	β_1	0.14	0.20	0.21
	x_2= C_{int}	β_2	3.80	5.62	5.87
WC01MD	Ind.Variables	β_0	0.38	0.38	0.38
	x_1= V	β_1	27.39	27.39	27.39
	x_2= C_{XY}	β_2	0.16	0.23	0.32
WC00QA	Ind.Variables	β_0	-2.00	-1.50	-1.10
	x_1= A	β_1	0.30	0.30	0.30
	x_2= C_{XY}	β_2	0.60	0.60	0.60

Table 14 - β -coefficients from MLR models for a, b and c parameters estimation

4.3. **Modelling Non-Qualities**

As previously mentioned in section 3.3.2 there are four different types of non-qualities: Scrap, Repair, Rework, and Use as Is, in decreasing order of severity. Any of these four types can occur at any given manufacturing step. Therefore, it would be useful to be able to predict the outcome of these events, at any given step, and account for its possible impacts on manufacturing costs.

In probability theory, binomial distributions are categorized as discrete probability functions of a random variable *X* that measures the number of successes, with a probability of success p, in a sequence of n independent experiments [66]. This could metaphorically translate to the amount of each type of non-quality (*X)* to occur, in a sequence of *n* production runs (production volume). In short, binomial distributions can be used to answer the following question: "Given the current efficacy $(1-p)$ of the activities completed in this step, how many non-qualities of each type will there be, for a certain amount of parts being produced (n)?"

In order to implement this type of distribution to the desired effect, a few conditions must be satisfied:

1. The experiment consists of n identical trials, where n is finite.
2. There are only two possible outcomes in each trial. Success, or failure.
3. The probability for success *p* remains the same for each trial in *n.*
4. All the trials are independent.

For this particular application, these could be interpreted as such:

1. The experiment consists of n identical production runs or manufacturing cycles.
2. For each type of non-quality (X - scrap, repair, rework, use as is), it either occurs (success) or not (failure).
3. The ratio between the number of non-qualities occurrences and the total number of parts produced stays the same during each production run.
4. Each production run is independent from previous runs.

On these grounds, the probability of getting exactly k successes in n trials is given by the probability mass function (PMF), in Equation 31,

$$f(k,n,p) = Pr(X = k) = \frac{n!}{k!\,(n-k)!}p^k(1-p)^{n-k}, \qquad \begin{matrix} n \in \mathbb{N} \\ p \in [0,1] \\ k = 0,1,2,\dots,n \end{matrix} \tag{31}$$

where p is the probability of success for the type of non-quality being evaluated.

This probability of success (p), for any of these four types of non-qualities, can be estimated by the ratio between the number of production cycles executed at each step, and the number of each non-quality occurrence at that respective step.

Equations 32 to 35 calculate each of the non-qualities type probabilities' success, represented in Table 15.

$$p_{rework} = \frac{\#reworks\ at\ step\ i}{\#cycles\ at\ step\ i} \tag{32}$$

$$p_{repair} = \frac{\#repair\ at\ step\ i}{\#cycles\ at\ step\ i} \tag{33}$$

$$p_{scrap} = \frac{\#scraps\ at\ step\ i}{\#cycles\ at\ step\ i} \tag{34}$$

$$p_{use\ as\ is} = \frac{\#use\ as\ is\ at\ step\ i}{\#cycles\ at\ step\ i} \tag{35}$$

	Probability of Sucess (p)			
WORK CENTER	Repair	Rework Total	Scrap	Use as Is
WC0001				
WC0002				
WC0003				
WC0004				
WC0005				
WC0006				
WC0008				
WC0009				
WC0016				
WC0017				
WC0018				
WC0019				
WC00QF				
WC01MD				
WC00QA				

Table 15 - Summary of non-qualities probability of success at each work center.(Values have been omitted to respect confidentiality.)

To determine this probable number of non-qualities at each process activity, the inverse cumulative distribution function (INVCDF), was employed. For a given u, defined as the confidence level of the estimate, the INVCDF is defined as

$$F^{-1}(u; n, p) = k\ ,$$

Where k is the smallest integer such that,

$$u \leq \sum_{i=0}^{k} \frac{n!}{i!\,(n-i)!} p^i (1-p)^{n-i}\ , \qquad \begin{matrix} n \in \mathbb{N} \\ p\ \in [0,1] \\ u\ \in [0,1] \\ i = 0,1,2,\dots,k \end{matrix} \tag{33}$$

This way, given a certain confidence level (u) it is possible to determine the minimum number of expected occurrences (k) of a certain non-quality at every step of the manufacturing process, based on the empirical chance of that non-quality to occur (p) and the targeted production volume (n) of the component being made. The confidence level (u), can be adjusted; Higher confidence levels will translate into a higher number of occurrences of non-qualities to be included in the cost model, which ultimately leads to more conservative and increased non-quality costs.

Lastly, the determined number of occurrences ($\#NQ$) is divided by the number of parts (NP_i) to measure the ratio of occurrences at that given step ($X_t\,\%$), required for the calculations of scrap costs in the process, as described in section 3.4.2.

$$X_i\,\% = \frac{\#NQ_t}{NP_i}\,, \qquad X = \{scrap, repair, rework, use\ as\ is\} \tag{34}$$

4.4. **Modelling Tooling Costs and Materials Quantities**

Different components have different requirements in terms of tooling and materials used. So, to estimate their costs, it is necessary to determine which tools and materials are going to be used and in what quantities.

Thus, following a similar approach as to what was done with cycle times, the available component's geometric properties were correlated with the tooling and materials data, in order to create regression models able to estimate tooling costs and materials quantities based on a new part geometry.

Because of the heterogeneity of the materials in the different parts, three distinct groups were created. Group 2 consists of spar type parts (Table 16), which, regardless of the differences in technology and processes, they are made of the same basic materials, although involving different classes within each material, which will ultimately be reflected in the different price points. Group 1 & 3 are comprised of very similar skin type components. However, Group 3 has additional co-cured stringers, which requires an additional resin film to be placed between the contact areas of the skin and the stringer, to promote bonding during the curing cycle. Also, the mixes between materials in these two groups are slightly different which could increase the variance in latter estimates, hence the separation of the two.

Group	Materials	Aircraft	Part Description	Part Tag
2	UD CF Prepreg Tape CF prepreg Copper Mesh GF prepreg	A	Skin 1	P_1
		A	Skin 2	P_2
		A	Skin 3	P_3
		A	Skin 4	P_4
		B	Skin 1	P_5
		B	Skin 2	P_6
1	UD CF Prepreg Tape CF prepreg GF prepreg	B	Spars 1	P_7
		B	Spars 2	P_8
		C	Spars 1	P_9
		C	Spars 2	P_{10}
3	UD CF Prepreg Tape CF prepreg Copper Mesh GF prepreg Epoxy Resin Film	C	Skin 1	P_{11}
		C	Skin 2	P_{12}
		C	Skin 3	P_{13}
		C	Skin 4	P_{14}

Table 16 - Component group identification and main materials used

Simple linear regression was used to fit the quantities of each material for each of the three groups as a function of the part surface area (Figure 41, Figure 42, Figure 43). Again, the idea is to use these regressions in the PBCM in order to allow for simple estimations of new components material quantities, and their respective costs.

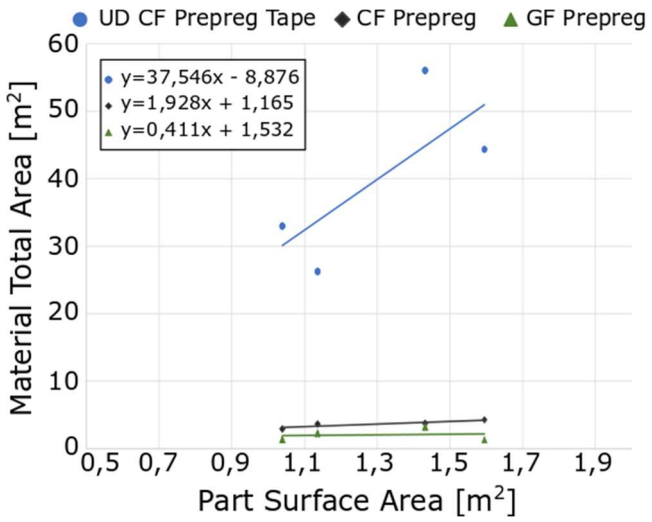

Figure 41 - Group 2 material quantity regression as function of parts' surface area in contact with mold surface

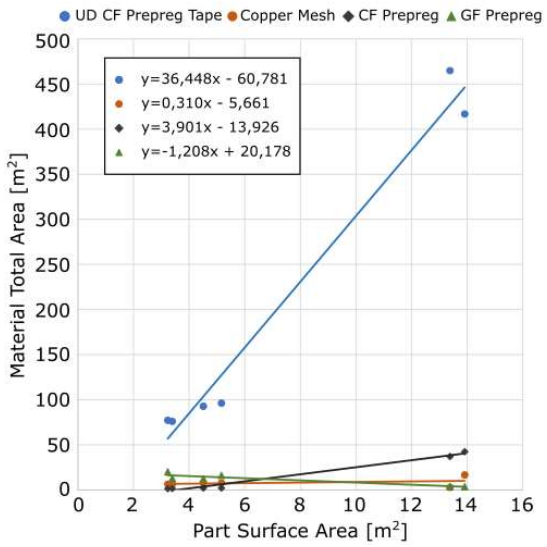

Figure 42 - Group 1 materials quantities linear regressions, as a function of parts' surface area in contact with the molds' surface

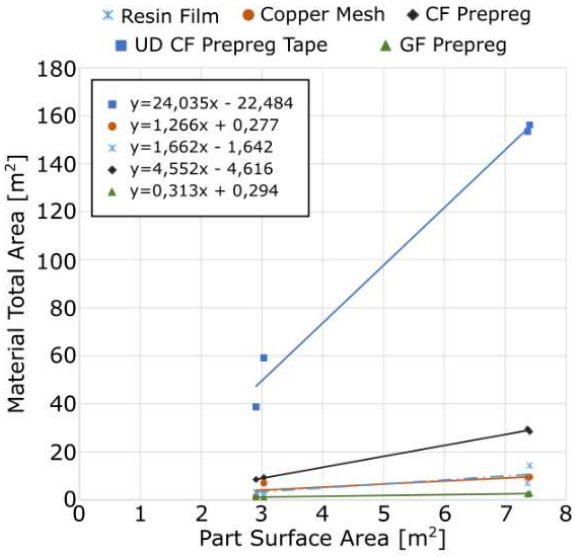

Figure 43 - Group 3 materials quantities regressions, as a function of parts' surface area in contact with the molds' surface

Tooling cost estimation follows a very similar approach. As mentioned in section 3.2, there is usually a main mold upon which the material is laminated, and depending on the type of manufacturing process, additional tooling can be required. These additional tools represent an added cost that must be brought into the equation, in order to properly assess the manufacturing costs of these special processes.

By plotting the current main mold and additional tooling costs versus the part surface area, it is possible to obtain the relationship between these two different quantities using SLR analysis (Figure 44, Figure 45)

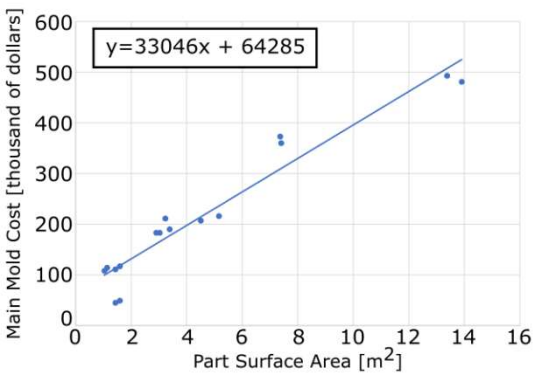

Figure 44 – Main mold cost linear regression. Part surface area refers parts' area in contact with mold surface.

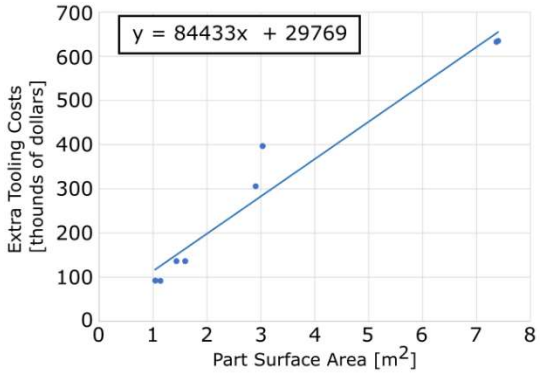

Figure 45 – Extra tooling costs linear regression. Part surface area refers to parts' area in contact with mold surface.

These regression models could be directly introduced into the PBCM allowing for the estimation of the necessary quantities of materials and tooling costs, limiting the inputs to a single variable of part surface area, instead of the multiple entries for each type of material and tooling.

Table 17 and Table 18 summarizes the accuracy of the implemented regressions for material quantities and tooling cost, respectively. It the cases of GF prepreg in Group 1 and Copper Mesh in both Group 2 and Group 3, the goodness-of-fit in very low and the p-value exceeds the 0.05 threshold, suggesting the lack of statistical significance in the regression. Ultimately, estimating the aforementioned quantities may yield poor results.

Group	Material	β_0	β_1	Pc	R^2	p-value
1	UD CF Prepreg Tape	-60.78	36.45	0.99	0.98	0.00
	CF prepreg	-13.93	3.90	0.99	0.98	0.0001
	Copper Mesh	5.66	0.31	0.34	0.11	0.52
	GF prepreg	20.18	-1.21	0.91	0.83	0.0112
2	UD CF Prepreg Tape	-8.88	37.54	0.74	0.55	3.65E-02
	CF prepreg	1.16	1.93	0.90	0.82	0.0020
	GF prepreg	1.53	0.41	0.12	0.01	0.78
3	UD CF Prepreg Tape	-22.48	24.04	0.99	0.98	0.0001
	CF prepreg	-4.62	4.55	1.00	1.00	8.08E-07
	Copper Mesh	0.28	1.27	0.75	0.56	0.0891
	GF prepreg	0.29	0.31	0.99	0.98	1.61E-04
	Epoxy Resin Film	-1.64	1.66	0.86	0.74	0.0288

Table 17- Statistical criteria summary and regression coefficients for material quantities

	β_0	β_1	Pc	R^2	p-value
Main Mold	33045	65285	0.96	0.93	2.12E-09
Extra Tooling	84433	29769	0.98	0.95	2.95E-05

Table 18 – Statistical criteria summary and regression coefficients for tooling costs

4.5. **Proposed Process-Based Cost Model**

After modelling the cycle times, non-qualities, material quantities, and tooling investment with respect to the part geometric properties, it is then possible to take advantage of these relations to build a new PBCM capable of estimating the cost of a new composite component in manufacturer's industrial environment.

Comparatively to the previous cost model, the α-PBCM (section 3.4), the amount of inputs required is significantly reduced. The inputs for the α-PBCM must be manually introduced, and the more steps the process has, the more inputs are required, many involving best guesses, resulting in a slow and arduous task. Moreover, to estimate the cost of new parts using the α-PBCM faces the obstacle of lack of data as its manufacturing process might not be yet designed or implemented. Integrating capabilities of estimating cycle times, non-quality effects and material, tooling, and equipment requirements based on knowledge retrieved from historical data, this new PBCM (β-PBCM) allows the cost estimation of new components not yet under production since it only requires component geometric characteristics as input. By estimating most of the process information from a limited set of part geometric properties, the new model reduces the number of inputs that must be manually introduced and at the same time automatically generates the necessary inputs for the cost estimations, based on the past performance.

These methods developed from section 4.2 to 4.4, can be viewed as additional modules built into the α-PBCM for estimating a specific input, namely cycle times, non-qualities occurrences, material quantities and tooling investments for the desired component. Furthermore, given the simplicity in the required inputs, it is expected that even at the early stages of design, this information is already fully available, thus allowing for cost estimation to be made at that point.

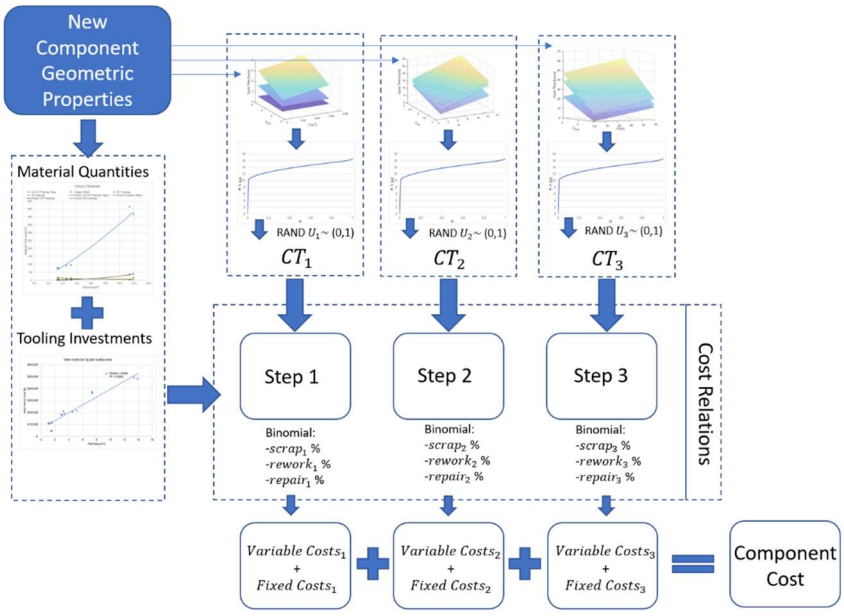

Figure 46 – New PBCM final component cost calculation framework

Figure 46 illustrates the basic framework of the developed PBCM, hereinafter referred to as β-PBCM, and the estimation modules behind it. For a manufacturing process and each of its steps, material quantities, tooling investments, cycle times, and non-quality occurrences are determined from an initial set of the component's geometric properties. Then, these estimated intermediate quantities are fed into each process step cost relations, where they are translated into their respective cost items. Additionally, because each step cycle time is generated from and expected distribution, it is possible to perform a Monte Carlo simulation to study the influence of time variability on manufacturing costs.

5. Results and Discussion

The main goal with the developed cost model is to be able to estimate the manufacturing costs of new structural parts made of carbon fiber composites, taking advantage of historical data from previously produced parts. It is intended to assess the cost impact of different designs and manufacturing routes, and therefore introduce cost as a decision variable since the early design and planning stages.

In this context, the validation of the outputs of the model is of extreme importance.

The component's final cost can be broken down either into the cost of each manufacturing step or into the different classes of cost items *i.e.* machine costs, material costs, labour costs, etc. This separation of costs favors a detailed analysis of the origin of costs, that can potentially allow for the identification and understanding of major sources of cost.

This next chapter focusses on these two topics, as well as exploring future technology tendencies than may impact manufacturing costs. Lastly, a sensitivity analysis is performed across every manufacturing step, evaluating possible performance improvements and deriving cost changes, underlying the potential for future interventions and process developments.

5.1. Test Case

The use of the developed models for a component cost estimation begins by collecting the geometric properties and compute the complexity metrics of the desired component. Generally, the geometry and complexity metrics entail the use of a CAD model to more easily extract its geometric features, alongside the MATLAB complexity script, in order to determine the complexity inputs. For this test case, aircraft's A Skin 4 (Figure 26) is used. Its input data is presented in Table 19.

Area [m^2]	Perimeter [m]	Volume [m^3]	C_XY	C_XZ	C_int
4.511	18.18	0.014	6.491	3.369	1

Table 19 – Aircraft A Skin 4 geometric and complexity properties

Based on these simple inputs, the model automatically estimates material quantities and tooling investments (Table 20). As a skin type component, with no co-curing of stringers or any additional reinforcements, the material quantities of aircraft's A Skin 4 are estimated from the Group 1 regression model (Figure 42). In this process, only the main mold is needed, whose cost is estimated from the equations in Figure 44.

Material Description	Estimated Material Quantity [m^2]	Estimated Tooling Cost [$]
Copper Mesh	7.45	$ 214,338.98
GF prepreg	14.73	
CF prepreg	3.67	
UD CF prepreg tape	103.62	

Table 20 - Estimated material quantities and tooling investment cost.

Similarly, for each step of the manufacturing process, cycle times and non-quality occurrences are estimated based on the triangular and binomial distributions, previously described in sections 4.2 and 4.3, respectively.

Considering the global inputs (Table 7), and step specific inputs (Table 8) a Monte Carlo simulation is performed for each stochastic variable. By doing so, the manufacturing cost distribution is obtained (Figure 45).

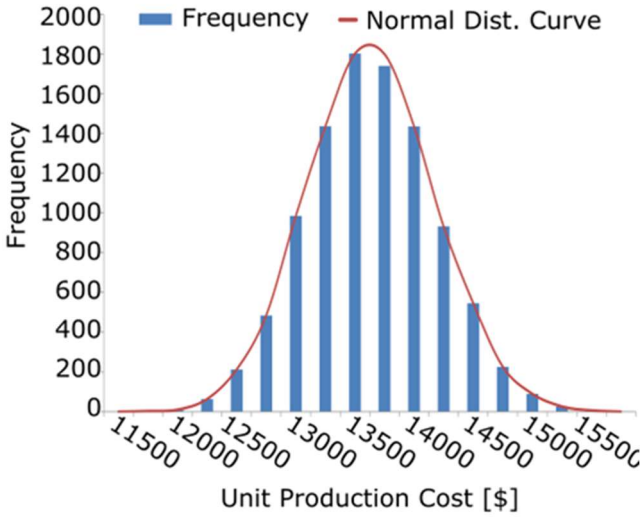

Figure 47 – Monte Carlo simulation 10000x output histogram for aircraft's A skin 4 unit cost estimation.

The costs in Figure 47 are the result of 10000 simulation runs for aircraft's A Skin 4. At each run, every manufacturing step cycle time is picked at random inside its respective time distribution, thus producing a cost distribution. This process of randomly picking a cycle time is the same as described in section 4.2, Figure 40.

It is interesting to note that, despite the cycle times at each work center being modeled according to a triangular distribution, the component final costs follow a normal distribution. This is a well-known consequence of the central limit theorem (CLT), stating that when independent samples from any distribution are added, their sum approximates a normal distribution even if the original samples themselves are not normally distributed. This assumption can be further supported by the Q-Q plots of the output data from the Monte Carlo simulation (Figure 48), where it is possible to observe that most of the points follow the ideal line of the normal distribution.

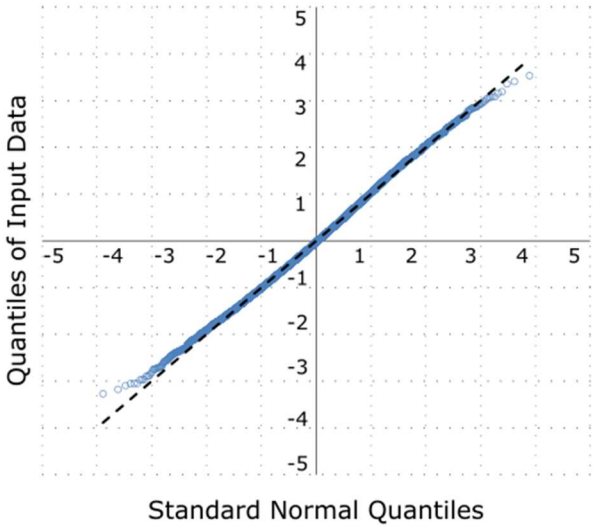

Figure 48 - Q-Q plot for the Monte Carlo output data in aircraft's A Skin 4 cost simulation.

The expected value of component cost can be determined as the average of all simulations, which in turn should be used as the cost metric reference when evaluating manufacturing and technology alternatives.

The range of costs resulting from the simulation, consequence of the different processes cycle time variabilities provides a realistic notion of final cost variability (Table 21). In this way, we move away from the more traditional and deterministic approach to cost estimation, where a single cost is provided and any cost differences that are likely to occur are neither contemplated of taken into account in the early project decisions. In this case, the average cost of the final component is expected to be within the interval [12,646; 14,774] with a confidence level of 95%, being this uncertainty due to variabilities on cycle times similar to the ones observed in the past.

Component	Lower 95% Bound (μ-2σ)	Average Cost (μ)	Upper 95% Bound (μ+2σ)
Aircraft A Skin 4	$ 12,646	$ 13,710	$ 14,774

Table 21 – Average component cost and cost variability after Monte Carlo simulation for Aircraft A Skin 4. (standard deviation = σ; average=μ)

Additionally, one could evaluate each manufacturing step (Figure 49) costs individually.

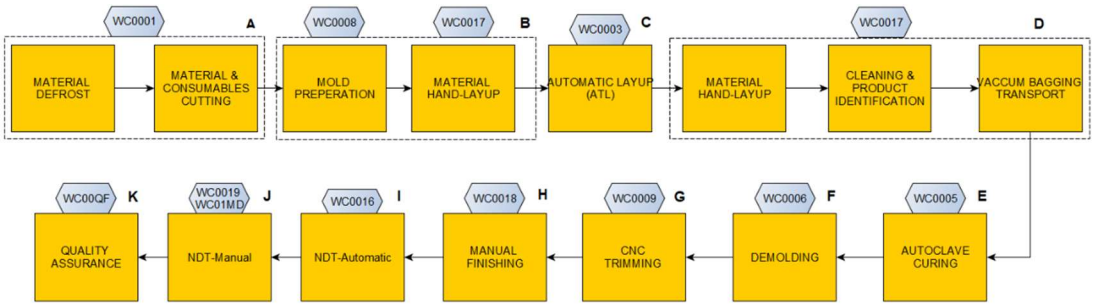

Figure 49 - Flowchart of aircraft's A skin 4 manufacturing process.

Some of the different process steps are grouped into larger steps, lettered from A to K in this example. This is because some manufacturing steps generate small contributions to the overall cost and are part of pre/post-processing steps to other, more impactful and primary steps in the manufacturing process. Thus, by aggregating some of these steps it is possible to tone down on the complexity of the analysis, and the amount of necessary calculations. Process steps costs are presented in Table 22, followed by a graphical representation of each step contribution in Figure 50.

Step	Description	Number of Parts (NP)	Cost Percentage	Average Step Cost
A	Storage and Material Cutting	†	5%	†
B	Preperation, Hand-Layup and Vaccum Bagging	†	7%	†
C	ATL	†	42%	†
D	Preperation, Hand-Layup and Vaccum Bagging	†	4%	†
E	Autoclave Curing	†	13%	†
F	Demolding	†	1%	†
G	CNC Trimming	†	14%	†
H	Manual Finishing	†	1%	†
I	NDT-Automatic	†	4%	†
J	NDT-Manual	†	5%	†
K	Quality Assurance	†	3%	†
Total		35		†

Table 22 - Manufacturing steps cost of aircraft's A skin 4 and number of parts (NP) produced for an annual production volume of 35 parts (effect of quality issues). (†Absolute cost values and step NP have been omitted to respect confidentiality.)

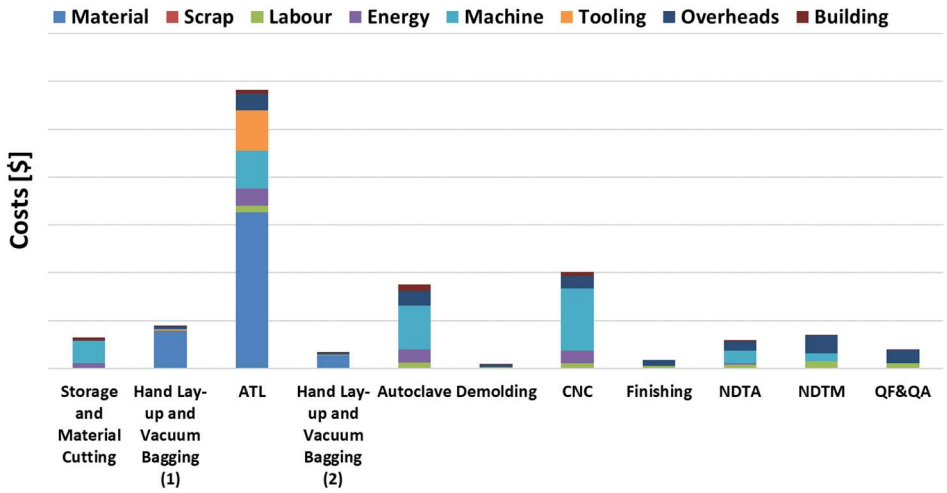

Figure 50 – Aircraft A skin 4 manufacturing steps cost items distribution. Annex 3 contains the remaining components manufacturing steps cost items distributions. (Cost values have been omitted to respect confidentiality.)

Table 22 also shows the increase in the required number of parts that must be produced to reach the targeted production volume of 35 units per year, since along the manufacturing process there is a loss in the number of required parts, due non-quality issues covered in previous sections. Therefore, it is necessary to launch more parts into production to compensate for the predicted losses. This increased number of parts has obvious effects in final component costs, as it represents an increase in both the amount of materials needed for the additional parts, as well as additional production time. Thus, from this combined increase in both materials and overall manufacturing time, unit component cost is higher than otherwise not having these issues emerge.

A more detailed analysis of each process step cost helps to better understand which cost items of the process are having a bigger impact on costs, and why costs were initially broken down into the different sources of variable and fixed costs. This cost breakdown can be performed at two different levels: at the process step level and the global process level.

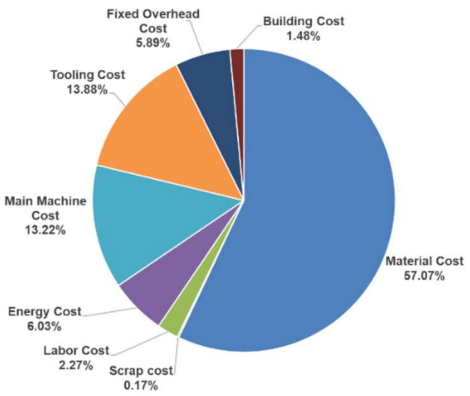

Figure 51 – Step (C) - ATL; Manufacturing costs items distribution

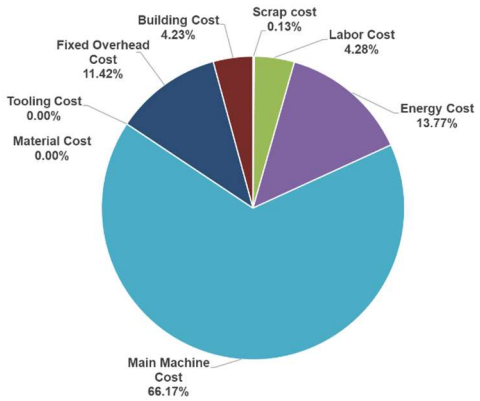

Figure 52 – Step (G) –CNC trimming; Manufacturing costs items distribution

At the process step level, the predominant cost item depends clearly on the technology and resources involved in each step. Material cost represents more than half (~57%) of the cost of ATL step (Figure 51), with machine and tooling costs being the second largest contributors to cost. This cost distribution is associated with the fact that most of the raw material necessary for the manufacturing of this component is used at this stage by the ATL machine, which, in turn, requires a mold for the material to be deposited. The combination of these three factors – materials, equipment, and tooling - is what drives most of the cost, but despite the high operation cost of the machine and the mold investment, material costs far outweigh the contributions from the previous two. On the other hand, in the part trimming (step G), the scenario is tremendously different (Figure 52). Here the cost of the equipment (CNC machine) used for part trimming clearly dominates cost.

Every process step performs a distinctive operation with distinctive characteristics in the manufacturing process, thus resulting in different cost distributions, as shown in the two previous examples. Ultimately, final component cost item distribution will be the combined result of each step distribution, which can be more weighed on material costs, machine, tooling, etc., and depends on the overall manufacturing strategy (Figure 53).

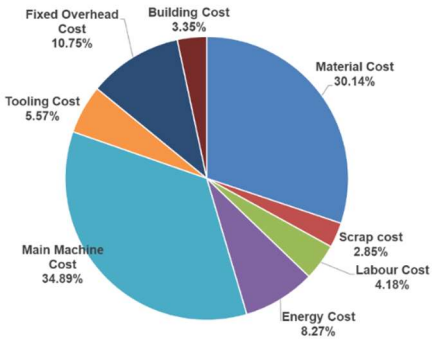

Figure 53 – Aircraft A skin 4 overall manufacturing costs breakdown. The remaining final cost distributions are shown in Annex 2 .

Materials and machine costs emerge as the two main sources of cost for aircraft's A Skin 4. Most of the material costs of the process originate from the ATL step, while machine costs are distributed across different steps of the process, namely Trimming, Autoclave, ATL, and NDT where high intensive capital equipment is needed (Figure 50). Comparatively, energy, labour, and overheads are significantly smaller. Building and tooling – with tooling being highly dependent on the process – represent a smaller portion of costs and smaller still are scrap costs, which in any case cannot be considered neglectable.

Production volume can also be considered, in order to explore the benefits of economy of scale (Figure 54).

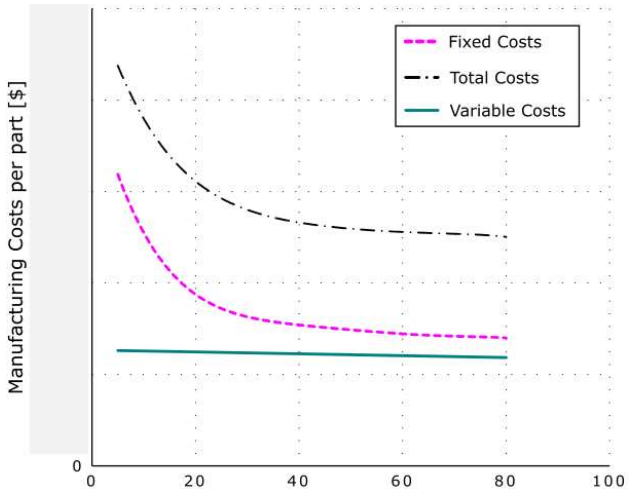

Figure 54 - Production Volume impact on aircraft A skin 4 manufacturing costs per part. (Cost values have been omitted to respect confidentiality.)

With the increase of production volume, there is a bigger diffusion of fixed costs, hence the observed reduction in component final costs. On the other hand, variable costs do not benefit from the same effect, as their costs – mostly associated with materials, labour, and energy – rise proportionally with the increase of production volume, and thus are maintained constant per unit produced.

As for the rest of the studied sample, applying the respective cost models yielded the cost distributions presented in Table 23 and Table 24.

Aircraft	Description	Part Tag	Material Cost	Scrap Cost	Labour Cost	Energy Cost	Machine Cost	Tooling Cost	Fixed Overhead Cost	Building Cost
A	Skin 1	P_1								
A	Skin 2	P_2								
A	Skin 3	P_3								
A	Skin 4	P_4								
B	Skin 1	P_5								
B	Skin 2	P_6								
B	Spars 1	P_7								
B	Spars 2	P_8								
C	Spars 1	P_9								
C	Spars 2	P_{10}								
C	Skin 1	P_{11}								
C	Skin 2	P_{12}								
C	Skin 3	P_{13}								
C	Skin 4	P_{14}								

Table 23 – Final components cost sources distribution.(Values have been omitted to respect confidentiality)

In general, machine and materials costs represent the biggest expenditures in most of the manufacturing processes, followed by overheads, energy, and tooling costs. Scrap costs favourably take one of the smallest fractions of total costs, indicative of relatively good processes' efficacy. Be that as it may, these numbers represent the developed models' interpretation of the physical manufacturing reality, thus, it can only be expected that in this approximation there may be some tenuous deviations between the model results and the reality.

Aircraft	Technologies	Part TAG		S_1 Storage and Material Cutting	S_2 Hand Lay-up and Vacuum Bagging (1)	S_3 ATL	S_4 AFP	S_5 Hand Lay-up and Vacuum Bagging (2)	S_6 Hand Lay-up and Vacuum Bagging (3)	S_7 ATL-Stringers	S_8 AFP-Stringers	S_9 Hand Lay-up and Vacuum Bagging (4)	S_{10} Hot Drape Forming	S_{11} Skins & Stringers Joining	S_{12} Autoclave	S_{13} Demolding	S_{14} CNC Trimming	S_{15} Manual Finish	S_{16} NDT-A	S_{17} NDT-M	S_{18} QF&QA	Final Cost
A	ATL	P_1	μ																			
			σ																			
A	ATL	P_2	μ																			
			σ																			
A	ATL	P_3	μ																			
			σ																			
A	ATL	P_4	μ																			
			σ																			
B	ATL	P_5	μ																			
			σ																			
B	ATL	P_6	μ																			
			σ																			
B	AFP	P_7	μ																			
			σ																			
B	AFP	P_8	μ																			
			σ																			
C	ATL+AFP+HD	P_9	μ																			
			σ																			
C	ATL+AFP+HD	P_{10}	μ																			
			σ																			
C	ATL+ATL+HD	P_{11}	μ																			
			σ																			
C	ATL+ATL+HD	P_{12}	μ																			
			σ																			
C	ATL+AFP+HD	P_{13}	μ																			
			σ																			
C	AFP+AFP+HD	P_{14}	μ																			
			σ																			

*Table 24 – Manufacturing steps average costs and standard deviation according to estimated cycle time distributions. *Process step not part of the component manufacturing process.(Cost values have been omitted to respect confidentiality.)*

5.2. **Developed model validation and accuracy**

Model validation is important to understand the reliability of the models' results so that any future decisions regarding process changes provide the desirable results indicated by it. One of the few ways to assess model acceptance is by comparing its cost outputs with real cost references, in this case, the manufacturer's own costing values for each of the different components (Figure 55). The real costs' data that was made available, is relative to five months of operations, with the latest time entry being relative to the end of February 2020.

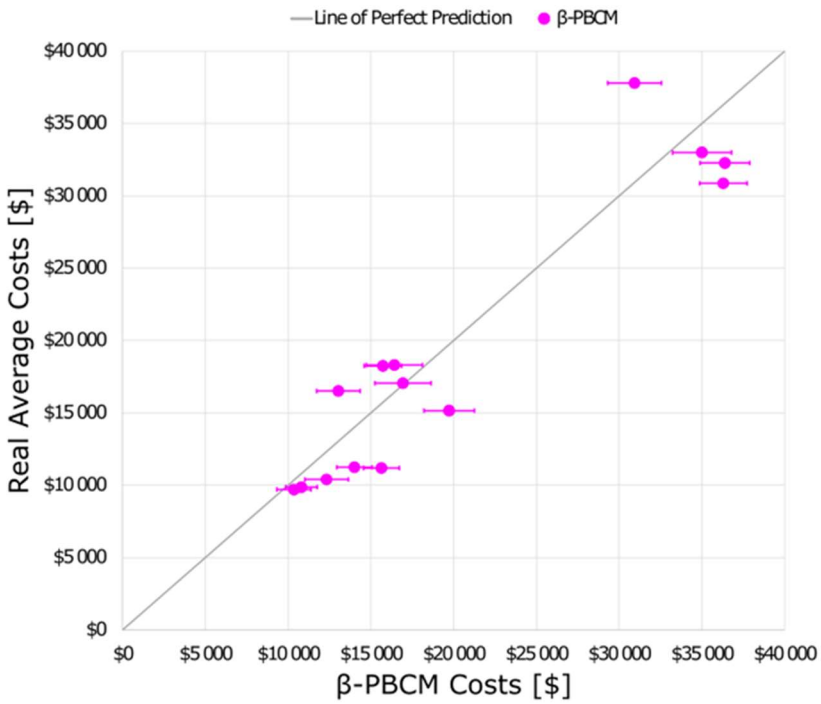

Figure 55 – Scatter plot of component cost distribution from the developed model (β-PBCM), compared to the real components' average costs provided by the manufacturer. Cost distribution for a 95% confidence interval, composed by 10000x simulations of its respective component cost.

Figure 55 demonstrates comparable results to the initial model (α-PBCM) that used real and manually inputted data, gathered from the current implemented processes (Figure 33). The results achieved by the developed model (β-PBCM) that uses multiple linear regressions, to estimate cycle times, materials consumption, and tooling costs based on part geometry data, show a very good fit with the parts' real costs. Certainly, due to possible intermediate estimation discrepancies between estimated and true cycle times, material quantities, and tooling costs, deviations are expected. That is true, but overall, final component cost accuracy remains acceptable, with values for Mean Average Percentual Error (MAPE) and Normalized Root Mean Square Error (NRMSE) of 16.4% and 5.1%, respectively. Regarding final cost distributions itself (Figure 56), there is a good level of agreement and overlapping of the models' distributions with real costs distributions, however, in a few cases, the latter shows an increased variance not fully contemplated by the model. One reason for this, in some cases, might stem from the reduced amount of parts produced, suggesting that the manufacturing process is still in early learning stages. Also, the variance in the more mature processes – with more components produced to date

(Table 2) – further supports this previous argument, as it is comparatively smaller than in the newer manufacturing processes, in which lower volumes are involved.

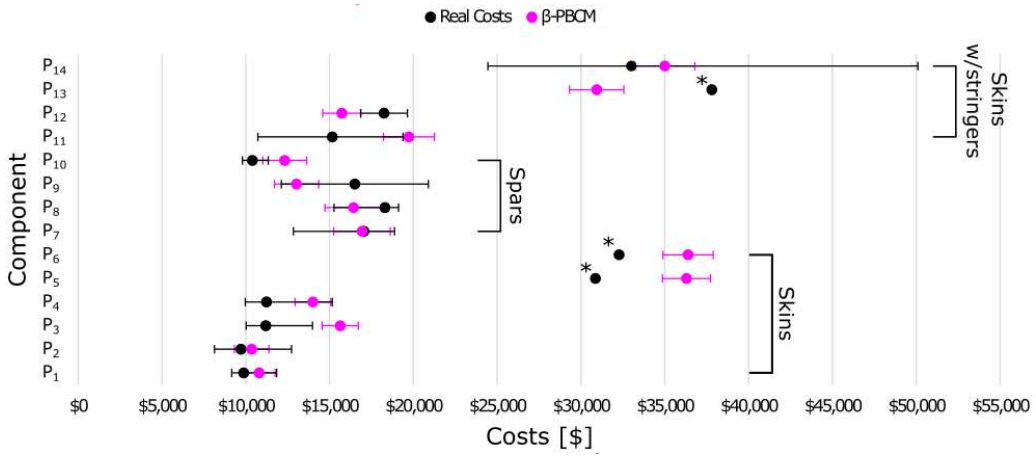

*Figure 56 – Manufacturer's Components Cost Distribution compared to β-PBCM cost distributions. *Insufficient data/no cost variations during the provided data period.*

The results shown thus far can somehow be taken as a validation of the β-PBCM behaviour in the estimation of components' costs, considering these are based on relationships established between components simple geometric properties and cost relevant data. Consequently, this last observation closes the initial research question (RQ): Can techno-economic relations/regressions be constructed based on historical parts data with enough merit to be used in the cost estimation model of the new component? One should note that this validation is in its essence a fitting validation. And in that sense, it can be argued that the descriptive power of the developed model is validated. Certainly, this does not guarantee its estimation (predictive) power. However, as far as new components, whose cost are to be estimated, are withing the bounds of characteristics to the ones used in this research, it can be expected that the model estimations have enough merit to be used to support decision making at the process design stage.

Transversely to all estimation methods, there are always three possible outcomes: The value is overestimated, underestimated, or perfectly estimated. Even in the unlikelihood of obtaining an exact match to the true/real value, having low deviations should produce reasonably accurate final cost results – assuming the competence of the implemented cost relations. However, poor estimations *i.e.* high deviations from the true observed values, can just as equally generate acceptable cost results. Initially, this may seem counter intuitive, but there is always the chance that two or more quantities could balance each other's relative deviations, resulting in error mitigation and thus, reach an admissible final cost estimation. All in all, depending on the magnitude of each estimated quantity relative deviation, these can work towards or against producing a more favourable result. Even if the former does occur, it adds no additional merit to the model itself.

The developed model (β-PBCM) provides intermediate estimations on cycle time, material quantities, and tooling costs to generate cost estimates for each manufacturing step, and the sum of these costs results in the final component cost. Unlike material and tooling estimations, that only influence material and tooling costs respectively, cycle times have an impact on multiple cost sources, namely: machine,

labour, energy, overheads, and building costs. These cost items will hereinafter be referred to as time-dependent cost items, as they are intrinsically associated with time itself.

Ultimately, it is expected, that any final cost deviation between the two models (*α* and *β*) stems from deviations between the true and estimated values of the three intermediate quantities – cycle times, materials, and tooling.

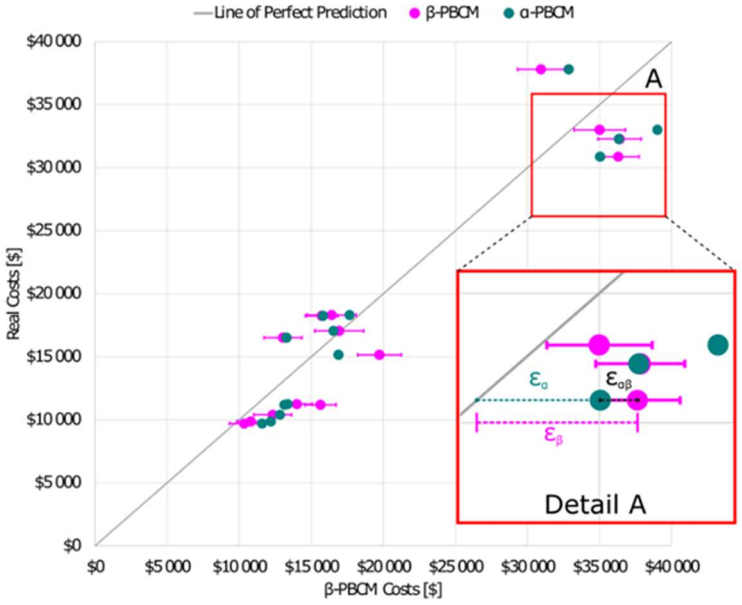

Figure 57 – Differences between the initial model (α-PBCM) and final implemented model (β-PBCM) costs, compared to the Real Costs. Detail A: Lack of agreement from α -PBCM (ε_α), combined with intermediate quantities estimation errors ($\varepsilon_{\alpha\beta}$), resulting in β -PBCM lack of agreement (ε_β).

Observing Figure 57, more often than not, the results achieved with the developed *β*-PBCM are more deviated from the true values (collected from the manufacturer) than the ones obtained with the α -PBCM model, *i.e* ε_β higher than ε_α. That is expected, as the α -PBCM was developed to use explicitly the field data as intermediate inputs in opposition to the *β*-PBCM model that generates these inputs based on regression relations over primary data of the part geometry. Overall, the β-PBCM cost results show an error increase of approximately 9% compared to the initial model (α-PBCM).

Table 25 presents the cost differences between the two PCBM models. It shows that the differences are not equal across every step, nor across every component.

Part TAG	S_1	S_2	S_3	S_4	S_5	S_6	S_7	S_8	S_9	S_{10}	S_{11}	S_{12}	S_{13}	S_{14}	S_{15}	S_{16}	S_{17}	S_{18}	Final Cost ($\varepsilon_{\alpha\beta}$)
P_1	-1%	4%	-32%	*	9%	*	*	*	*	*	*	-1%	10%	1%	37%	133%	-12%	119%	-11%
P_2	-1%	8%	-25%	*	17%	*	*	*	*	*	*	0%	13%	-3%	-35%	83%	-28%	70%	-11%
P_3	0%	14%	13%	*	24%	*	*	*	*	*	*	0%	16%	11%	62%	295%	14%	215%	19%
P_4	0%	6%	-2%	*	10%	*	*	*	*	*	*	0%	22%	-3%	39%	9%	97%	261%	5%
P_5	0%	-13%	3%	*	6%	*	*	*	*	*	*	0%	170%	7%	33%	11%	52%	-13%	4%
P_6	0%	36%	-11%	*	14%	*	*	*	*	*	*	0%	169%	18%	-8%	19%	21%	18%	0%
P_7	1%	3%	*	3%	4%	*	*	*	*	*	*	1%	1%	1%	1%	3%	1%	1%	2%
P_8	-1%	4%	*	-10%	1%	*	*	*	*	*	*	0%	-42%	21%	97%	-38%	10%	24%	-7%
P_9	0%	-8%	26%	13%	-5%	-6%	*	*	*	7%	*	0%	5%	-17%	35%	-13%	66%	-30%	-2%
P_{10}	2%	-16%	29%	-6%	-17%	-17%	*	*	*	3%	*	0%	4%	-27%	4%	12%	-9%	-16%	-4%
P_{11}	-3%	-22%	-9%	*	-10%	-17%	-8%	*	-12%	1%	-4%	0%	3%	69%	14%	145%	46%	87%	17%
P_{12}	2%	28%	3%	*	-1%	-12%	-6%	*	-7%	4%	7%	0%	9%	-26%	27%	13%	125%	-1%	-1%
P_{13}	1%	5%	6%		6%	21%	*	18%	5%	0%	-6%	1%	26%	-24%	7%	-7%	-34%	-50%	-6%
P_{14}	0%	1%	*	-21%	2%	23%	*	-17%	0%	0%	11%	0%	20%	-4%	7%	-3%	0%	16%	-10%

*Table 25 - Manufacturing steps relative cost difference in β-PBCM compared to α-PBCM costs. *Process step not part of component's manufacturing process.*

In some steps, the relative cost deviations are quite significant, hinting at significant error on the estimation of intermediate quantities. Even so, final component cost is not as heavily influenced by the suggested numbers across the different steps for two reasons. Different steps have different operational costs, due to the type of technologies involved and its supporting equipment's, meaning that high relative cost deviations, may translate into much smaller absolute cost deviations. Also, while some steps are overestimated, others are underestimated, balancing the total estimation error, into a more acceptable final error. This, in turn, confirms the initial hypothesis that the individual errors of each step might balance each other in the final result.

For the reasons stated above, each step cost difference becomes more perceptible in absolute terms (Table 26). It is possible to see that, in some steps, smaller relative differences in terms of cost resulted in higher absolute differences, and thus, higher impacts on the final cost difference. The opposite also happens. The total balance from all the steps deviations results in the final cost deviations between the two models ($\varepsilon_{\alpha\beta}$).

Part TAG	S_1	S_2	S_3	S_4	S_5	S_6	S_7	S_8	S_9	S_{10}	S_{11}	S_{12}	S_{13}	S_{14}	S_{15}	S_{16}	S_{17}	S_{18}	Final Cost ($\varepsilon_{\alpha\beta}$)
P_1	$ -9	$ 28	$-1,863	*	$ 31	*	*	*	*	*	*	$ -19	$ 7	$ 23	$ 36	$ 282	$ -77	$ 167	$ -1,394
P_2	$ -5	$ 61	$-1,408	*	$ 58	*	*	*	*	*	*	$ -7	$ 8	$ -42	$ -38	$ 198	$ -161	$ 99	$ -1,236
P_3	$ 1	$ 139	$ 811	*	$ 131	*	*	*	*	*	*	$ 1	$ 12	$ 198	$ 68	$ 802	$ 85	$ 256	$ 2,502
P_4	$ -1	$ 61	$ -141	*	$ 51	*	*	*	*	*	*	$ 0	$ 15	$ -70	$ 51	$ 50	$ 343	$ 282	$ 641
P_5	$ -2	$ -415	$ 589	*	$ 125	*	*	*	*	*	*	$ -5	$ 153	$ 196	$ 85	$ 250	$ 379	$ -103	$ 1,253
P_6	$ -2	$ 719	$-2,364	*	$ 261	*	*	*	*	*	*	$ -7	$ 154	$ 576	$ -39	$ 402	$ 232	$ 117	$ 49
P_7	$ 5	$ 15	*	$ 323	$ 14	*	*	*	*	*	*	$ 13	$ 0	$ 11	$ 1	$ 13	$ 3	$ 2	$ 401
P_8	$ -5	$ 16	*	$-1,201	$ 4	*	*	*	*	*	*	$ -8	$ -21	$ 177	$ 36	$-308	$ 36	$ 34	$ -1,239
P_9	$ -3	$ -15	$ 129	$ 448	$ -11	$-11	*	*	*	$42	*	$ 5	$ 4	$ -338	$ 45	$-401	$ 24	$ -162	$ -252
P_{10}	$ 10	$ -32	$ 131	$ -233	$ -38	$-38	*	*	*	$20	*	$ -2	$ 3	$ -536	$ 4	$ 278	$ -5	$ -67	$ -504
P_{11}	$ -25	$ -89	$ -358	*	$ -62	$-15	$-141	*	$-34	$ 3	$ -53	$ 3	$ 1	$ 2,014	$ 12	$ 709	$ 717	$ 156	$ 2,839
P_{12}	$ 12	$ 62	$ 85	*	$ -7	$ -7	$ -84	*	$-17	$24	$ 83	$ 4	$ 4	$-1,162	$ 21	$ 92	$ 789	$ -3	$ -91
P_{13}	$ 6	$ 36	$ 496	*	$ 36	$ 13	*	$ 580	$ 26	$ 9	$-127	$ 20	$ 26	$-1,489	$ 18	$-140	$-1,130	$ -312	$ -1,932
P_{14}	$ 3	$ 9	*	$-3,164	$ 13	$ 15	*	$-901	$ 1	$ -1	$ 187	$ -1	$ 18	$ -179	$ 15	$ -61	$ -3	$ 42	$ -4,005

*Table 26 - Manufacturing steps absolute cost difference in β -PBCM compared to α-PBCM costs. *Process step not part of component's manufacturing process.*

The differences between the two models are due to the regression estimation errors for cycle time, materials, and tooling. Therefore, the errors of the β-PBCM (ε_{β}), shown in Figure 57, are related to the initial model lack of agreement (ε_{α}), coupled with the intermediate quantities estimation errors ($\varepsilon_{\alpha\beta}$), which, in itself, are a function of time, material, and tooling costs errors. Further breaking down these models' cost differences into the time-dependent costs, materials costs, and tooling costs, provides a better sense of the impact of each individual quantity error and weight to the cost differences (Table 27).

Part TAG	Cost Type	S_1	S_2	S_3	S_4	S_5	S_6	S_7	S_8	S_9	S_{10}	S_{11}	S_{12}	S_{13}	S_{14}	S_{15}	S_{16}	S_{17}	S_{18}
P_1	Time	-$9	-$161	-$822	*	-$5	*	*	*	*	*	*	-$20	$8	$29	$33	$304	-$69	$171
	Mat	$0	$187	-$591	*	$34	*	*	*	*	*	*	$0	$0	$0	$0	$0	$0	$0
	Tool	$0	$0	-$449	*	$0	*	*	*	*	*	*	$0	$0	$0	$0	$0	$0	$0
P_2	Time	-$5	-$156	-$631	*	-$58	*	*	*	*	*	*	-$8	$9	-$41	-$41	$218	-$152	$101
	Mat	$0	$214	-$461	*	$113	*	*	*	*	*	*	$0	$0	$0	$0	$0	$0	$0
	Tool	$0	$0	-$323	*	$0	*	*	*	*	*	*	$0	$0	$0	$0	$0	$0	$0
P_3	Time	$1	$17	$251	*	$23	*	*	*	*	*	*	$1	$11	$198	$66	$787	$84	$244
	Mat	$0	$121	$436	*	$108	*	*	*	*	*	*	$0	$0	$0	$0	$0	$0	$0
	Tool	$0	$0	$123	*	$0	*	*	*	*	*	*	$0	$0	$0	$0	$0	$0	$0
P_4	Time	-$1	$8	-$42	*	$11	*	*	*	*	*	*	$0	$14	-$70	$50	$49	$338	$270
	Mat	$0	$53	-$79	*	$40	*	*	*	*	*	*	$0	$0	$0	$0	$0	$0	$0
	Tool	$0	$0	-$20	*	$0	*	*	*	*	*	*	$0	$0	$0	$0	$0	$0	$0
P_5	Time	-$2	-$39	$251	*	$13	*	*	*	*	*	*	-$5	$149	$196	$84	$247	$378	-$100
	Mat	$0	-$375	$208	*	$111	*	*	*	*	*	*	$0	$0	$0	$0	$0	$0	$0
	Tool	$0	$0	$130	*	$0	*	*	*	*	*	*	$0	$0	$0	$0	$0	$0	$0
P_6	Time	-$2	$68	-$999	*	$29	*	*	*	*	*	*	-$7	$150	$575	-$38	$398	$231	$114
	Mat	$0	$649	-$849	*	$232	*	*	*	*	*	*	$0	$0	$0	$0	$0	$0	$0
	Tool	$0	$0	-$514	*	$0	*	*	*	*	*	*	$0	$0	$0	$0	$0	$0	$0
P_7	Time	$5	$3	*	$220	$2	*	*	*	*	*	*	$13	$0	$11	$0	$13	$1	$2
	Mat	$0	$12	*	$72	$12	*	*	*	*	*	*	$0	$0	$0	$0	$0	$0	$0
	Tool	$0	$0	*	$31	$0	*	*	*	*	*	*	$0	$0	$0	$0	$0	$0	$0
P_8	Time	-$5	$3	*	-$845	$1	*	*	*	*	*	*	-$8	-$11	$177	$19	-$308	$11	$34
	Mat	$0	$13	*	-$246	$4	*	*	*	*	*	*	$0	$0	$0	$0	$0	$0	$0
	Tool	$0	$0	*	-$110	$0	*	*	*	*	*	*	$0	-$1	$0	$1	$0	$0	$0
P_9	Time	-$3	-$8	$64	$290	-$3	-$3	*	*	*	$19	*	$5	$4	-$312	$45	-$401	$23	-$162
	Mat	$0	-$7	$64	$140	-$4	-$5	*	*	*	$2	*	$0	$0	$0	$0	$0	$0	$0
	Too	$0	$0	$0	$18	-$4	-$4	*	*	*	$20	*	$0	$0	-$25	$0	$0	$0	$0
P_{10}	Time	$10	-$17	$68	-$154	-$10	-$11	*	*	*	$10	*	-$2	$3	-$490	$4	$278	-$4	-$67
	Mat	$0	-$15	$62	-$68	-$15	-$15	*	*	*	$1	*	$0	$0	$0	$0	$0	$0	$0
	Too	$0	$0	$0	-$9	-$13	-$12	*	*	*	$10	*	$0	$0	-$46	$0	$0	$0	$0
P_{11}	Time	-$25	-$19	-$154	*	-$62	-$6	-$97	*	-$15	$2	-$8	$3	$1	$1,931	$12	$689	$711	$139
	Mat	$0	-$69	-$154	*	$0	-$4	-$43	*	-$20	$0	-$12	$0	$0	$0	$0	$2	$2	$5
	Tool	$0	$0	-$49	*	$0	-$6	$0	*	$0	$1	-$34	$0	$0	$83	$0	$15	$0	$0
P_{12}	Time	$12	$16	$41	*	-$7	-$3	-$61	*	-$8	$16	$15	$4	$3	-$1,091	$20	$88	$778	-$3
	Mat	$0	$45	$34	*	$0	-$2	-$23	*	-$8	$0	$18	$0	$0	$0	$0	$0	$4	$0
	Tool	$0	$0	$10	*	$0	-$2	$0	*	$0	$7	$50	$0	$0	-$71	$0	$3	$0	$0
P_{13}	Time	$6	$4	$246	*	$36	$2	*	$185	$3	$6	-$10	$20	$16	-$1,482	$15	-$139	-$1,050	-$288
	Mat	$0	$32	$201	*	$0	$11	*	$305	$23	$0	-$66	$0	$0	-$1	$0	-$1	-$7	-$24
	Tool	$0	$0	$48	*	$0	$0	*	$76	$0	$3	-$51	$0	$0	$0	$0	$0	$0	$0
P_{14}	Time	$3	$1	*	-$1,607	$13	$3	*	-$357	$0	-$1	$15	-$1	$10	-$178	$11	-$61	-$2	$42
	Mat	$0	$8	*	-$1,312	$0	$12	*	-$417	$1	$0	$97	$0	$0	$0	$0	$0	$0	$0
	Tool	$0	$0	*	-$247	$0	$0	*	-$106	$0	$0	$76	$0	$0	$0	$0	$0	$0	$0

Table 27 - Time-dependent, material, and tooling costs differences between α- and β-PBCM estimations at each process step.

As expected, it is found that absolute cost differences are mostly attributed to time-dependent and materials costs. Also, these errors are more noticeable in critical process steps, typically involving the use of expensive equipment with high operational costs. For this reason, any discrepancies regarding these operation's cycle time estimates, will results in higher absolute differences in cost, when compared to other process steps.

Recalling the cycle time estimation method, the cycle time distribution parameters (a,b,c) are determined from multiple regression models using as independent variables the most appropriated components' geometric properties, for every manufacturing process step. These parameters define the cycle time distribution from which each cycle time is picked in the simulation process. Consequently, each of these estimated parameters can introduce an error, depending on their deviations to the true value, as described in Figure 58. Thus, depending on the magnitude of each parameter deviation, the distribution average could increase or decrease, leading to higher or lower cycle times to be estimated. Additionally, the distribution variance can also be affected, leading to a wider or narrower time spread. These situations become unrepresentative of the current industrial performance, which is an undesirable characteristic in operation planning purposes.

Table 28 presents the percentual comparison between the estimated cycle times distribution average and the real cycle times average collected in the company registers.

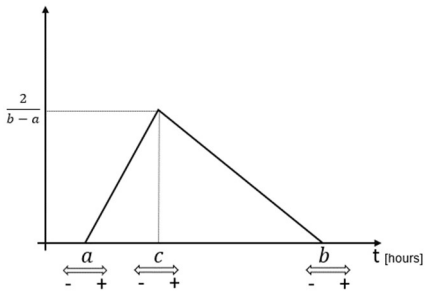

Figure 58 - Triangular distribution parameters variation possibilities. Each of the independent distribution parameters can be underestimated (-) or overestimated (+).

Aircraft	Description	WC0001	WC0002	WC0003	WC0004	WC0006	WC0008	WC0009	WC0016	WC0017	WC0018	WC0019	WC00QA	WC00QF	WC01MD
A	Skin 1	-31%	-11%	*	22%	13%	51%	3%	141%	8%	42%	-11%	142%	175%	*
A	Skin 2	-31%	-2%	*	13%	16%	38%	-3%	86%	17%	-34%	-27%	43%	191%	*
A	Skin 3	6%	-5%	*	23%	16%	60%	12%	306%	-2%	62%	14%	158%	204%	*
A	Skin 4	-17%	-17%	*	0%	21%	62%	-4%	104%	-14%	42%	6%	202%	213%	*
B	Skin 1	-1%	6%	*	**	**	97%	7%	12%	-4%	37%	56%	3%	-20%	-17%
B	Skin 2	-1%	-7%	*	**	**	**	19%	20%	2%	-7%	23%	59%	-11%	-16%
B	Spars 1	46%	*	2%	4%	65%	**	38%	113%	-20%	30%	-40%	15%	*	-63%
B	Spars 2	-4%	*	-3%	**	**	**	48%	25%	2%	106%	-41%	-35%	*	-37%
C	Spars 1	-10%	23%	8%	**	11%	**	-19%	-18%	100%	43%	75%	-63%	*	44%
C	Spars 2	33%	102%	-8%	**	21%	**	-30%	21%	11%	22%	-20%	-55%	*	-30%
C	Skin 1	-30%	-5%	*	**	**	153%	74%	206%	-1%	15%	46%	163%	**	29%
C	Skin 2	40%	-19%	*	**	**	103%	-27%	57%	-23%	30%	81%	-3%	**	0%
C	Skin 3	-8%	10%	87%	**	49%	34%	-24%	11%	1%	7%	-36%	-52%	**	-71%
C	Skin 4	16%	*	-34%	**	45%	33%	-3%	0%	13%	9%	0%	53%	**	-35%

*Table 28 -Percentual differences in estimated cycle time distributions averages to the real cycle times average. **Insufficient manufacturing data to allow for the definition of the initial parameters. *Work center not part of components' manufacturing process. Annex 4 shows both the model and the gathered data individual averages.*

The observed differences between cycle time distribution averages are quite significant for some cases and are highly correlated to the time-dependent cost differences from Table 27. In turn, one possible reason behind these work centre cycle time discrepancies could be tied to the recency in some components' manufacturing processes and thus, reduced amount of parts produced (Table 3). This led to a scarcity and scattering of data which had negative impacts when trying to find techno-economic correlations. Over time, with the increase in production runs, more adequate fittings are expected to be made. It should be noted however, that correlation does not always imply causation, meaning that despite having found a good statistical correlation between the component geometric properties and cycle time (Table 13), does not mean that some other property, unbeknown and outside of the range of available properties, could not produce a better fit. The underlying conclusion is that the models can be quite sensitive to changes in cycle times, affecting their overall capability in correctly assessing component costs.

From the observations stated above, it is suggested that in the future, better methods - besides MLR - should be explored to attenuate these issues. This is not only true for cycle times, but for materials and tooling costs as well. Compared to cycle times, these later quantities estimations errors have a lower impact on the cost estimation scheme, but the simple regression methods they are based on have the potential for further improvement and enable better cost estimations to be made, given larger sample sizes.

5.3. **PBCM as a Decision-Making Tool**

Besides being utilized to estimate manufacturing costs, PBCMs can also be used as a testbench to enable the finetuning of process variables, with the intent of studying its influence in production costs and evaluate the most economical manufacturing routes. However, with hundreds of different variables, some more controllable than others, it becomes difficult to target those that may provide meaningful results or significantly influence component final costs. With this in mind, the scope of this analysis involves three different scenarios, where mainly cycle time, materials costs and material quantities are the main cost items driving decisions. These scenarios are as follow:

- Scenario A: Considers the drop of the market price of the materials used, and consequently a component cost reduction. This reduction in material price can be linked to future improvements in material manufacturing processes, that ultimately drive prices down [67][68].
- Scenario B: Explores potential technological progress on composite manufacturing technologies, enabling higher rates of deposition and therefore smaller cycle times during automatic layup steps [69]. Improvements to layup times can also be achieved by optimizing the machine layup paths and stoppages [70].
- Scenario C: Takes into account potential reductions to overall material usage for the manufacturing of the component. This could be achieved in two ways: (1) materials mechanical properties improve over time, and to achieve the same mechanical strength, smaller quantities are required [71]; (2) by developing further knowledge on composite materials behavior, design safety factors can be reduced and design can be optimized with lower materials usage [72].

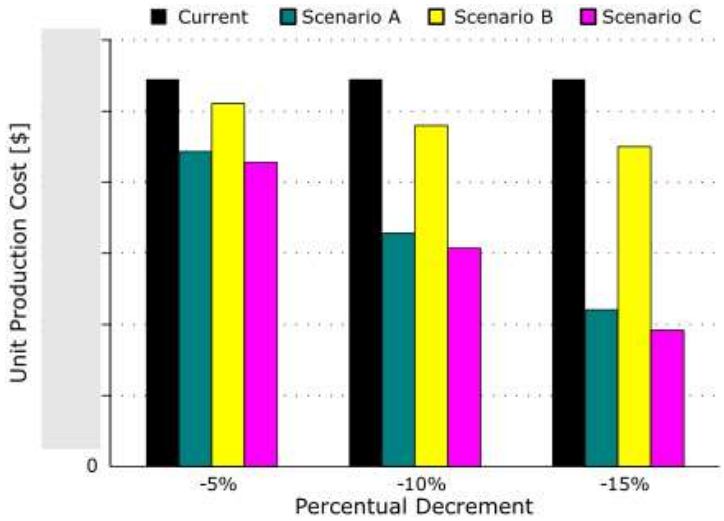

Figure 59 – Aircraft A skin 4 scenarios cost reduction comparison. (Cost values have been omitted to respect confidentiality.)

Figure 59 details the component cost reduction, concerning a 5% decrement in the quantities associated with each scenario. Scenario A considers the lowering of material price and achieves a 1,49% reduction to final component cost per 5% decrement of price.

Scenario B considers possible technical evolutions in current layup technologies, that may improve overall deposition rates. With this increase in deposition rates, lower cycle time times can be achieved, resulting in higher efficiencies in product manufacturing, thus reducing final component costs. The cost impact of this reduction – 0,5% reduction per 5% cycle time decrement - is not as effective as it was evidenced in Scenario A. Therefore, an equivalent percentual reduction to cycle times has diminishing returns when compared to a reduction to material costs, which hints at the preference of one over the other. Still, it should be noted that this cycle time reduction was only targeted at the layup step. Implementing this cycle time decrease across multiple process steps would yield cost reductions that far surpass any realistic material cost reduction.

The premise for Scenario C, revolves in reductions to overall material usage, owing to technological improvements on material properties, or design optimizations, that allow smaller quantities of material to be used, while still guarantying the components' mechanical integrity. Since there is a reduction in the amount of material being deposited during the automated layup cycle, an equal reduction on cycle time is to be expected. Therefore, under this scenario, there is a double reduction in cost drivers - one in material quantities, and another in the automated layup cycle time. This is effectively a combination of Scenario A and B, as the percentual material cost and quantities drop, have the same effect. For the aforementioned reasons, this scenario generates the greatest gains in terms of cost reduction, with a cost drop of 1,72% in the final cost.

Additionally, these scenarios can be explored considering two similar manufacturing routes for the same component, where the main difference lies in the automatic deposition technology used, namely ATL or AFP, in order to assess the economic viability of one over the other (Figure 60).

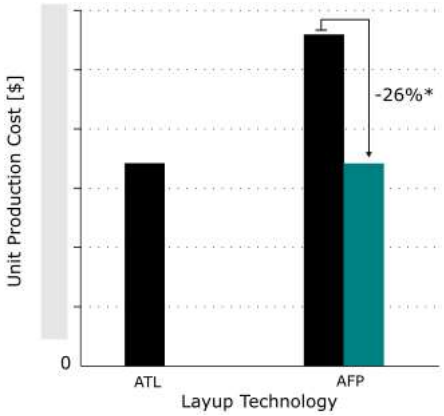

*Figure 60 – Aircraft A Skin 4 manufacturing costs comparison using ATL or AFP as main layup technology. ** 26% decrement under scenario C. (Cost values have been omitted to respect confidentiality.)*

The differences in cost are very noticeable when the only difference in the manufacturing route is on whether using AFP instead of ATL. These are mostly due to the increased cost in both materials and AFP equipment as well as the apparent lower processing performance of AFP, resulting in increased cycle times when compared to ATL. These differences between the cycle times estimated for the two technologies are quite significant and could be tied to an estimation failure of AFP cycle times for this case. This might stem, once again, from the lack of data regarding the AFP process (Table 2), when

compared to ATL, which besides reducing the fitting power of the regression, may signal a technological process in an early development phase in the company, yet far from its maturity.

For the component currently produced under the ATL route to be manufactured by AFP (Figure 60) without losing economic competitiveness, it would require a reduction of 26% in both material quantities and layup cycle time. Interestingly, in one other study, it was concluded that a 5% reduction to material costs, would make AFP less costly than ATL [6]. That such a small reduction would suffice in making AFP more cost efficient, suggests that the cost of equipment and materials considered for the two technologies were not as distinct as observed in this study. What the current model and data suggest, for this example, is that ATL is the better solution to have implemented, from an economical point of view. If AFP was to be considered - or the only viable option due to geometrical constraints - only trough very aggressive reductions, hardly achievable in the foreseeable future, in materials quantities and layup cycle times, could it become as economically competitive as ATL. This sort of conclusion is extremely useful to be drawn out, especially at the early stages of design, where different manufacturing routes are being assessed, or when considering present manufacturing processes changes.

Cycle Time Sensitivity

Cycle times have noticeably influenced components' costs and in some process steps, cycle time sensitivity is more exposed, due to its greater effects on costs. In such particular steps, managing and possibly improving its performance could contribute to the final components' final cost reductions. Thus, in future interests for operations improvements, effort and resources would be better allocated into refining these steps performances, than in other less rewarding. In order to track down these specific cases, a cycle time sensitivity analysis was performed across each work center, and components' cost changes due to forced cycle time variations were recorded. These variations are explored by overriding each process work centers' maximum and most likely cycle time, to a percentage of their initial values, as described in Figure 61 a). From this lowering of cycle times, a cost reduction is observed in the final cost distribution, Figure 61 b), alongside final cost distribution spread reductions.

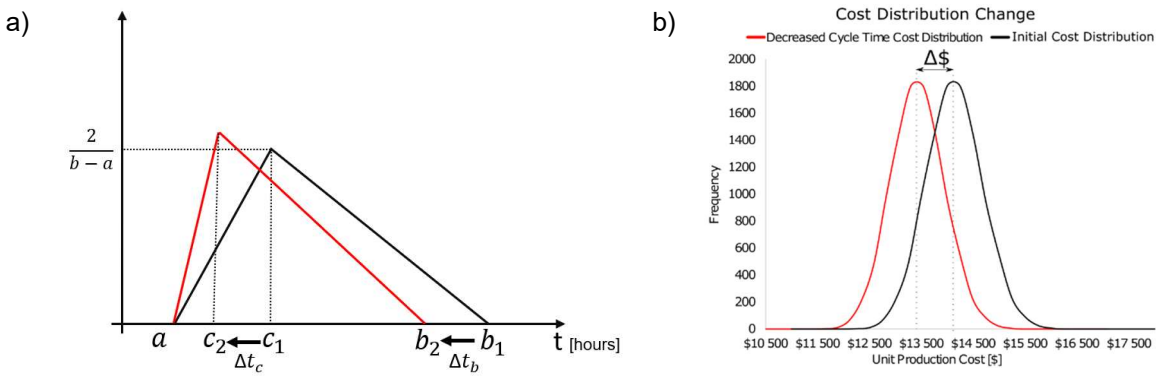

Figure 61 – a) Forced cycle time shift, by reducing the maximum and most likely cycle times. Percentual Δt_c reduction equal to percentual Δt_b b) Example of cost distribution reduction (Δ$) as a result of the forced time shift.

Aircraft	Description	Part Tag	WC0001	WC0002	WC0003	WC0004	WC0006	WC0008	WC0009	WC0016	WC0017	WC0018	WC0019	WC00QA	WC00QF	WC01MD
A	Skin 1	P_1	0.4%	1.8%	*	0%	0%	0%	1.8%	0.5%	0.7%	0.7%	0.6%	0.3%	0.7%	*
A	Skin 2	P_2	0%	1.9%	*	0.1%	0.1%	0.1%	1.6%	0.5%	0.4%	0.1%	0.6%	0.2%	0.1%	*
A	Skin 3	P_3	0.1%	1.4%	*	0.1%	0.1%	0.1%	1.5%	0.8%	0.3%	0.1%	0.6%	0.1%	0.3%	*
A	Skin 4	P_4	0%	1.5%	*	0.1%	0.1%	0.1%	1.7%	0.5%	0.2%	0.2%	0.6%	0.1%	0.4%	*
B	Skin 1	P_5	0%	1.3%	*	0.1%	0.1%	0%	0.9%	0.7%	0.2%	0.1%	0.3%	0.1%	0.2%	*
B	Skin 2	P_6	0%	1.2%	*	0.1%	0.1%	0%	1.2%	0.8%	0.2%	0.1%	0.4%	0%	0.4%	*
B	Spars 1	P_7	0%	*	4.8%	0%	0%	0%	0.9%	0.7%	0.1%	0%	0.1%	0%	*	0.1%
B	Spars 2	P_8	0%	*	5.0%	0%	0.1%	0.1%	0.9%	0.8%	0.1%	0%	0.1%	0%	*	0.0%
C	Spars 1	P_9	0%	0.2%	1.8%	0.2%	0.1%	0.0%	1.5%	1.9%	0.1%	0.1%	0%	0%	*	0.0%
C	Spars 2	P_{10}	0.1%	0.5%	2.1%	0%	0.1%	0.1%	1.4%	2.0%	0.3%	0%	0%	0.1%	*	0.1%
C	Skin 1	P_{11}	0%	0%	*	0.1%	0.1%	0%	3.4%	0.9%	0.1%	0.1%	1.6%	0.3%	*	0.1%
C	Skin 2	P_{12}	0.1%	0%	*	0.1%	0.1%	0%	2.9%	0.7%	0.3%	0.2%	1.3%	0.2%	*	0.1%
C	Skin 3	P_{13}	0%	1.8%	0.4%	0%	0.1%	0%	2.0%	0.5%	0%	0.1%	0.4%	0.2%	*	0.1%
C	Skin 4	P_{14}	0.2%	*	2.5%	0.1%	0.0%	0%	1.6%	0.6%	0.1%	0.1%	0.7%	0%	*	0.2%
	Average		**0.1%**	**1.1%**	**2.8%**	**0.1%**	**0.1%**	**0.0%**	**1.7%**	**0.8%**	**0.2%**	**0.1%**	**0.5%**	**0.1%**	**0.4%**	**0.1%**

Table 29 - Final components' cost decrease as a result of a 15% reduction of current maximum and most likely cycle times for each work center. Total reduction represents a 15% reduction across all work centers simultaneously

From Table 29, some conclusions can be drawn out. Work centers that display the highest sensitivities to cycle time variation are tied to manufacturing steps that are mostly dominated by machine operations, where either increases or decreases to cycle times will massively influence final component costs. Contrarily, less critical and manual tasks, usually performed as intermediate steps of the manufacturing process, not involving the use of major equipment, have a very small to gain in reducing its cycle time.

These analyses are constantly being pushed by companies, looking for continuum improvements that can effectively reduce manufacturing costs, and thus, to have a clear target as to where the effort should be channelled, is always of great help to meet those goals.

Similar studies could be conducted in order to understand how different manufacturing parameters influence components' costs, besides cycle time and material quantities. Being able to perform these tests, at any given project stage, further cements the usefulness of having a tool that can accurately represent cost changes owning to process parameters variations. Ultimately, the developed model allows for thoughtful and readily available decisions to be made regarding manufacturing processes, mindful of their impacts on costs.

6. Conclusions and Future work

In the current manufacturing paradigm, the control of manufacturing costs should begin at the product and process design stages. When manufacturing operations are already taking place, actions for cost reduction have normally a narrower impact and/or involve high investments, which are too expensive [4][44]. Therefore, cost engineering within aircraft design, and certainly in many other areas, should play a more significant role inside the multidisciplinary design teams, to more effectively balance trade-offs between cost and performance. However, there is still the need for tools that help cost engineers to work in tandem with product and process designers, in order to make reasonable and measured cost estimations, often difficult to perform due to the lack of detailed design information during the initial stages of development. With this in mind, this work was set out to attenuate these issues, by developing a tool based on Process-Based Cost Models (PBCMs) to provide a manufacturing cost assessment, based on a limited amount of inputs, easily obtained even at the early stages of design. For a particular industrial environment and for aeronautics components made of composites, this was done taking advantage of a significant amount of rich historical data to generate techno-economic regressions that materialize powerful knowledge, which can then feed the core of the PBCM tool.

Across many different manufacturing industries, process variability is often encountered, influencing operations cycle time and therefore the component's final cost. To emulate its effects in the developed cost model, the common deterministic approach to cost modelling was abandoned, and instead, a stochastic method was introduced. It was shown that the modelled variabilities can significantly impact the components' final cost, and provide a broader view of expected costs, that may surpass the cost target. Additionally, by introducing cost variability into the cost estimation process, additional awareness is raised on the need for close process monitoring, allowing for the identification of process steps whose improvements can deliver positive results in terms of final cost reduction. Outside of the cost estimation process, the modelled variabilities can also be used for process capacity planning purposes. Using part-specific data as the basis for cycle time determination proved to be efficient in the current cost estimation scheme, although, in the future, the method could be further refined in several ways by (1) adding additional part properties (independent variables) to the time regressions or (2) adopting non-linear fittings or machine learning methods. Either in the current of future states, these methods would benefit from the maturity of some of the current processes, whose data randomness and uncertainty from the limited number of production runs hinder the accuracy of the developed methods.

Non-qualities are estimated based on a method that assumes that their occurrence is random and independent from one another. For the intended purposes of cost estimation, this is an effective and reasonable approach, but these events are usually dominated by the principle of causality – a cause that triggers an event. Given the abundance and detail of the available data, future studies should be performed that explore the possible cause-and-effect mechanisms in non-quality occurrences. Any new-found knowledge could be applied in line with the cost modelling problem, but more importantly, it

would provide valuable information to non-quality causes and how to better prevent them, so that its effects are less noticeable on future costs.

It was also found that tooling costs were surprisingly well correlated with part surface area, and a simple linear regression was used to describe its costs based on the parts' surface area. A similar approach was followed to determine the manufacturing process material quantities, but the method was not as suited as it was with tooling costs, given the clustering of different part types. The heterogeneity between the different parts results in different material demands that stem from the type of component itself, rather than some quantitative part property such as its area. For that reason, future methods should be able to combine qualitative and quantitative data to distinguish the different types of components and consequently better determine their required material quantities.

From the cost analysis of the studied sample, the results show the bigger the part, the higher the material percentage cost represents in the total manufacturing costs, followed by machine costs. In processes involving multiple parts integrations, labour and tooling costs become more significant, given the increased manufacturing steps required and additional tools to ensure the correct alignment of parts.

The results from this study support the initial hypothesis that manufacturing cost can be automatically estimated based on simple geometric characteristics available in the very front end of the design and process planning if good historical data is available. It should be noted, however, that the predictive power of the current method is not fully validated, and further testing with parts outside of the learning sample would be required. Still, given the method's descriptive power, it can be expected acceptable predictive results on components' costs, whose properties are within the bounds of the studied samples. The achieved estimation errors of the manufacturing costs are substantially low (MAPE=16.4%;NRMSE=5.1%), and a clear step forward to support engineering decision making before production is initiated, or to launch cost reduction initiatives in current processes. Additionally, with further development, the cost estimation could be embedded as a CAD tool and become a design parameter during parts' design stages. In the future, the scope of this analysis may be broadened to include assembly costs and thus enable the economic evaluation of one of composites main advantages that is part consolidation.

7. References

[1] G. Marsh, “Aerospace composites - the story so far,” *Reinf. Plast.*, vol. 40, no. 9, pp. 44–48, 1996.

[2] J. Sloan, “ATL & AFP: Defining the megatrends in composite aerostructures,” *High Perform. Compos. 16 (4) (2008) 68–71.* .

[3] J. A. Barton, D. M. Love, and G. D. Taylor, “Design determines 70% of cost? A review of implications for design evaluation,” *J. Eng. Des.*, vol. 12, no. 1, pp. 47–58, 2001.

[4] R. RUSH, Christopher; ROY, “Expert judgement in cost estimating: modelling the reasoning process.,” *Concurr. Eng.*, vol. 9, no. 4, pp. 271–284, 2001.

[5] D. H.-J. A. Lukaszewicz, C. Ward, and K. D. Potter, “The engineering aspects of automated prepreg layup: History, present and future,” *Compos. Part B Eng.*, vol. 43, no. 3, pp. 997–1009, Apr. 2012.

[6] B. A. R. Soares, E. Henriques, I. Ribeiro, and M. Freitas, “Cost analysis of alternative automated technologies for composite parts production,” *Int. J. Prod. Res.*, vol. 0, no. 0, pp. 1–14, 2018.

[7] G. Dorey, “Carbon fibres and their applications,” *J. Phys. D. Appl. Phys.*, vol. 20, no. 3, pp. 245–256, 1987.

[8] J. . R. C. H. Dr. Ravi B.Deo; Dr. James H. Starnes, “Low-Cost Composites Materials and Structures for Aircraft Applications,” 臨床整形外科, vol. 38, no. 5, pp. 607–612, 2003.

[9] M. Maria, “Advanced composite materials of the future in aerospace industry,” *Incas Bull.*, vol. 5, no. 3, pp. 139–150, 2013.

[10] E. Hutchinson, “Chapter 1 - Introduction,” *Environ. Heal. Sustain. Dev.*, no. forthcoming, pp. 1–23, 2016.

[11] “Boeing sets pace for composite usage in large civil aircraft : CompositesWorld.” [Online]. Available: https://www.compositesworld.com/articles/boeing-sets-pace-for-composite-usage-in-large-civil-aircraft. [Accessed: 25-Sep-2019].

[12] “AERO - Boeing 787 from the Ground Up.” [Online]. Available: https://www.boeing.com/commercial/aeromagazine/articles/qtr_4_06/article_04_5.html. [Accessed: 25-Sep-2019].

[13] R. Stewart, “Carbon fibre composites poised for dramatic growth,” *Reinf. Plast.*, vol. 53, no. 4, pp. 16–21, May 2009.

[14] M. Holmes, “Global carbon fibre market remains on upward trend,” *Reinf. Plast.*, vol. 58, no. 6,

pp. 38–45, Nov. 2014.

[15] M. Holmes, “Carbon composites continue to find new markets,” *Reinf. Plast.*, vol. 61, no. 1, pp. 36–40, Jan. 2017.

[16] “Boeing: 777X.” [Online]. Available: https://www.boeing.com/commercial/777x/#/overview. [Accessed: 25-Sep-2019].

[17] “777X: Bigger-than-expected carbon fiber impact: CompositesWorld.” [Online]. Available: https://www.compositesworld.com/blog/post/777x-bigger-than-expected-carbon-fiber-impact. [Accessed: 25-Sep-2019].

[18] “Boeing opens $1 billion 777X Composite Wing Center : CompositesWorld.” [Online]. Available: https://www.compositesworld.com/news/boeing-opens-1-billion-777x-composite-wing-center. [Accessed: 25-Sep-2019].

[19] J. Huber, “Automated lamination of production advanced composite aircraft structures,” *SAE Tech. Pap.*, 1981.

[20] Grimshaw MN, “Automated Tape Laying,” *Cincinnati Cincinnati Mach.*, 2001.

[21] Anon, “MIL-HDBK-17-3F-composite materials handbook,” *Dep. Def.*, vol. 3F, 2002.

[22] T. G. Gutowski, *Advanced composites manufacturing*, vol. 1. 1997.

[23] Åström, “Manufacturing of polymer composites,” 1997.

[24] MTorres, “Diseños Industriales S. Torres layup - Tape Layer Machine,” 2010. [Online]. Available: http://www.mtorres.es/pdf/torreslayup.pdf.

[25] M. K. Hagnell and M. Åkermo, “A composite cost model for the aeronautical industry: Methodology and case study,” *Compos. Part B Eng.*, vol. 79, pp. 254–261, Sep. 2015.

[26] and J. M. L. D. M. N. Grimshaw, C. G. Grant, “Advanced Technology Tape Laying for Affordable Manufacturing of Large Composite Structures,” in *Int. Smape Symp Exhib*, 2001, pp. 2484–2494.

[27] W. B. Goldsworthy, “Geodesic path length compensator for composite-tapeplacement method.,” 1974.

[28] A. W. Blom, C. S. Lopes, P. J. Kromwijk, Z. Gürdal, and P. P. Camanho, “A theoretical model to study the influence of tow-drop areas on the stiffness and strength of variable-stiffness laminates,” *J. Compos. Mater.*, vol. 43, no. 5, pp. 403–425, 2009.

[29] T. Oldani, “Increasing productivity in fiber placement processes,” in *SAE Aerospace manufacturing and automated fastening conference & exhibition*, 2008.

[30] Y. R. Larberg, M. Åkermo, and M. Norrby, “On the in-plane deformability of cross-plied unidirectional prepreg,” *J. Compos. Mater.*, vol. 46, no. 8, pp. 929–939, 2012.

[31] D. F. Walczyk, J. F. Hosford, and J. M. Papazian, “Using reconfigurable tooling and surface

heating for incremental forming of composite aircraft parts," *J. Manuf. Sci. Eng. Trans. ASME*, vol. 125, no. 2, pp. 333–343, 2003.

[32] W. T. Wang, H. Yu, K. Potter, and B. C. Kim, "Improvement of composite drape forming quality by enhancing interply slip," *ECCM 2016 - Proceeding 17th Eur. Conf. Compos. Mater.*, no. June, pp. 26–30, 2016.

[33] J. Sjölander, P. Hallander, and M. Åkermo, "Forming induced wrinkling of composite laminates: A numerical study on wrinkling mechanisms," *Compos. Part A Appl. Sci. Manuf.*, vol. 81, pp. 41–51, 2016.

[34] T. J. Dodwell, R. Butler, and G. W. Hunt, "Out-of-plane ply wrinkling defects during consolidation over an external radius," *Compos. Sci. Technol.*, vol. 105, pp. 151–159, 2014.

[35] M. Kuwata and P. J. Hogg, "Interlaminar toughness of interleaved CFRP using non-woven veils: Part 2. Mode-II testing," *Compos. Part A Appl. Sci. Manuf.*, vol. 42, no. 10, pp. 1560–1570, 2011.

[36] K. C. Teng and F. C. Chang, "Single-phase and multiple-phase thermoplastic/thermoset polyblends: 2. Morphologies and mechanical properties of phenoxy/epoxy blends," *Polymer (Guildf).*, vol. 37, no. 12, pp. 2385–2394, 1996.

[37] T. G. Gutowski, G. Dillon, S. Chey, and H. Li, "Laminate wrinkling scaling laws for ideal composites," *Compos. Manuf.*, vol. 6, no. 3–4, pp. 123–134, Jan. 1995.

[38] X. X. Bian, Y. Z. Gu, J. Sun, M. Li, W. P. Liu, and Z. G. Zhang, "Effects of processing parameters on the forming quality of C-shaped thermosetting composite laminates in hot diaphragm forming process," *Appl. Compos. Mater.*, vol. 20, no. 5, pp. 927–945, 2013.

[39] U. R. Dean EB, "Elements of designing for cost.," in *Irvine Proceedings of AIAA 1992 aerospace design conference*.

[40] M. J. Wood, "Design to cost," *Wiley Intersci.*

[41] T. Kruckenberg and R. Paton, *Resin transfer molding for aerospace structures*. 1998.

[42] P. M. Mukhopadhyay T, Vicinanza S, "Examining the feasibility of a case-based reasoning model for software effort estimation," *MIS Quart*, vol. 155, no. 71.

[43] S. E. Myrtveit I, "A controlled experiment to assess the benefits of estimating with analogy and regression models," *IEEE Trans. Softw. Eng.*, vol. 510, no. 25, 1999.

[44] R. Curran, S. Raghunathan, and M. Price, "Review of aerospace engineering cost modelling: The genetic causal approach," *Prog. Aerosp. Sci.*, vol. 40, no. 8, pp. 487–534, Nov. 2004.

[45] R. Corporation., "Military jet acquisition:technology basics & cost-estimating methodology. MR-1596," 2002.

[46] T. G. ICM, "(Integrated Cost Modelling) business case.," in *BAE SYSTEMS, Internal*

presentation, 2002.

[47] B. JA., “Feature costing:beyond ABC.,” *J Cost Manag*, vol. 6, no. 12, 1998.

[48] N. K. Nachtmann H, “Fuzzy activity based costing:a methodology for handling uncertainty in activity based costing systems.,” *Eng Econ*, vol. 46(4):245, 2001.

[49] A.-H. A. Kishk M, “An integrated framework for life cycle costings in buildings.,” *RICS Res. Found.*, 1999.

[50] S. R. Villarreal JA, Lea RN, “Fuzzy logic and neural network technologies,” in *30th Aerospace sciences meeting and exhibit*.

[51] B. J., “Neural networks for cost estimation.,” *Cost Eng*, vol. 40(1):25–3, 1998.

[52] J.-L. Loyer, E. Henriques, M. Fontul, and S. Wiseall, “Comparison of Machine Learning methods applied to the estimation of manufacturing cost of jet engine components,” *Int. J. Prod. Econ.*, vol. 178, pp. 109–119, Aug. 2016.

[53] O. K. Joshi, “The effect of moisture on the shear properties of carbon fibre composites,” *Composites*, vol. 14, no. 3, pp. 196–200, Jul. 1983.

[54] J. P. M. de Silva Luis, “Effect of out-time aging in composite prepreg material Towards a testing methodology for material properties characterization,” no. May, p. 36ff, 2014.

[55] M. Gagné and D. Therriault, “Lightning strike protection of composites,” *Prog. Aerosp. Sci.*, vol. 64, pp. 1–16, Jan. 2014.

[56] L. Liu, B.-M. Zhang, D.-F. Wang, and Z.-J. Wu, “Effects of cure cycles on void content and mechanical properties of composite laminates,” *Compos. Struct.*, vol. 73, no. 3, pp. 303–309, Jun. 2006.

[57] L. M. P. Durão, J. M. R. S. Tavares, V. H. C. de Albuquerque, J. F. S. Marques, and O. N. G. Andrade, “Drilling damage in composite material,” *Materials (Basel).*, vol. 7, no. 5, pp. 3802–3819, 2014.

[58] L. F.Vosteen, “Fibrous Composites in Structural Design,” J. J. B. Edward M.Lenoe, Donald W.Oplinger, Ed. Springer, 1980, pp. 7–24.

[59] A. Y. Akbulut-Bailey, J. Motwani, and E. M. Smedley, “When Lean and Six Sigma converge: A case study of a successful implementation of Lean Six Sigma at an aerospace company,” *Int. J. Technol. Manag.*, vol. 57, no. 1–3, pp. 18–32, 2012.

[60] J. Ziv and A. Lempel, “Compression of Individual Sequences via Variable-Rate Coding,” *IEEE transactions on Information Theory*, vol. IT24. p. 530, 1978.

[61] K. E. V. L. B. Pfahler, “The Role of Normal Data Distribution in Pharmaceutical Development and Manufacturing.”

[62] B. W. Yap and C. H. Sim, “Comparisons of various types of normality tests,” *J. Stat. Comput. Simul.*, vol. 81, no. 12, pp. 2141–2155, 2011.

[63] G. T. F. W. Edward Back, Walter W. Boles, “DEFINING TRIANGULAR PROBABILITY DISTRIBUTIONS FROM HISTORICAL COST DATA,” *J. Constr. Eng. Manag.*, vol. 126, no. February, pp. 29–37, 2000.

[64] “Fitting a triangular distribution.” [Online]. Available: https://www.johndcook.com/blog/2015/03/24/fitting-a-triangular-distribution/. [Accessed: 12-Oct-2019].

[65] “(No Title).”

[66] S. Rivas-tumanyan, *Random variables*. 2017.

[67] H. Mainka *et al.*, “Lignin - An alternative precursor for sustainable and cost-effective automotive carbon fiber,” *J. Mater. Res. Technol.*, vol. 4, no. 3, pp. 283–296, 2015.

[68] S. N. Rao, S. T. G A, R. K. P, and R. G. Kumar V V, “Carbon Composites Are Becoming Competitive and Cost Effective,” *Infosys Ltd.*, pp. 1–12, 2018.

[69] M. Assadi, “AFP Processing of Dry Fiber Carbon Materials (DFP) for Improved Rates and Reliability,” pp. 1–6, 2020.

[70] C. Ückert, D. Delisle, T. Bach, D.-I. Christian Hühne, and D.-I. Jan Stüve, “Design Optimization of a CFRP Wing Cover for the AFP Process,” 2017.

[71] R. L. Zhang *et al.*, “Enhanced mechanical properties of multiscale carbon fiber/epoxy composites by fiber surface treatment with graphene oxide/polyhedral oligomeric silsesquioxane,” *Compos. Part A Appl. Sci. Manuf.*, vol. 84, pp. 455–463, 2016.

[72] S. Guo, D. Li, and Y. Liu, “Multi-objective optimization of a composite wing subject to strength and aeroelastic constraints,” *Proc. Inst. Mech. Eng. Part G J. Aerosp. Eng.*, vol. 226, no. 9, pp. 1095–1106, 2012.

Annex 1 – Tooling costs data and geometric part data (Detailed data has been omitted to respect confidentiality)

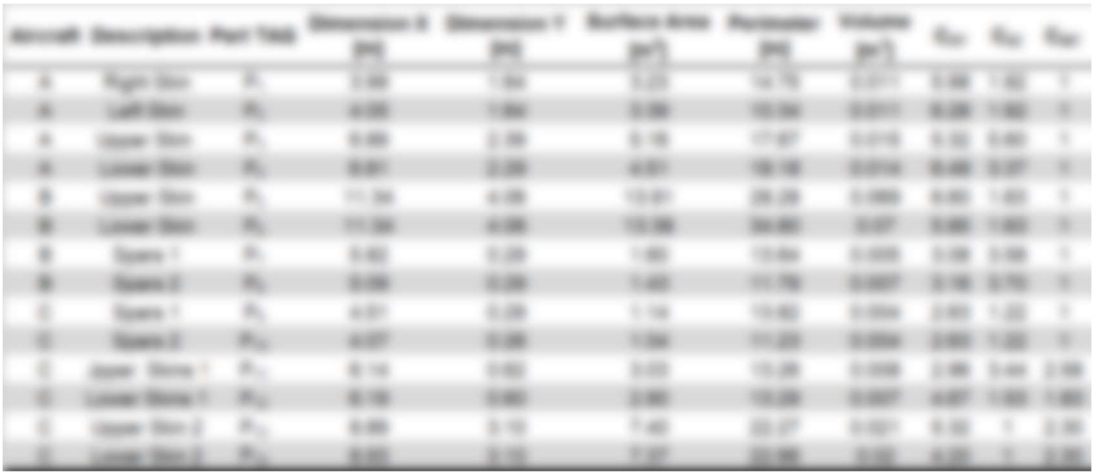

Aircraft	Description	Part Yield	Tooling Costs	Extra Tooling Costs
A	Right Skin	P_1	$ [illegible]	-
A	Left Skin	P_2	$ [illegible]	-
A	Upper Skin	P_3	$ [illegible]	-
A	Lower Skin	P_4	$ [illegible]	-
B	Upper Skin	P_5	$ [illegible]	-
B	Lower Skin	P_6	$ [illegible]	-
B	Spars 1	P_7	$ [illegible]	$ [illegible]
B	Spars 2	P_8	$ [illegible]	$ [illegible]
C	Spars 1	P_9	$ [illegible]	$ [illegible]
C	Spars 2	P_{10}	$ [illegible]	$ [illegible]
C	Upper Skins 1	P_{11}	$ [illegible]	$ [illegible]
C	Lower Skins 1	P_{12}	$ [illegible]	$ [illegible]
C	Upper Skin 2	P_{13}	$ [illegible]	$ [illegible]
C	Lower Skin 2	P_{14}	$ [illegible]	$ [illegible]

Equipment	Acquisition Cost ($ USD)	Depreciation Years
[illegible]	[illegible]	[illegible]
[illegible]	[illegible]	[illegible]
[illegible]	[illegible]	[illegible]
[illegible]	[illegible]	[illegible]
[illegible]	[illegible]	[illegible]
[illegible]	[illegible]	[illegible]

Annex 2 – Components Final Cost Sources Distributions

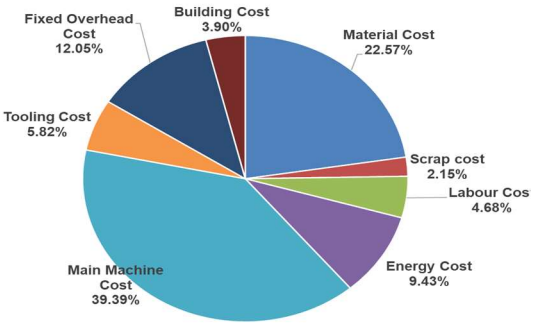

P_1

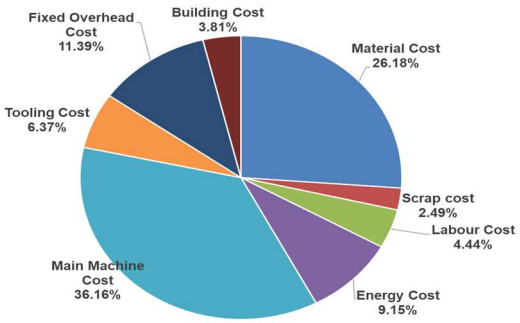

P_2

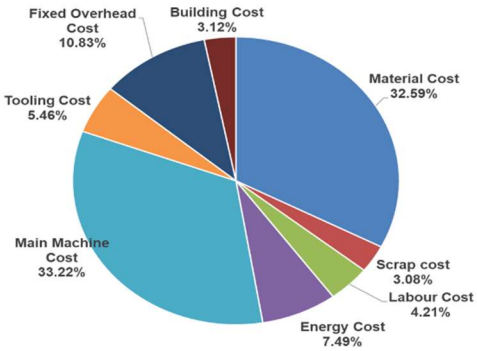

P_3

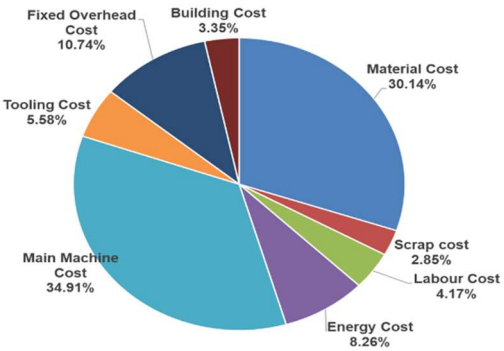

P_4

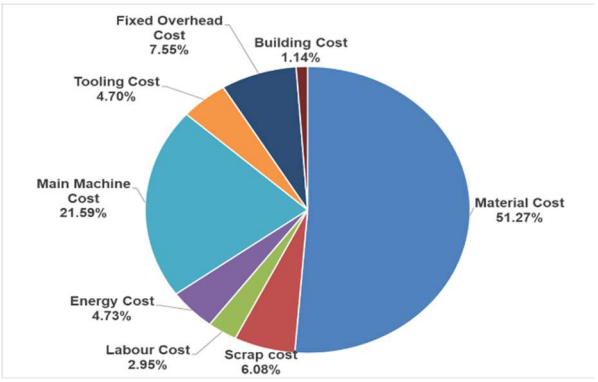

P_5

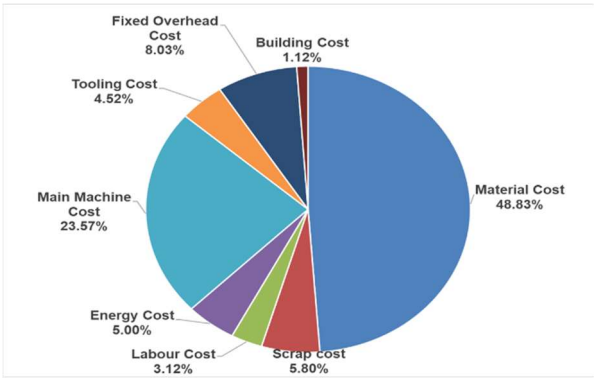

P_6

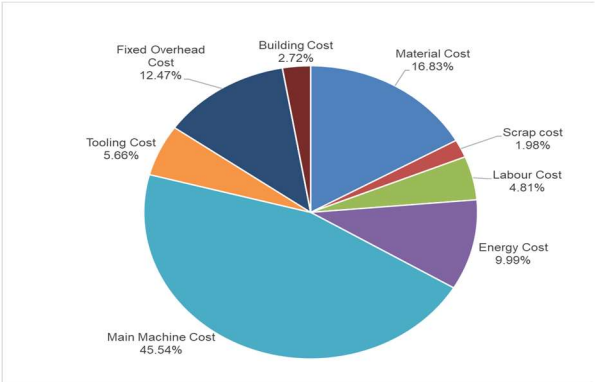

P_7

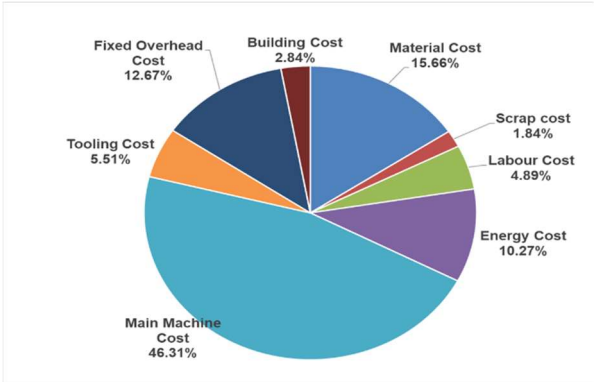

P_8

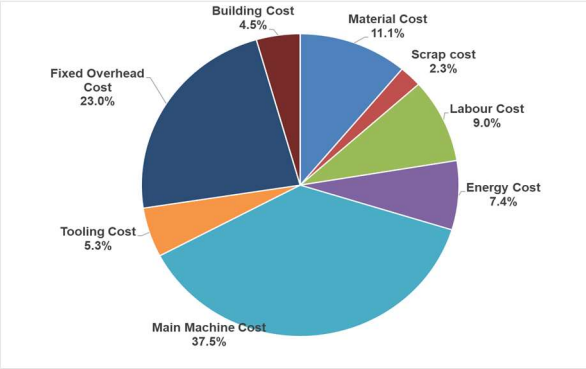

P_9

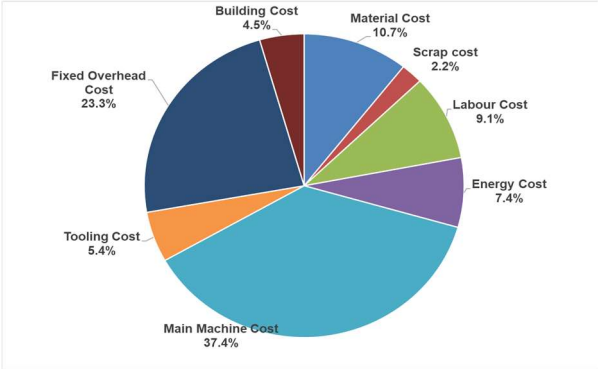

P_{10}

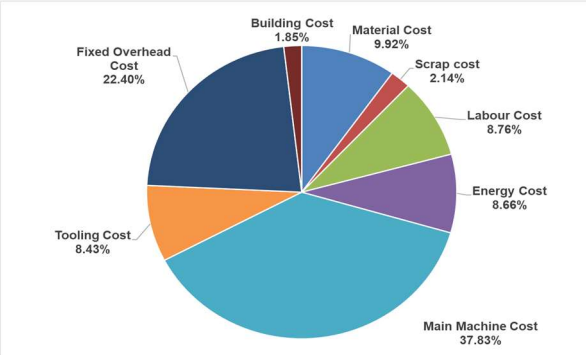

P_{11}

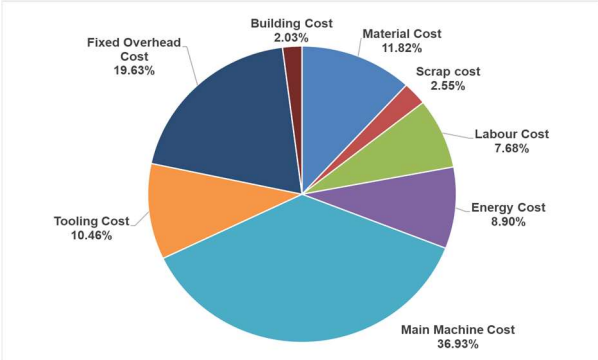

P_{12}

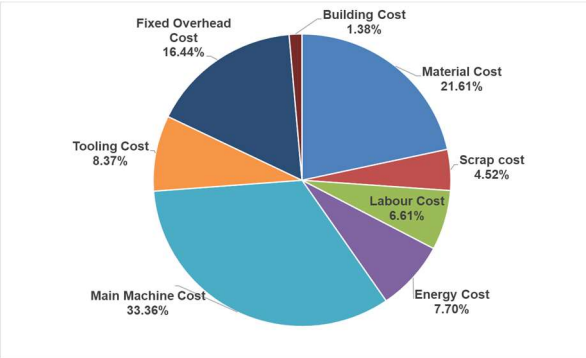

P_{13}

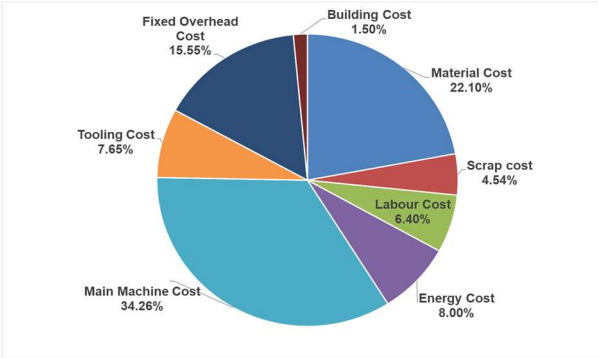

P_{14}

Annex 3 – Components manufacturing steps cost sources distribution (Absolute cost values have been omitted from the axis to respect confidentiality.)

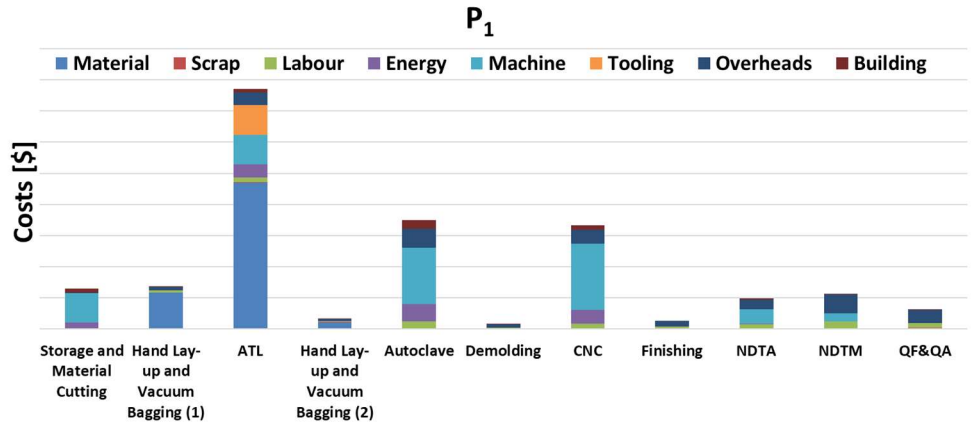

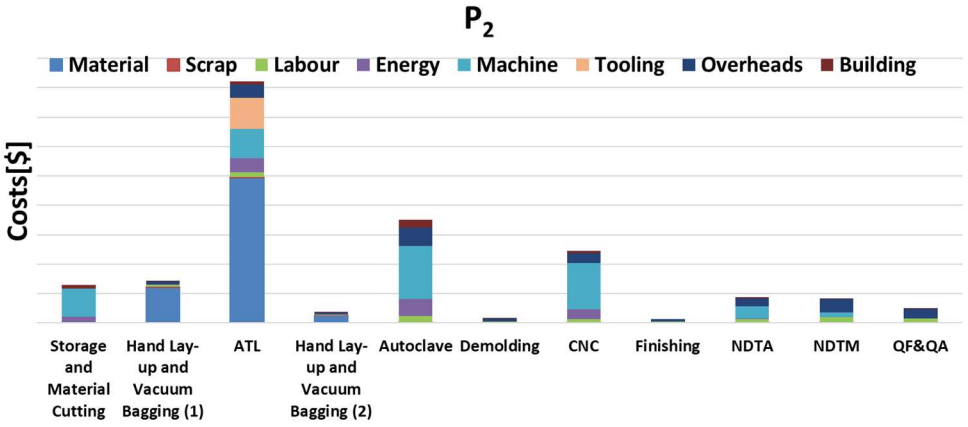

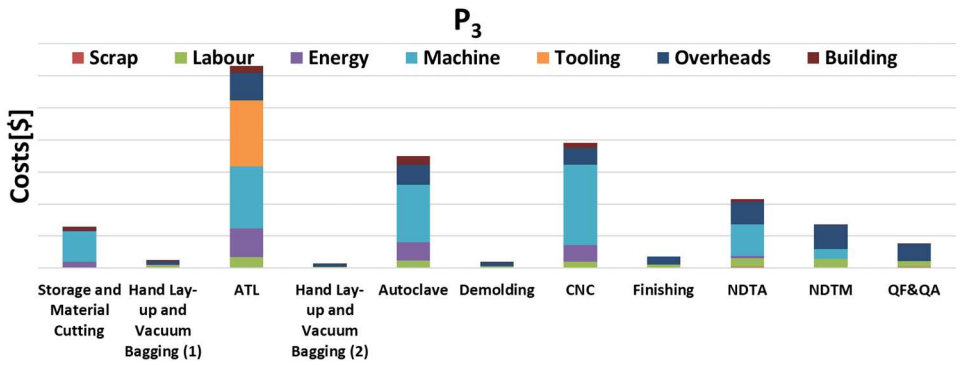

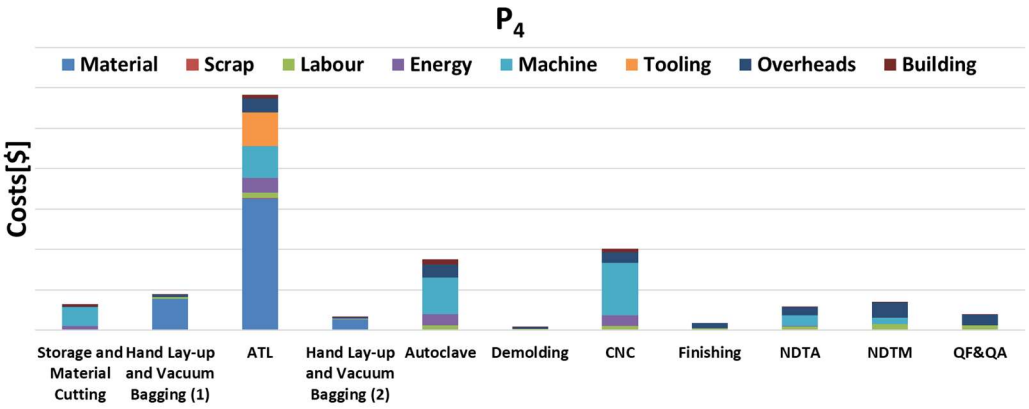
P4
Material
Scrap
Labour
Energy
Machine
Tooling
Overheads
Building
Costs[$]
Storage and Material Cutting
Hand Lay-up and Vacuum Bagging (1)
ATL
Hand Lay-up and Vacuum Bagging (2)
Autoclave
Demolding
CNC
Finishing
NDTA
NDTM
QF&QA

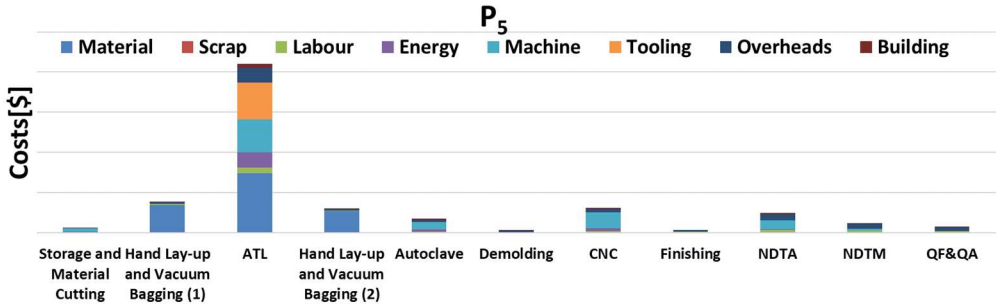
P5
Material
Scrap
Labour
Energy
Machine
Tooling
Overheads
Building
Costs[$]
Storage and Material Cutting
Hand Lay-up and Vacuum Bagging (1)
ATL
Hand Lay-up and Vacuum Bagging (2)
Autoclave
Demolding
CNC
Finishing
NDTA
NDTM
QF&QA

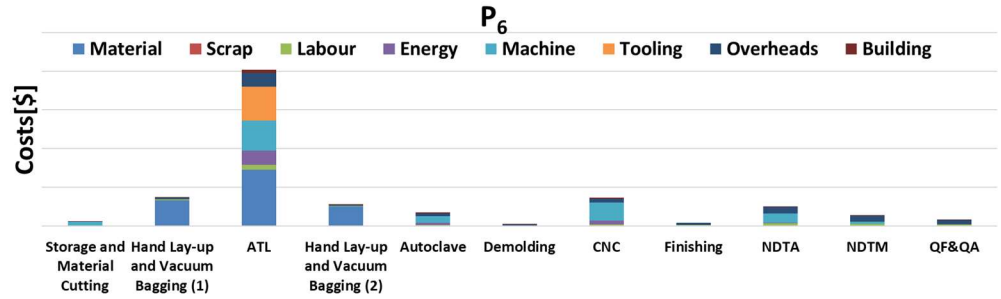
P6
Material
Scrap
Labour
Energy
Machine
Tooling
Overheads
Building
Costs[$]
Storage and Material Cutting
Hand Lay-up and Vacuum Bagging (1)
ATL
Hand Lay-up and Vacuum Bagging (2)
Autoclave
Demolding
CNC
Finishing
NDTA
NDTM
QF&QA

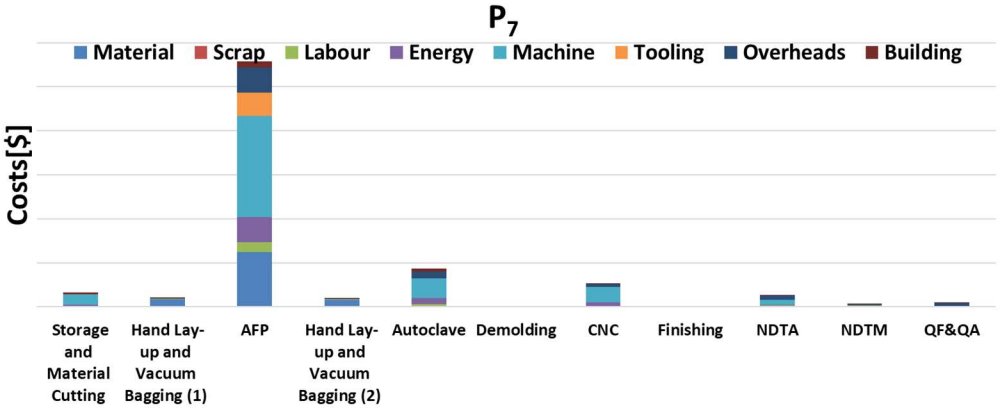
P7
Material
Scrap
Labour
Energy
Machine
Tooling
Overheads
Building
Costs[$]
Storage and Material Cutting
Hand Lay-up and Vacuum Bagging (1)
AFP
Hand Lay-up and Vacuum Bagging (2)
Autoclave
Demolding
CNC
Finishing
NDTA
NDTM
QF&QA

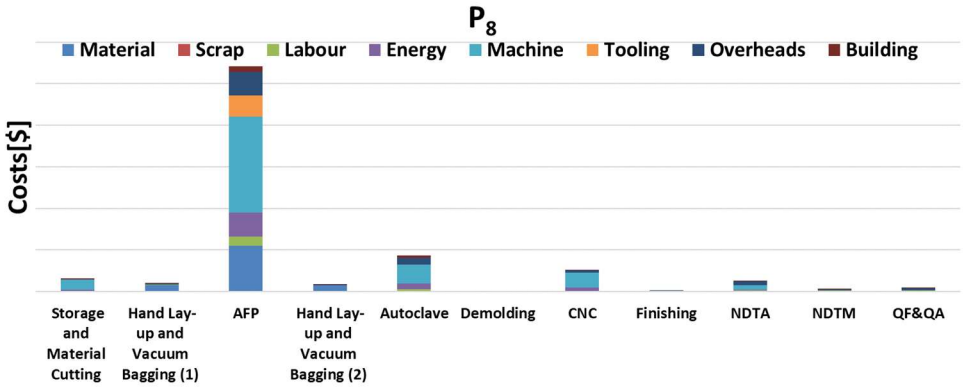
P8
Material
Scrap
Labour
Energy
Machine
Tooling
Overheads
Building
Costs[$]
Storage and Material Cutting
Hand Lay-up and Vacuum Bagging (1)
AFP
Hand Lay-up and Vacuum Bagging (2)
Autoclave
Demolding
CNC
Finishing
NDTA
NDTM
QF&QA

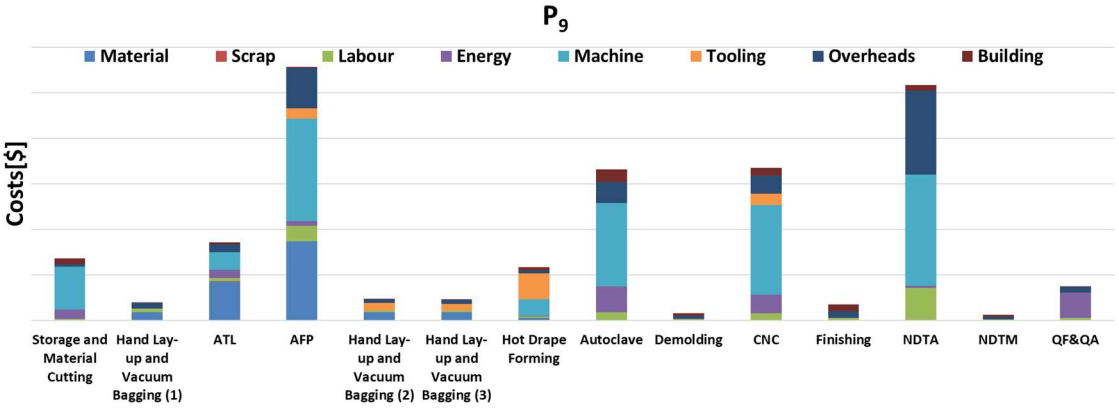
P9
Material
Scrap
Labour
Energy
Machine
Tooling
Overheads
Building
Costs[$]
Storage and Material Cutting
Hand Lay-up and Vacuum Bagging (1)
ATL
AFP
Hand Lay-up and Vacuum Bagging (2)
Hand Lay-up and Vacuum Bagging (3)
Hot Drape Forming
Autoclave
Demolding
CNC
Finishing
NDTA
NDTM
QF&QA

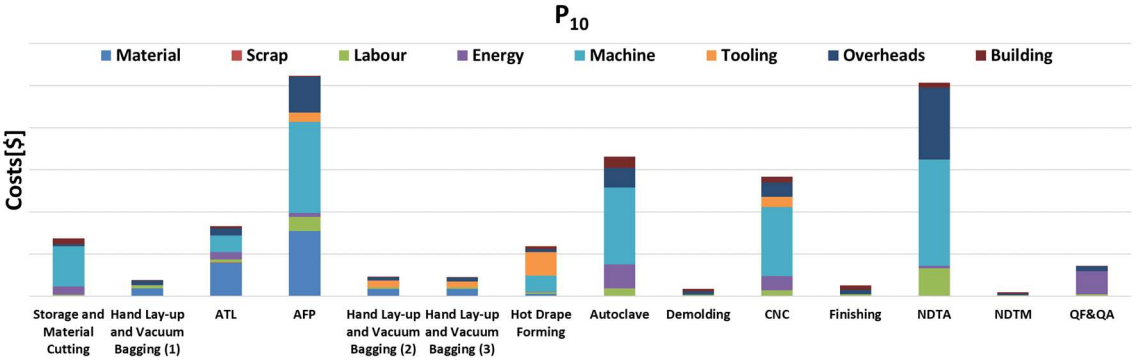
P10
Material
Scrap
Labour
Energy
Machine
Tooling
Overheads
Building
Costs[$]
Storage and Material Cutting
Hand Lay-up and Vacuum Bagging (1)
ATL
AFP
Hand Lay-up and Vacuum Bagging (2)
Hand Lay-up and Vacuum Bagging (3)
Hot Drape Forming
Autoclave
Demolding
CNC
Finishing
NDTA
NDTM
QF&QA

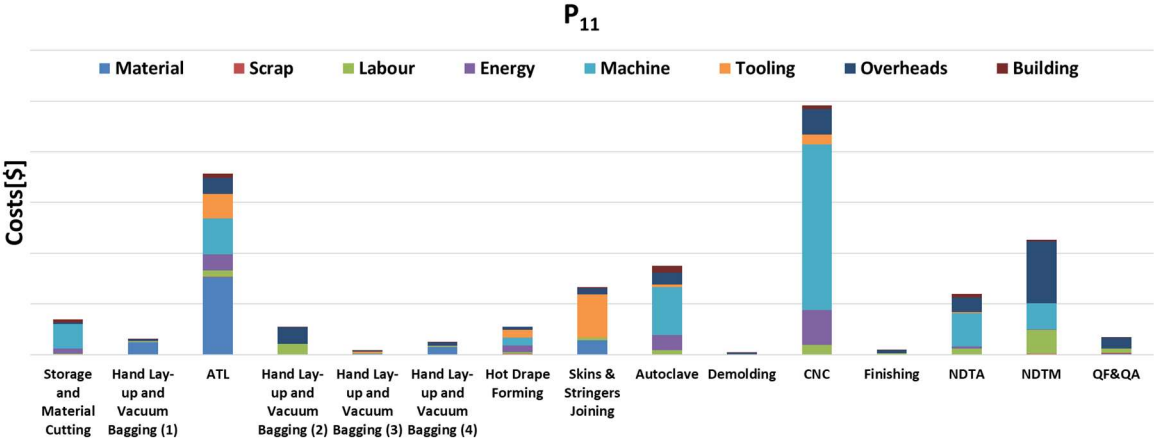
P11
Material
Scrap
Labour
Energy
Machine
Tooling
Overheads
Building
Costs[$]
Storage and Material Cutting
Hand Lay-up and Vacuum Bagging (1)
ATL
Hand Lay-up and Vacuum Bagging (2)
Hand Lay-up and Vacuum Bagging (3)
Hand Lay-up and Vacuum Bagging (4)
Hot Drape Forming
Skins & Stringers Joining
Autoclave
Demolding
CNC
Finishing
NDTA
NDTM
QF&QA

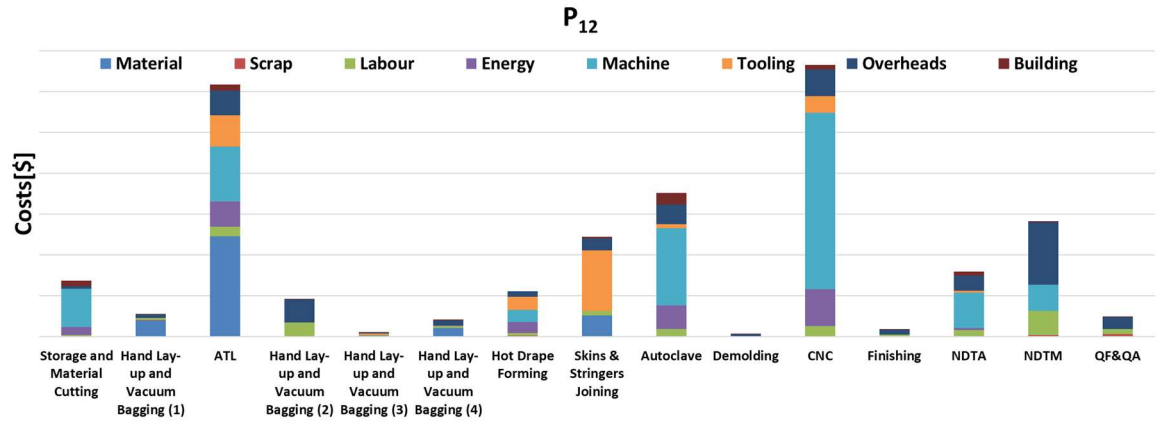
P12
Material
Scrap
Labour
Energy
Machine
Tooling
Overheads
Building
Costs[$]
Storage and Material Cutting
Hand Lay-up and Vacuum Bagging (1)
ATL
Hand Lay-up and Vacuum Bagging (2)
Hand Lay-up and Vacuum Bagging (3)
Hand Lay-up and Vacuum Bagging (4)
Hot Drape Forming
Skins & Stringers Joining
Autoclave
Demolding
CNC
Finishing
NDTA
NDTM
QF&QA

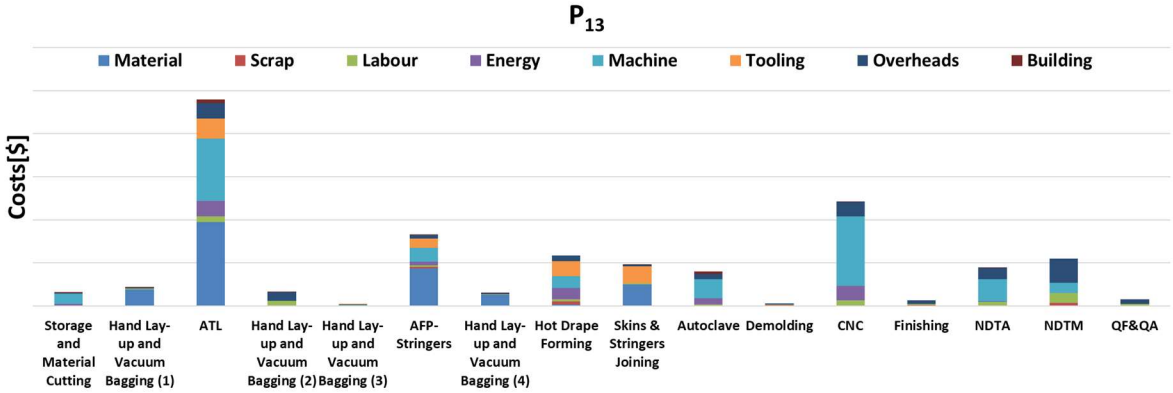
P13
Material
Scrap
Labour
Energy
Machine
Tooling
Overheads
Building
Costs[$]
Storage and Material Cutting
Hand Lay-up and Vacuum Bagging (1)
ATL
Hand Lay-up and Vacuum Bagging (2)
Hand Lay-up and Vacuum Bagging (3)
AFP-Stringers
Hand Lay-up and Vacuum Bagging (4)
Hot Drape Forming
Skins & Stringers Joining
Autoclave
Demolding
CNC
Finishing
NDTA
NDTM
QF&QA

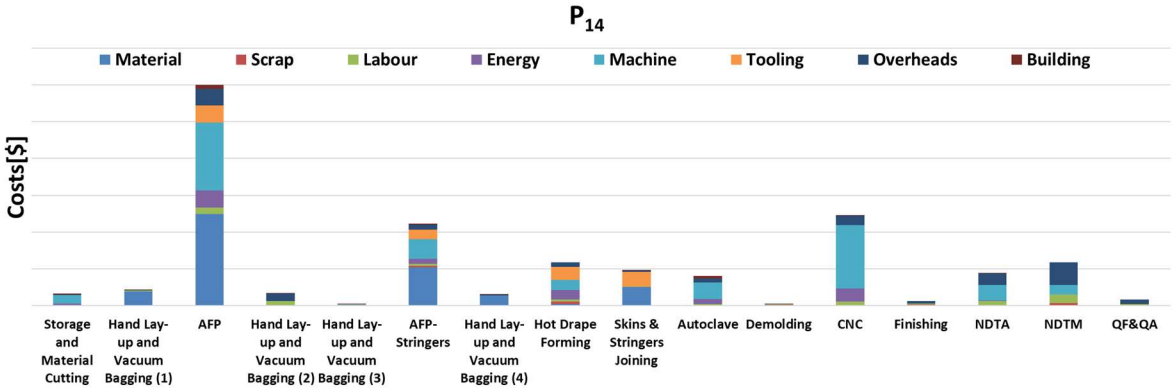
P14
Material
Scrap
Labour
Energy
Machine
Tooling
Overheads
Building
Costs[$]
Storage and Material Cutting
Hand Lay-up and Vacuum Bagging (1)
AFP
Hand Lay-up and Vacuum Bagging (2)
Hand Lay-up and Vacuum Bagging (3)
AFP-Stringers
Hand Lay-up and Vacuum Bagging (4)
Hot Drape Forming
Skins & Stringers Joining
Autoclave
Demolding
CNC
Finishing
NDTA
NDTM
QF&QA

Annex 4 – Work centers' MLR model distribution average cycle time and historic data distribution averages

Estimate Mean															
Aircraft	Description	CE0001	CE0002	CE0003	CE0004	CE0006	CE0008	CE0009	CE0016	CE0017	CE0018	CE0019	CE00QF	CE00QA	CE01MD
A	Skin 1	2.1	6.6	*	1.3	1.5	1.3	6.4	7.9	4.6	2.7	7.4	2.0	2.5	*
A	Skin 2	2.1	6.8	*	1.3	1.5	1.3	4.8	7.0	4.7	1.4	5.4	1.2	2.7	*
A	Skin 3	3.3	8.7	*	1.4	1.7	1.6	7.5	17.0	5.8	3.6	8.8	2.5	2.7	*
A	Skin 4	2.6	8.0	*	1.4	1.6	1.5	7.7	9.4	5.4	3.7	9.0	2.6	3.1	*
B	Skin 1	2.6	18.3	*	4.8	4.6	3.1	11.5	37.7	10.8	6.7	13.7	4.5	6.0	3.8
B	Skin 2	2.7	17.7	*	4.8	4.7	3.1	14.0	39.7	10.5	8.7	16.8	5.7	5.4	3.7
B	Spars 1	2.6	*	26.2	0.9	1.2	1.0	6.0	16.9	3.7	2.4	6.9	1.8	*	1.2
B	Spars 2	2.6	*	26.4	1.0	1.3	1.0	5.3	16.0	3.6	1.9	6.0	1.4	*	1.3
C	Spars 1	1.9	4.3	8.6	0.9	1.1	1.0	6.1	17.7	3.4	2.5	7.0	1.8	*	1.1
C	Spars 2	1.9	4.2	8.2	0.9	1.1	0.9	5.1	17.4	3.4	1.7	5.8	1.3	*	1.1
C	Skin 1	2.6	12.6	*	1.0	1.0	1.3	20.0	21.9	11.4	2.6	31.1	9.8	0.9	1.3
C	Skin 2	2.0	9.5	*	1.1	1.1	1.2	13.3	13.3	8.0	2.4	19.5	5.9	1.7	1.7
C	Skin 3	2.0	16.2	29.8	1.9	1.7	2.0	20.9	23.9	12.7	5.2	30.9	10.0	3.4	2.2
C	Skin 4	2.0	16.2	29.7	1.9	1.7	2.0	21.1	29.2	12.7	5.3	31.2	10.1	2.8	1.9

*Work centers' distribution average cycle time obtained from MLR models. *Work center not part of components' manufacturing process*

Real Mean															
Aircraft	Description	CE0001	CE0002	CE0003	CE0004	CE0006	CE0008	CE0009	CE0016	CE0017	CE0018	CE0019	CE00QF	CE00QA	CE01MD
A	Skin 1	3.09	7.42	*	1.05	1.31	0.86	6.26	3.29	4.28	1.92	8.32	0.82	0.89	*
A	Skin 2	3.10	6.89	*	1.14	1.28	0.96	4.88	3.74	4.03	2.17	7.37	0.83	0.91	*
A	Skin 3	3.08	9.18	*	1.13	1.47	1.00	6.74	4.19	5.90	2.23	7.68	0.98	0.89	*
A	Skin 4	3.15	9.60	*	1.41	1.36	0.93	8.00	4.59	6.27	2.65	8.55	0.87	0.99	*
B	Skin 1	2.68	17.29	*	**	**	1.58	10.80	33.74	11.33	4.92	8.82	4.35	7.43	4.60
B	Skin 2	2.68	19.07	*	**	**	**	11.74	33.17	10.32	9.37	13.69	3.55	6.14	4.36
B	Spars 1	1.77	*	25.71	0.83	0.70	**	4.34	7.92	4.64	1.84	11.47	1.55	*	3.33
B	Spars 2	2.72	*	27.24	**	**	**	3.58	12.78	3.52	0.90	10.30	2.24	*	2.09
C	Spars 1	2.09	3.49	7.96	**	0.99	**	7.47	21.57	1.71	1.71	4.01	4.95	*	0.77
C	Spars 2	1.41	2.07	8.93	**	0.91	**	7.25	14.42	3.02	1.38	7.19	2.99	*	1.59
C	Skin 1	3.66	13.26	*	**	**	0.50	11.51	7.15	11.44	2.22	21.22	3.72	**	1.01
C	Skin 2	1.43	11.66	*	**	**	0.61	18.29	8.43	10.47	1.87	10.73	6.11	**	1.67
C	Skin 3	2.15	14.77	15.94	**	1.16	1.47	27.60	21.67	12.53	4.84	48.22	20.66	**	7.65
C	Skin 4	1.70	**	44.97	**	1.16	1.47	21.73	29.28	11.19	4.84	31.25	6.59	**	2.96

*Work centers' distribution average cycle time, obtained from historic data. **Insufficient manufacturing data to allow for initial parameters definition. *Work center not part of components' manufacturing process*